UNIVERSITY OF CALIFORNIA, SAN DIEGO

Reliability-Based Characterization of Prefabricated FRP Composites for Rehabilitation of Concrete Structures

A thesis submitted in partial satisfaction of the requirements for the degree

Master of Science

in

Structural Engineering

by

Sung-Jun Jin

Committee in charge

Professor Vistasp M. Karbhari, Chair
Professor Francesco Lanza di Scalea
Professor Chia-Ming Uang

2008

The thesis of Sung-Jun Jin is approved and it is acceptable quality and form for publication on microfilm and electronically:

_____

_____

_____

Chair

University of California, San Diego

2008

TABLE OF CONTENTS

LIST OF FIGURES

LIST OF TABLES

ACKNOWLEDGEMENTS

I greatly acknowledge the guidance, time, and support of my research advisor Professor Vistasp Karbhari. I would like to thank Professors Francesco Lanza di Scalea and Chia-Ming Uang for service on my thesis committee.

I would like to thank the California Department of Transportation (Caltrans) for sponsoring this research. I would also like to thank Dr. Quan Yang and Dr. Rebecca Atadero for conducting many of the experiments used in this research.

I am deeply grateful to my family and friends for their love, support, and understanding during my studies. I give all honor to my loving parents, without whom I would not have achieved my goal.

ABSTRACT OF THE THESIS

Reliability-Based Characterization of Prefabricated FRP Composites for Rehabilitation of Concrete Structures

by

Sung-Jun Jin

Master of Science in Structural Engineering

University of California, San Diego, 2008

Professor Vistasp M. Karbhari, Chair

In order to further utilize fiber reinforced polymer (FRP) composites for strengthening of existing concrete structures, the load and resistance factor design (LRFD) approach is proposed as a design framework. The statistical nature of LRFD provides a good match for the application of prefabricated FRP composites in a reliability-based design approach. In this work, probabilistic models to describe tensile properties of prefabricated FRP materials are developed and durability test results are

used with a degradation prediction model to determine the design value of FRP material properties used in strengthening of concrete over time. Stochastic variation in the FRP is characterized based on tensile testing of several sets of prefabricated FRP composites obtained from three suppliers. A general procedure to determine the design characteristic values of the FRPs is proposed using a two-parameter Weibull distribution. This procedure is then incorporated with predictive degradation equations derived based on the experimental durability data to predict the time-dependent tensile properties of the prefabricated FRP strips and to assess the reliability of the materials over time. The proposed predictive model is used on example girders for illustration of differences between the guidelines design property values and those determined based on considerations of time and reliability. A reliability analysis is performed to compare the results. The philosophy proposed in this work provides a sound approach of considering time-dependent material degradation and reliability to determine FRP material properties values for design so that the values used are reliable and accurate over time.

Chapter 1. Introduction

1.1 Research Motivation

Externally bonded fiber reinforced polymer (FRP) composites are increasingly considered as a viable means of strengthening existing concrete structures. These materials can offer significant advantages over more traditional techniques of strengthening, such as placing more concrete, bonding steel plates, or applying some sort of post-tensioning to the structure (The Concrete Society, 2004). Due to its ease of use and adaptability, FRP provides engineers opportunities for use not available with other construction materials. FRP composites are best known for their high specific strength and stiffness. Other advantageous properties of composites include their enhanced fatigue resistance at the materials level, resistance to corrosion, and tailorability. At the present time, the application of FRP strengthening as a means of rehabilitation of civil structures is growing rapidly. In order to facilitate the continued growth of this technology and to provide for long-term safe design using FRP materials, it is essential that a design standard is developed for their use in strengthening. However, there are many challenges to be overcome in design code development including the inherently unique characteristics of FRP materials, the absence of a comprehensive statistical database of material properties, and the absence of an understanding of long-term FRP durability. The motivation of this research is to provide answers to overcome some of these challenges in order to advance the development of a design standard for FRP materials through development following the rationale of Load and Resistance Factor Design (LRFD).

1.2 Problem Description

FRP strengthening of concrete structures is currently under utilized due in large part to a lack of design standards incorporating Load and Resistance Factor Design (LRFD) principles, designer experience, and an understanding of long-term durability. A number of design guidelines are already available for the use of FRP for strengthening concrete structures. However, these guidelines are based on a deterministic approach for design. Given the high level of material variability that is inherent to FRP systems, deterministic design is likely to produce an unacceptably large range of project reliabilities.

The development of a FRP design standard similar to those of concrete and steel utilizing LRFD has been the subject of a growing body of research (Okeil et al., 2002; Atadero and Karbhari, 2005; Zureick et al., 2006). However, the creation of a comprehensive design standard is complicated by the numerous different possible combinations of fiber and resin types available for FRP composites. Methodologies for determining accurate and consistent design values and development of reliability-based design procedures must be studied.

Time-dependent material properties have not been considered in the development of design codes for other materials; however, this is an important concern for FRP materials that will be exposed to severe environments. Although the determination of long-term durability of FRP materials has been the subject of recent research, there are

only a few studies particularly related to prefabricated FRP materials used as externally bonded reinforcement in infrastructure rehabilitation over time (Yang and Karbhari, 2008).

1.3 Research Objectives

The fundamental objectives of this research are: (1) to investigate the consideration of statistical variation in the response of prefabricated FRP composites for use in rehabilitation of concrete structures, (2) to develop a reliability-based approach for determining FRP design value with the explicit considerations of an anticipated service life and effects of time-dependent material degradation due to aging and exposure conditions. This work thus serves to integrate research on LRFD with that of durability.

1.4 Research Approach

Although the development of the design procedure is intended to accommodate the full range of FRP materials, the specific examples given herein are for carbon fiber reinforced prefabricated epoxy-based composites. This choice of material was motivated by the frequent use of carbon/epoxy composites for strengthening and by the availability of previous data and material for assessing the variability of prefabricated composites. While the general format of the design procedure presented in this thesis is applicable to all types of structures, the specific design example considered in this thesis is the class of T-beam bridge girders. This choice was motivated by the sponsor of this research, the

California Department of Transportation, and the availability of data and information regarding the girders from previous research (Atadero, 2006). Furthermore, the limit state considered in the design examples is the flexural capacity of the girders. This choice was made based on the availability of load and resistance models available from previous research (Atadero, 2006; Wilcox, 2008) and will be discussed further later in Chapter 6.

1.5 Outline of the Thesis

This thesis follows the progressive development of a reliability-based procedure to determine FRP design values for flexural rehabilitation of concrete structures. Chapter 2 begins with the background for the research including current design guideline approaches for use of FRP with concrete structures, ingredients for the development of reliability-based procedure, and structural reliability methods chosen for this research. Chapter 3 describes the experimental testing and data used in this research. Statistical data sets are described representing the three material systems and the combined set of all material systems considered in this study. The results of several sets of material test data are analyzed to determine appropriate statistical descriptors for FRP, including distribution type and ranges for the mean and standard deviation of material properties. Chapter 4 introduces a reliability-based approach to determine characteristic values of the FRP and defines the characteristic values for the FRP material using the two-parameter Weibull distribution. The use of confidence levels to account for statistical uncertainty due to limited experimental data is also discussed. The durability prediction of the FRP is illustrated in Chapter 5 and predictive degradation equations are derived to determine the

degraded value of material properties over time. Environmental modification factors for various exposure conditions are developed and comparisons are made between the degraded property values predicted by a deterministic factor based current guideline approach and the property value predicted by the predictive degradation equations with the use of an environmental modification factor. Chapter 6 offers design examples to demonstrate the use of the proposed predictive reliability-based approach to determine FRP design values and a comparison to current guideline recommendations is made using reliability analysis. A summary of the ACI 440 design procedure (ACI 440, 2002) for FRP strengthening of concrete girders and the reliability method of calculation of the reliability index for the example girders is also provided. Finally, Chapter 7 concludes this thesis with a summary of the main accomplishments of this investigation and discussion of the areas remaining for further study. Several appendices supplement the thesis by providing programming scripts utilized for statistical treatment of data and reliability analysis and additional tabulated data.

Chapter 2. Background to Reliability-based Approach for FRP Material Characterization

This chapter provides general background of current application of existing design guidelines and the development of reliability-based approaches to determine FRP design values for rehabilitation of concrete structures. Discussions will include current design guideline approaches to determine FRP design values, reliability-based procedures for modeling the time-dependent FRP degradation and environmental effects, and structural reliability methods.

2.1 Current Guideline Approach to Determine FRP Design Values

There are currently a number of different design guidelines for the use of FRP in strengthening applications:

1. American Concrete Institute Committee 440 (ACI 440), *Guide for the Design and Construction of Externally Bonded FRP Systems for Strengthening Concrete Structures*, published by the American Concrete Institute , 2002
2. Technical Report 55 (TR 55), *Design Guidance for Strengthening Concrete Structure using Fibre Composite Materials (2nd Edition)*, published by the Concrete Society in the United Kingdom, 2004

3. Canadian Highway Bridge Design Code (CHBDC), published by the Canadian Standards Association (CSA), 2006
4. *Design Guidelines for FRP Strengthening of Existing Concrete Structures*, published by Björn Täljsten, 2002
5. *Strengthening Reinforced Concrete Structures with Externally-Bonded Fibre Reinforced Polymers,* published from ISIS Canada, 2001
6. *Recommendations for Upgrading of Concrete Structures with Use of Continuous Fiber Sheets*, published from the Japanese Society of Civil Engineers, 2001
7. *Externally Bonded FRP Reinforced for RC Structures,* published by the International Federation for Structural Concrete (fib), 2001

Although these guidelines were developed by different organizations from different countries, their approaches to specifying composite material properties for design are similar. Current design guidelines for FRP strengthening typically use a certain percentile of experimental results or manufacturer reported mean properties to specify FRP material properties for design (Atadero, 2006). Among the various guidelines considered for this study, the main similarity is that they generally disregard the time-dependent degradation of the tensile modulus and use the mean value as the design value of modulus. Some of the guidelines use modulus-specific safety factors to account for the property variability and degradation, but most of them generally use the mean modulus as a deterministic design variable. Overall, the guidelines have very similar approaches to define the design value for the ultimate tensile strength or ultimate tensile strain. Details related to some of

the major current guideline approaches to determine FRP design values for rehabilitation of concrete structures and the shortcomings of their approaches from the standpoint of reliability-based design are discussed briefly in this section.

2.1.1 Determination of Material Characteristic Values

The general approach of the aforementioned guidelines to determine a design value for FRP strength is to define a "characteristic" value. The characteristic value is specified as a certain percentile of test results. Instead of specifying a percentile, some of the guidelines use an equation similar to Eq. 2-1 from which the mean and standard deviation are used to define the characteristic value.

$$x_c = \mu_x - n\sigma_x \qquad \textbf{Eq. 2-1}$$

where μ_x and σ_x are the mean value and standard deviation of the test results or manufacturer reported data for property x, respectively, and n is a guideline-specific factor for property x. The characteristic value can also be expressed in terms of the coefficient of variation (COV) as shown in Eq. 2-2 (Atadero, 2006):

$$x_c = \mu_x \left[1 - n\left(COV_x\right)\right] \qquad \textbf{Eq. 2-2}$$

where x_c is the characteristic value of a particular property x.

The approach described above provides for a specified probability that the FRP strength will fail (i.e. fall below the "characteristic" value). For example, selecting the lower 5^{th} percentile as the characteristic strength means that the FRP has a 5% probability of failure. An increase in the value of n, as used in Eq. 2-1, decreases the probability that the FRP strength will fail below the characteristic strength. A summary of different values of n used in some of the existing design guidelines is provided in Table 2-1. Details related to some of the guidelines described in Table 2-1 will be discussed in the following sections.

Table 2-1. Different Values of n Used to Specify the Characteristic Value for FRP Tensile Strength

Guideline	n	n Specified or Calculated
ACI 440 (ACI, 2002)	3	Specified
TR 55 (The Concrete Society, 2000)	2	Specified
CHBDC (CSA, 2006)	1.64	Calculated from 5th percentile
Täljsten (2002)	1.64	Calculated from 5th percentile
ISIS Canada (Neale, 2001)	3	Specified
Japanese (Maruyama, 2001)	3	Specified
fib (International, 2001)	1.64	Calculated from 5th percentile

Among the above guidelines listed in Table 2-1, some use a certain percentile instead of a value of n factor to define their characteristic values. However, for the purpose of direct comparison of the different guidelines, a normal distribution was used to determine the

equivalent value of n to the specified percentile. Since unidirectional FRP materials are generally assumed to have linear-elastic behavior, the above equations would also apply to the ultimate tensile strain, assuming that the modulus is a constant value.

2.1.2 Consideration of Time-Dependent Property Degradation

After the characteristic value is determined following a specific guideline, additional factors are applied to further reduce the characteristic design value to the final design value. These additional factors are guideline-dependent and in some cases are intended to account for long-term degradation of FRP material properties due to environmental effects and fatigue and sustained loading (Atadero, 2006). The current design guidelines typically use a reduction factor to account for material degradation due to environmental effects. The general approach to consider the effects of fatigue and sustained loading is to provide limits on the FRP material stress. Among the guidelines discussed above, three design guidelines, ACI 440 (2002), TR 55 (The Concrete Society, 2004), and CHBDC (2006), are selected to give a comprehensive insight of use of FRP materials and to illustrate how the effects of time-dependent degradation behavior is considered in the determination of the FRP design values in these design guidelines.

2.1.2.1 ACI 440

ACI 440 (2002) suggest that the design ultimate strength, f_{fu}, be determined by modifying the characteristic design strength, f_{fu}^{*}, by an environmental reduction factor, C_E, such that:

$$f_{fu} = C_E f_{fu}^{*} \qquad \textbf{Eq. 2-3}$$

where the characteristic design strength is as follows:

$$f_{fu}^{*} = \left(\overline{f}_{fu} - 3\sigma\right) \qquad \textbf{Eq. 2-4}$$

where $\overline{f}_{fu}$ is the mean ultimate strength and σ is the standard deviation of the test population. The environmental reduction factor, C_E, used in ACI 440 (2002) is specifically intended to consider the long-term degradation of FRP ultimate strength. The factor is selected based on the type of fiber and the type of exposure environments. Environmental factors for various fiber types and exposure levels are shown in Table 2-2.

Table 2-2. Environmental Reduction Factor Used in ACI 440 (2002)

Exposure Level	Fiber Type	Environmental Reduction Factor, C_E
Interior Exposure	**Carbon**	0.95
	Glass	0.75
	Aramid	0.85
Exterior Exposure (i.e. bridges and piers)	**Carbon**	0.85
	Glass	0.65
	Aramid	0.75
Aggressive Environment (i.e. chemical plants and waste treatment plants)	**Carbon**	0.85
	Glass	0.50
	Aramid	0.70

ACI 440 (2002) accounts for fatigue and sustained loading by imposing a stress limitation. This limit is expressed as a percentage of the ultimate design strength of the FRP: a stress limit of 55% for carbon, 20% for glass, and 30% for aramid fiber reinforced FRP composites.

2.1.2.2 TR 55

Many other design guidelines do not use a specific factor for material degradation but include partial factors to reduce the material properties to account for the degradation throughout the expected FRP lifetime. TR 55 (The Concrete Society, 2004) uses partial factors that are dependent on the fiber type and the method of manufacture and application of the composite. Individual partial factors are included for ultimate modulus and strain, as shown in Table 2-3.

Table 2-3. Partial Factors for Modulus and Strain Used in TR 55 (2004)

Material	Partial Factor for Modulus, γ_E	Partial Factor for Strain, γ_ε
Carbon FRP	1.1	1.25
E-Glass FRP	1.8	1.95
Aramid FRP	1.1	1.35

An additional set of partial factors is intended to consider the effects of various composite manufacturing methods and applications and is shown in Table 2-4.

Table 2-4. Partial Factors for Method of FRP Manufacture and Application

FRP Application	FRP Processing Type	Partial Factor, γ_{mm}
Plates	**Pultruded**	1.05
	Prepreg	1.05
	Preformed	1.1
Sheets of Tapes	**Machine-Controlled Application**	1.05
	Vacuum Infusion	1.1
	Wet Layup	1.2
Prefabricated Shells	**Filament Winding**	1.05
	Resign Transder Molding	1.1
	Hand Layup	1.2
	Hand Sprayup	1.5

The ultimate design properties are calculated as:

$$P_{fd} = \frac{P_f}{\gamma_{mP}} \quad \textbf{Eq. 2-5}$$

where

$$\gamma_{mP} = \left(\gamma_{mE} \text{ or } \gamma_{m\varepsilon}\right) \times \gamma_{mm} \quad \textbf{Eq. 2-6}$$

where the subscript P represents the property of interest, modulus or strain, P_f is the characteristic value, γ_{mP} is the final factor, calculated as the product of the two sets of partial factors. The design tensile strength is calculated from the design modulus and strain following Hook's Law, as shown in Eq. 2-7.

$$f_{fd} = E_{fd} \cdot \varepsilon_{fd} \quad \textbf{Eq. 2-7}$$

For example, the resulting factors of the tensile strength for pultruded strips can be determined as 1.5 for carbon FRP, 3.9 for E-glass FRP, and 1.6 for aramid FRP. These factors are intended to account for time-dependent degradation behavior due to environmental effects. Similar to ACI 440, TR 55 has a stress limit on the FRP stress due to service loads to prevent stress rupture and a different limit on the maximum stress to prevent fatigue failure, as shown in Table 2-5 (The Concrete Society, 2004).

Table 2-5. Stress Limits on Sustained and Fatigue Loading Used in TR 55 (2004)

Fiber Type	Stress Limit on Sustained Loading	Stress Limit on Fatigue Loading
Carbon	65%	80%
Glass	55%	30%
Aramid	40%	70%

2.1.2.3 CHBDC

The Canadian Highway Bridge Design Code (CHBDC) outlines changes in material durability from a previous edition and considers environmental degradation based on research results which best describe Canadian conditions (CHBDC, 2006). Material factors are different in magnitude and method of application than in ACI 440 (2002), especially in the case of carbon fiber. Details related to various application types considered by CHBDC can be found from Tables 16.5.3 and C16.5.3 (b) (CHBDC, 2006), separating type of fiber and type of environmental exposure. The overall resistance safety factor for FRP materials, ϕ_{FRP} , is the product of an environmental factor, C_E, and a production material factor, ϕ_{pul} and ϕ_{hl} for factory and field-produced FRP materials, respectively. The production material factors used are shown in Table 2-6.

Table 2-6. CHBDC material safety factors by fiber type and method of production

Fiber Type	ϕ_{pul}	ϕ_{hl}
AFRP	0.8	0.6
CFRP	0.8	0.6
GFRP	0.8	0.6

Environmental factors in CHBDC vary with averages of 0.64, 0.95, and 0.66 for aramid, carbon, and glass fibers respectively, depending on the type of environmental exposure to which they are subjected. Carbon fibers were used as the basis for the determination of factors and a value of 0.95 was set based on the statistical variation in the results (CHBDC, 2006). Thus, the overall material resistance factor used in design is the product of the production material factor and the environmental factor, resulting in different resistance factors for different production types (factory or field) and environmental conditions. For the case of prefabricated carbon FRP, as would be used for the current research, the resistance factor, ϕ_{FRP}, is 0.75.

2.1.3 Issues with the Current Design Guideline Approach

The previous sections illustrate a few examples of the many ways design characteristic values are determined and safety factors, to account for environmental effects, and other time-dependent degradation behavior are used in current FRP design guidelines. In the context of reliability-based design and analysis, it is important to recognize the presence of uncertainty in the design and analysis of engineering systems (Haldar, 2000). However, the current approaches simplify the problem by considering the

uncertain parameters to be deterministic and accounting for the uncertainties, such as material variability and environmental effects, thorough the use of empirical safety factors. Safety factors are derived based on past experience but do not absolutely guarantee safety or satisfactory performance. Also, they do not provide any information on how the different parameters of the system contribute to the safety of the system. Therefore, it is difficult to design a system with a uniform distribution of safety levels among the different components using empirical safety factors. In reality, the failure probability may vary from a low to an intolerably high value for the same value of safety factor (Dai, 1992). For this reason, the current design approaches do not satisfy the requirements for reliability and are not adequate from the standpoint of reliability-based design.

The current approach described above to determine characteristic values such as those recommended by ACI 440 (2002) and TR 55 (2004) where a number of standard deviations are subtracted from the mean ultimate material properties has an undesirable statistical implication for FRP materials in a reliability-based design. The method described above for determining the characteristic design strength provides for a certain probability that the FRP strength will fail, provided that a composite strength below the design characteristic strength is considered to have failed. The intent of the method used in the current guidelines is to fix the probability of structural failure by fixing the probability that the composite falls below the characteristic value. This approach neglects the fact that the reliability of a structure is determined by the interaction of load and resistance, not by resistance alone and therefore results in an undesirable design

consequence. For example, a larger standard deviation directly correlates to a smaller characteristic design value. When determining how much material to use for a given design project, a smaller characteristic value would imply that a greater amount of material should be used. The final outcome of using a smaller characteristic value is a design with a larger margin of safety due to the use of a greater amount of material. Using a larger characteristic value, then, relates to a smaller margin of safety but represents a material manufactured with more precision. When using characteristic values determined in this manner with differing standard deviations in a reliability-based design or when calibrating a reliability based design guideline, further complications arise (Atadero, 2006). The use of a material with a greatly penalized design value increases the structural reliability index. The opposite is true for materials with higher design values, penalizing those with lower variability, or higher quality controlled products (Atadero, 2006).

Some of the guidelines discussed above do not consider the specific environment to which the FRP will be exposed in service. Prediction of time-dependent property degradation cannot be accurate without sufficient knowledge of the exposure environment. More importantly, these guidelines do not explicitly consider the required service life of the strengthened material or system. Often, strengthened structures are not expected to have a lifetime equivalent to that of new construction. Thus, knowledge of the expected service life of strengthening is important to predict the amount of material degradation that could occur during the expected lifetime. Factors developed without

explicitly considering the environmental and service life demands on the strengthening are likely to be highly conservative or inaccurate in most cases.

Based on the aforementioned shortcomings, the current design approach is considered to be inadequate for use with reliability-based design procedures. Thus, reliability-based design methodology which considers the statistical nature of the design related parameters, including the material, loading, and geometric properties, is needed, so that reliability of a material or structure can be determined at the design stage.

2.2 Reliability-Based Approach for FRP Design Values

In the context of reliability-based design and analysis, reliability-based properties refer to material properties that are characterized as random variables, not as deterministic properties (Haldar, 2000). The determination of the statistical descriptors and probability distributions of the random variables describing material properties is a crucial step towards the characterization of such random variables and therefore plays an important role in determining reliability-based design values (HDBK-MIL17, 2002).

2.2.1 Probabilistic Model for FRP Tensile Properties

In composite design, tensile property data for unidirectional composites are obtained from experimental tests and aid the material selection and design. When modeling experimental data, statistical distributions are typically used to describe the

tensile properties of composite specimens. The selected probability distribution that represents the material property data has a significant effect on the estimated strength and the calculated reliability of a structural component (Ellingwood, 1994).

Among many other statistical distributions that are commonly used in engineering, the Weibull distribution is widely used to predict the strength of composite materials (King, 1986). Compared to the Normal distribution which is predominantly used for traditional metallic structural materials, the Weibull distribution is more flexible and suitable and has been very successful in predicting the strength of composite materials (Bury 1999). In order to study the use of the Weibull distribution in FRP material characterization, it is important to understand the fundamental theory upon which the distribution is based. The statistical theories developed to describe the strength behavior of brittle materials are often generically classified as weakest link theory (Sutherland 1997). A composite material is made of a large number of small fibers whose properties, dimensions, and initial flaws can only be described realistically by a probabilistic approach. Thus, the purpose of the probabilistic theory of the strength of composite materials is to predict the strength related properties considering the probability of failure of a given component of such materials under a prescribed loading.

For the purposes of the current investigation, the use of the Weibull distribution will be proposed for the determination of reliability-based FRP characteristic values and details related to the validation of using the Weibull distribution over other common

distributions and the procedure to determine the Weibull design values will be further discussed in the following chapters.

2.2.2 Reliability-Based Approach for Consideration of Time-Dependent Degradation

The proposed approach to consider the material degradation for the determination of FRP design values in the current research is based on a service life evaluation of the FRP strengthening. Since the material is expected to ensure safety of the rehabilitation over the service life of the structure, it is essential that design values be chosen considering not just the variation in value around the mean of the characteristic, but also the performance degradation of the property under consideration that would take place due to anticipated environmental exposure. To this end, with a known value of expected service life, the mean value of a material property can be predicted using predictive equations of material degradation derived using experimental accelerated aging procedures. Application of the experimentally determined environmental factors allows the material property values to be calculated accurately for reasonable levels of expected service life. These design values can then be used in design with sufficient confidence that the value of the material will not fall below the expected threshold during the lifetime of the strengthening.

2.3 Reliability-Based Design for FRP Rehabilitation

FRP materials have been increasingly used in combination with concrete structures for a number of years for strengthening existing bridge girders through external bonding. However, the increased use of FRP materials has been hindered by the lack of established design standards (Chambers, 1997). Therefore, the need for FRP composites to have a design standard for rehabilitation of concrete structures is apparent. In order to be compatible with design codes for other common construction materials, this standard must be based on probabilistic design and analysis. A load and resistance factor design (LRFD) format would facilitate their use in civil infrastructure by providing a basis for structural design that is comparable with existing LRFD standards for other civil materials, such as the AASHTO LRFD Highway Bridge Design Code (2004) and the American Institute of Steel Construction Code (AISC LRFD, 2004; Ellingwood, 2003). The development of a design standard for FRP materials similar to those of concrete and steel utilizing LRFD method has been the focus of current and ongoing research (Okeil et al., 2002; Atadero, 2006; Zureick et al., 2006). The basis of these codes based on LRFD is the use of load and resistance factors such that final designs meet predetermined target reliabilities which can be related to a predetermined and acceptable probability of failure of a structure (Ellingwood, 2003). Due to the fact that the conceptual basis for LRFD is founded in classical reliability theory, the LRFD based design can be interchangeably termed as a reliability-based design and this term will be used for this study.

2.3.1 Consideration of Design Uncertainties

In many fields of engineering, it is important to understand the presence of uncertainty in the analysis and design of engineering systems. A primary goal of structural design is to create a structure such that the resistance capacity is greater than the load demands acting on it. This can be complicated by design related uncertainties since, in their presence, resistance and load cannot be described by deterministic quantities. Instead, uncertainties result in a range of possible resistance and load values and introduce the possibility that the applied load will exceed the capacity of the structure. To illustrate the relation between load and resistance, the most basic situation, where a single resistance variable acts against a single load variable, is shown in Figure 2-1.

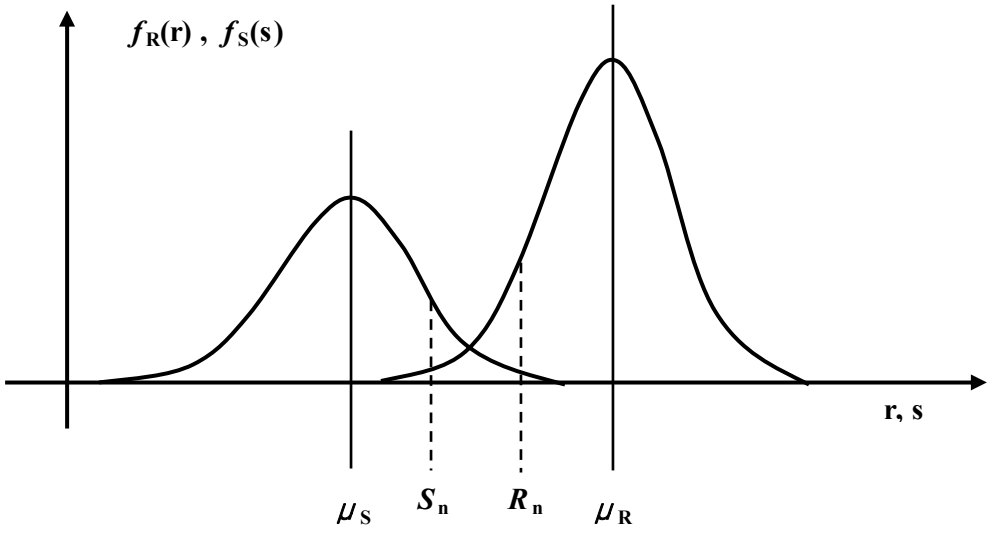

Figure 2-1. Basic Structural Reliability Problem

In the above figure, the uncertainty in the resistance, R, and the load effect, S, are represented by probability density functions $f_R(r)$ and $f_S(r)$, respectively, μ_S and μ_R

are the mean of the load and resistance, respectively, and S_n and R_n are the nominal load and capacity used for design, respectively. The nominal value is determined according to the design procedure in use. In traditional deterministic design, a safety factor would be calculated as the ratio of the nominal resistance to the nominal load. However, since they do not account for the full distributions of load and resistance, safety factors determined in this manner do not provide an accurate assessment of design safety (Melchers, 1999; Haldar, 2000). The structural system whose load and resistance curves are shown in Figure 2-1 will fail if the load effect exceeds the resistance of the system. As can be seen from Figure 2-1, the probability of failure will change as the relative position of the two distributions changes, as the amount of spread in one or both of the distributions changes, and as the shape of the distributions changes (Madsen et al., 1986). The distribution parameters are significantly dependent on the type of probability distributions selected to describe the load and resistance variables. Therefore, it is essential to select the most appropriate distribution to describe the variable of interest and to use the corresponding distribution parameters to account for design uncertainties.

2.3.2 Basic Reliability Methodology

The fundamental aspect of structural reliability is to use statistical knowledge of uncertainties to compute the probability of structural failure (Melchers, 1999). The method used to make decisions regarding reliability design of a structure can often be formulated as follows:

$$R = P\ [\text{strength}(r)\ \geq\ \text{stress}(s)] = P\ [g(r,s) \geq 0] \qquad \textbf{Eq. 2-8}$$

where R is reliability, $P[.]$ is probability, r is a vector of the design parameters affecting design strength, s is a vector of the design parameters affecting applied stress, and $g(r,s)$ is called the limit state function. The limit state of failure surface is defined as the boundary between "safe" and "failure" regions in the design parameter space; i.e.

$$g(r,s) = 0 \qquad \textbf{Eq. 2-9}$$

Then g(r,s) > 0 is the safe state, and g(r,s) < 0 is the failure state, and the probability of failure is given by:

$$P_f = P\ [g(r,s) < 0] \qquad \textbf{Eq. 2-10}$$

In the most general case, load and resistance may be correlated random variables, and in order to evaluate the probability of limit state failure, the joint probability density function (PDF), $f_{RS}(r,s)$, is required. Figure 2-2 shows contour lines of a general joint PDF.

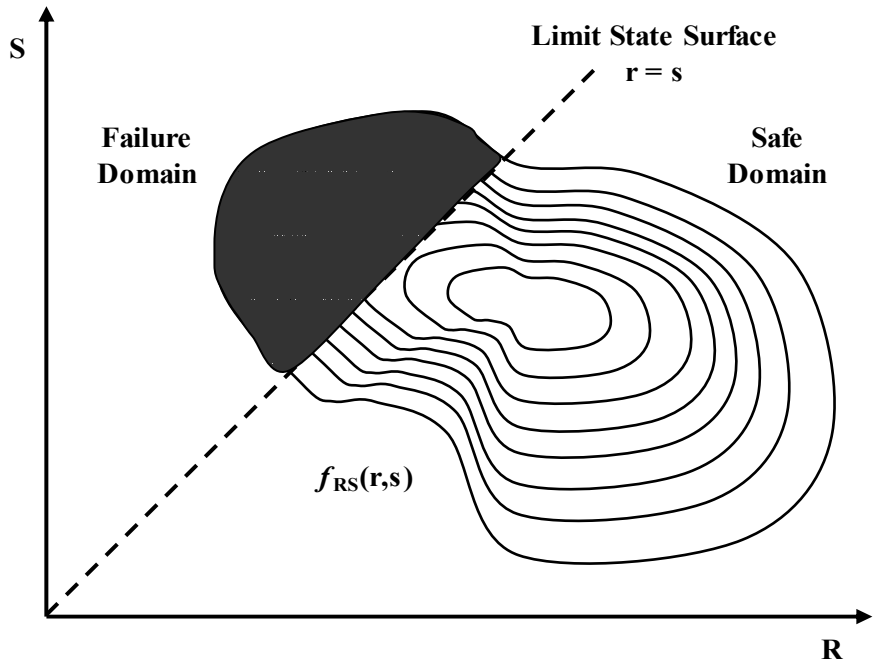

Figure 2-2. Graphical Representation of Limit State Function and Probability of Failure (Dai, 1992)

The area of the joint PDF shaded in grey, as shown in Figure 2-2, represents the values for R and S where the limit state function is violated. In order to calculate the probability of failure, integration must be used to compute the total volume of probability under the joint PDF. This integral is expressed in Eq. 2-11.

$$P_f = \iint_{g()\leq 0} f_{RS}(r,s)drds \qquad \textbf{Eq. 2-11}$$

Eq. 2-11 may be generalized to account for as many as random variables as are present in the problem by using the joint PDF for all variables. In general, obtaining a joint PDF for

all variables is very difficult and thus a reliability method is often used to estimate the reliability.

2.3.3 Reliability Methods Used for the Thesis

The reliability of a structure strengthened with FRP materials, where the interaction between the load and resistance variables is more complicated than that of a material system, will be evaluated in Chapter 7. The reliability of the strengthened structure is the probability that the structure will not fail, or more accurately, reach a limit state (Melchers, 1999). The reliability index, denoted by the symbol β is often used as a substitute for the probability of failure and thus a measure of reliability. β may be used to compare different structural systems and can be used as the target in reliability-based design without mentioning a specific probability of failure. In order to accurately assess the reliability of the structure for a prescribed limit state, it is important to use an appropriate method to determine the reliability index.

The purpose of this section is not to provide a comprehensive literature review of currently available reliability methods to compute β, but to provide detailed background of the reliability method used for the current research. The method chosen for the current investigation is a hybrid reliability approach using a first-order reliability method (FORM) and Monte Carlo Simulation (MCS) as used by Plevris (Nowak, 1999; Rackwitz and Fiessler, 1978; Plevris, 1995; Atadero, 2006). MCS was used to evaluate the mean and standard deviation of the resistance, and then FORM was used to compute the reliability index. MCS was chosen for several reasons: it is very robust, generally simple

to implement, can accommodate many variables without convergence concerns, and more importantly can directly assess structural reliability (Atadero, 2006). This procedure is consistent with the methods that described in the National Cooperative Highway Research Program (NCHRP) Report 368, "Calibration of the LRFD Bridge Design Code", by Nowak (1999). This approach is chosen due to the fact that it offers a higher level of accuracy than some approximate methods, while remaining simple to implement (Atadero, 2005). The method was used for the calibration of the ASSHTO LRFD code for bridges (AASHTO, 2004) and therefore is appropriate for use in assessing the structural reliability for FRP strengthening of concrete bridges.

The reliability index in this method is based on the load and resistance distributions, S and R respectively, their means μ_S and μ_R, standard deviations, σ_S and σ_R, and the coefficient of variation of resistance, COV_R defined as:

$$COV_R = \frac{\mu_R}{\sigma_R} \qquad \textbf{Eq. 2-12}$$

It is assumed that the resistance variable, R, can be described by a Lognormal distribution and the load variable, S, is modeled by a Normal distribution (Atadero, 2006; Wilcox, 2008).

Given the required information of load and resistance distributions, MCS is used as described in Section 6-6 to determine the mean and standard deviation of resistance of the structural system. The essential steps of this procedure are described below.

(i) Assume that the resistance design point, R^*, can be estimated as:

$$R^* = \mu_R \left(1 - k \cdot COV_R\right) \qquad \textbf{Eq. 2-13}$$

where k is the unknown constant. To start the iteration, k is assumed to be 2 for this investigation as suggested by Nowak (1999) as a good starting point.

(ii) The standard deviation and mean of the normal distribution used to approximate the non-normal distribution for resistance at the design point, R^*, can be approximated as:

$$\sigma'_R = \frac{\varphi\left\{\Phi^{-1}\left[F\left(R^*\right)\right]\right\}}{f\left(R^*\right)} \qquad \textbf{Eq. 2-14}$$

$$\mu'_R = R^* - \sigma'_R \cdot \Phi^{-1}\left[F\left(R^*\right)\right] \qquad \textbf{Eq. 2-15}$$

where $F(\ )$ and $f(\ )$ are the cumulative distribution function and probability density function, respectively, of the non-normal distribution that is being approximated. $\Phi(\ )$ and $\varphi(\ )$ are the standard normal cumulative and density functions, respectively.

(iii) For the lognormal distribution of resistance, the cumulative density function, $F(\ )$ and probability density function, $f(\ )$, of the design point, R^*, can be expressed as:

$$F_{\mathrm{R}}\left(R^*\right)=\Phi[\alpha] \qquad \textbf{Eq. 2-16}$$

$$f_{\mathrm{R}}\left(R^*\right)=\frac{\varphi[\alpha]}{COV_{\mathrm{R}}\cdot R^*} \qquad \textbf{Eq. 2-17}$$

where

$$\alpha=\frac{\ln R^*-\ln \mu_{\mathrm{R}}}{COV_{\mathrm{R}}} \qquad \textbf{Eq. 2-18}$$

(iv) Based on $F_{\mathrm{R}}\left(R^*\right)$ and $f_{\mathrm{R}}\left(R^*\right)$, the transformation equations of step (ii) can be simplified to:

$$\sigma'_{\mathrm{R}}=COV_{\mathrm{R}}\cdot R^* \qquad \textbf{Eq. 2-19}$$

$$\mu'_{\mathrm{R}}=R^*-\alpha\cdot\sigma'_{\mathrm{R}} \qquad \textbf{Eq. 2-20}$$

(v) The reliability index can now be calculated using the distribution parameters of the load and resistance variables at the design point, R^*, as:

$$\beta = \frac{\mu'_R - \mu_S}{\sqrt{\sigma'^2_R - \sigma^2_S}} \qquad \textbf{Eq. 2-21}$$

Eq. 2-21 can be extended as:

$$\beta = \frac{R^* - \alpha \cdot COV_R \cdot R^* - \mu_S}{\sqrt{\left(COV_R \cdot R^*\right)^2 + \sigma^2_S}} \qquad \textbf{Eq. 2-22}$$

(vi) From here, the new design point can be determined as:

$$\hat{R}^* = \mu'_R - \frac{\beta \cdot \left(COV_R \cdot R^*\right)^2}{\sqrt{\left(COV_R \cdot R^*\right)^2 + \sigma^2_S}} \qquad \textbf{Eq. 2-23}$$

(vii) If this new design point, $\hat{R}^*$, matches the initial design point, R^*, assumed in step (i), the computation is complete and β is as calculated in step (v). If they do not match, one is required to go back to step (iv) with the new design point, $\hat{R}^*$, and continue the iteration.

For ease of computation, the above procedure can be automated through the use of a difference term comparing the initial and new design points as:

$$R_{ERR} = \left(R^* - \hat{R}^*\right)^2 \qquad \textbf{Eq. 2-24}$$

For the purposes of this investigation, convergence is assumed to be achieved when the error between the design points, R_{ERR}, is within an acceptable tolerance. A tolerance can be evaluated for each application depending on how much accuracy of the estimated reliability is desired for calibration purposes. For the purposes of this investigation, the tolerance is assumed to be 1.0×10^{-10} as used in previous research (Wilcox, 2008). Details related to the application of this reliability method to reliability analysis of a strengthened girder will be further discussed in Chapter 7.

Chapter 3. Characterization of Composite Properties for Reliability-based Design

This chapter provides detailed discussions on testing and material used for the current research and discusses the incorporation of the durability test data from previous research (Yang and Karbhari, 2008). Special attention is given to the statistical treatment and analysis of data as a means for statistical characterization of FRP materials.

3.1 Materials and Test Methods

3.1.1 Description of Materials

The materials chosen for the purposes of this investigation were prefabricated FRP strips and the associated adhesives. These were obtained from three different suppliers; SIKA, SCCI, and Fyfe Co. All strips were of carbon fiber reinforced epoxy and were fabricated by the pultrusion or pullforming processes. Details related to the strips and adhesives are given in Table 3-1 and Table 3-2, respectively.

Table 3-1. Details of Prefabricated Unidirectional Strips (Manufacturer Reported Data)

Characteristic	SIKA	SCCI	Fyfe Co.
Designation	S-512	CS-02	Tyfo UC75
Fiber Volume Fraction [%]	> 68%	-	62%
Density [g/cm^3]	1.6	-	-
Tensile Modulus [N/mm^2]	> 165,000	-	155,000
Tensile Strength [N/mm^2]	3,050	-	2,790
Ultimate Strain [%]	1.7	-	1.8

Table 3-2. Details of Adhesive Systems (Manufacturer Reported Data)

Characteristic	SIKA	SCCI	Fyfe Co.
Designation	Sikadur 30	-	Tyfo TC Epoxy
Viscosity [cps]	Non-sag paste	-	46,000
Gel Time [minutes]	70	-	58
7-day Compressive Strength [MPa]	59.3	-	-
7-day Tensile Strength [MPa]	24.8	-	-
7-day Tensile Modulus [MPa]	4,482	-	-
12-day Elongation at Break [%]	1	-	-
14-day Shear Strength [MPa]	24.8	-	-
2-day Bond Strength (Dry Cure) [MPa]	22.0	-	-

Each of the strips was a unidirectional carbon/epoxy and the adhesive was a two-part epoxy system with high solids content. These material systems were chosen due to the fact that they were commercially available and already being used for FRP strengthening of concrete structures.

3.1.2 Characterization Procedures

All materials considered in the study were extensively characterized through mechanical testing, and assessment of fiber volume fraction in the case of the FRP strips. In order to develop equations for time and environment related deterioration, tests were also conducted at routine intervals after immersion of the materials in deionized water at 23 ˚C, 37.8 ˚C, and 60 ˚C, and in a 5% NaCl solution (simulating sea water at 23 ˚C), and in a concrete based alkali solution (with a pH of 12 at 23 ˚C). As will be discussed later much larger sets were used for the initial tests with only 5 repetitions being used to characterize deterioration trends. It is noted that the level of repetition chosen meets the requirements of ASTM specifications. Details related to durability testing are given in Yang and Karbhari (2008).

3.1.2.1 Tensile Testing

In order to account for the higher loads required to test carbon/epoxy composites, tabs were used to ensure uniform load introduction, protect the specimen from damage by high pressure grips of the loading device and to reduce high stress concentrations at the grips, which could cause premature failure. Glass/epoxy tabs were used and they have been most commonly used for tensile specimens (Adams, 2003). The tapered tabs were bonded to the full width of the composite strips from which individual specimens were later cut to the specified size.

In order to minimize possible misalignment and provide sufficient compressive pressure during bonding, typical compression tabbing jigs were used. Prior to the bonding of tabs, the bonding surfaces of the specimen strips as well as the tab surfaces were lightly roughened and cleansed with acetone to remove any remaining loose particles for a better contact surface. SIKADUR 30, a two-part adhesive system supplied from SIKA, was applied to the bonding surfaces of both the specimen and the tabbing strips. Care was taken to keep bond lines of uniform thickness. Then, the assembly was ambient cured under pressure for 24 hours followed by post-curing for 6 hours at 55 ˚C. The tabbed strip was then cut into individual specimens, using a diamond tip saw, having 12.7 mm (0.5 in) width and 254 mm (10 in) length. A schematic showing coupon dimensions for the tensile specimens from the prefabricated strips are shown in Figure 3-1.

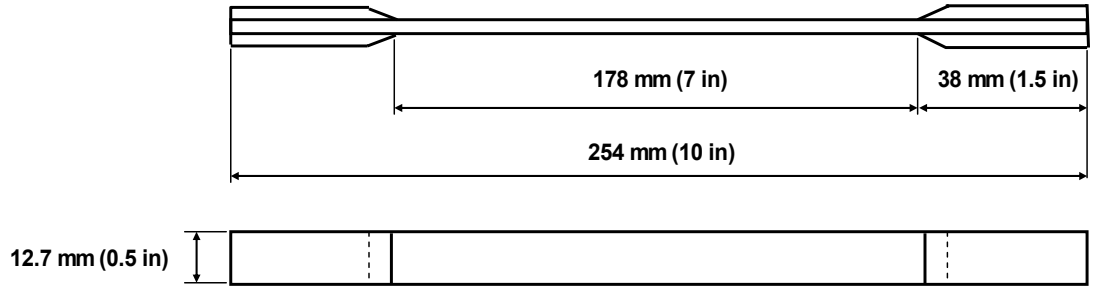

Figure 3-1. Tensile coupon dimensions.

It should be noted that specimens exposed to the aforementioned environmental exposures were not tabbed so as to avoid failures and changes at the adhesive and tab-specimen interface level.

Prior to testing, width and thickness measurements were taken at three different locations along the gage length of each specimen. The prefabricated strip specimens were tested at a strain rate of 2mm/min until failure following ASTM D3039 (ASTM, 2005). Displacement was measured using a clip-on extensometer. The tensile modulus was determined by fitting a straight line to the stress versus strain data over the range from 0.1 to 0.3 percent strain, as recommended by ASTM D3039 (ASTM, 2005). For all tensile samples, the stress versus strain curve was linear until the maximum load was reached, and therefore the strain-to-failure was calculated from the ultimate stress and elastic modulus.

3.1.2.2 Determination of Fiber Volume Fraction

Fiber volume fraction is the ratio of the volume of fiber to the volume of the composite. The tensile strength and modulus of composites are strongly dependent on the fiber volume fraction, and therefore this parameter is a very important measure of such materials. The fiber volume fraction of a composite may be determined by acid digestion and the burn-off technique. The two common methods are standardized as ASTM D3171 (ASTM, 2005) and ASTM D2584 (ASTM, 2005), respectively. For carbon fiber reinforced polymer (CFRP) composites, the burn-off method is not applicable since carbon (as opposed to glass fibers) is not resistant to oxidation at the temperatures required to burn off the matrix (typically 500 to 600˚C) (Adams, 2003) and therefore the acid digestion method was used. Prior to testing, three specimens for each of the three material systems were cut from the FRP strips. Each test specimen was cut to

approximately 12.7 mm (0.5 in) by 12.7 mm (0.5) and the mass of the specimen was less than 1 gram as recommended by ASTM D3171 (ASTM, 2005). Concentrated nitric acid was used to dissolve the epoxy matrix of the carbon/epoxy composite. After the matrix was dissolved, the fibers were weighed, and the weight of the matrix was also determined. From the weights of the fibers and matrix (W_f and W_m), and their known densities (ρ_f and ρ_m), the fiber volume fraction, V_f, is determined as

$$V_f = \frac{\rho_m W_f}{\rho_f W_m + \rho_m W_f} \qquad \textbf{Eq. 3-1}$$

where it is assumed that the void content of the composite is negligible since these are prefabricated using a highly controlled, automated process.

3.2 Statistical Characterization

Statistical methods for obtaining probability-based properties from composite material test data are discussed herein. In the context of reliability-based design and analysis, probability-based properties refer to material properties that are characterized as random variables, not as deterministic properties (HDBK-MIL17, 2002). The determination of the statistical descriptors and probability distributions of the random variables describing material properties is a crucial step towards the characterization of such random variables and therefore plays an important role in determining probability-based design values.

Variability in composite material property data may result from a number of sources, such as batch-to-batch variability of raw materials, testing variability, and inherent materials variability. Although the characterization of all the sources of variability is not practical, it is clear that the identification of as many sources of variability as possible and the incorporation of such variability in material design values are desired. Details related to statistical methods, including data normalization, outlier analysis, determination of statistical distribution, and goodness-of-fit testing, are discussed. With use of the statistical methods, procedures for determining probability-based material properties can account for some, but not all, of these sources of variability.

3.2.1 Description of Experimental Data Sets

Each of the three material systems, SIKA, SCCI, and FYFE, consists of a number of tensile specimens tested in accordance with ASTM D3039 (ASTM, 2005). Due to the geometric constraint of the compression tabbing jigs from which only a limited amount of specimens can be produced, different number of sets consisting of different number of specimens were obtained: 4 sets with a total of 35 specimens for SIKA, 4 sets with a total of 36 specimens for SCCI, and 5 sets with a total of 36 specimens for FYFE. A summary of the data sets is given in Table 3-3, which gives the sample size and statistics of the experimental data.

Table 3-3. Summary of Prefabricated FRP Strips Data Sets

Material System	Materials	Data Set	Number of Samples	
			Per Set	Total
SIKA	Carbon/Epoxy	SIKA-1	8	35
		SIKA-2	9	
		SIKA-3	9	
		SIKA-4	9	
SCCI	Carbon/Epoxy	SCCI-1	9	36
		SCCI-2	9	
		SCCI-3	9	
		SCCI-4	9	
FYFE	Carbon/Epoxy	FYFE-1	7	35
		FYFE-2	7	
		FYFE-3	7	
		FYFE-4	7	
		FYFE-5	7	

3.2.1.1 Incorporation of Previous Durability Test Data

As discussed previously, the durability test data (Yang and Karbhari, 2008) were used in this research for the purpose of characterizing time-dependent degradation behavior of the composite materials. It is noted that the material systems used for the durability test are identical to that used for this current research. Although times at which the two tests were performed are different, considering that the material systems were prefabricated composites and maintained appropriately in a controlled laboratory environment, the following assumptions were made: (1) test-to-test material property variability is negligible, and (2) all of the data are obtained from the tests under identical conditions. With these assumptions made, the incorporation of the previous durability test data into the current research was validated.

For the durability tests, tensile tests were conducted following ASTM D3039. A minimum of 5 tensile specimens were prepared and tested at each exposure condition and time period, following the minimum sample size recommendation per ASTM D3039 (ASTM, 2005). The durability tensile specimens were immersed in five different exposure conditions: (1) deionized water at 23 °C, (2) deionized water at 37.8 °C, (3) deionized water at 60.0 °C, (4) a 5% NaCl solution at 23 °C, and (5) a concrete based alkali solution with a pH of 12 at 23 °C. An additional set of specimens was stored in 30 % relative humidity chamber as control (baseline) condition. The specimens were tested prior to the initiation of exposure and then at periods of 8, 24, 48, 72, and 96 weeks to obtain time-dependent degradation trends. The durability data were incorporated with the current data in order to determine predictive equations of material degradation using experimental accelerated aging procedures. Details related to the development of a degradation model will be discussed in Chapter 4. The durability test results are summarized in Table 3-4 through Table 3-12.

Table 3-4. Durability Experimental Data for Tensile Strength for SIKA FRP Strips

Condition	Exposure Level	Time [weeks]	Mean [MPa]	Standard Deviation [MPa]	COV	Minimum [MPa]	Maximum [MPa]
Control	Stored in a controlled humidity chamber at 30% RH and 23ºC	0	2833.87	71.98	0.03	2733.63	2901.05
		8	-	-	-	-	-
		24	2748.58	110.40	0.04	2588.53	2888.39
		48	2774.28	64.00	0.02	2696.80	2873.83
		72	2742.41	47.28	0.02	2697.38	2816.29
		96	2732.16	192.03	0.07	2500.81	2899.27
Immersed in Deionized Water	23 ºC	0	2833.87	71.98	0.03	2733.63	2901.05
		8	2693.99	198.22	0.07	2347.70	2814.98
		24	2671.56	155.95	0.06	2557.60	2849.29
		48	2451.22	50.06	0.02	2403.69	2525.52
		72	2271.35	138.78	0.06	2111.35	2458.01
		96	2266.99	114.33	0.05	2156.28	2441.57
	37.8 ºC	0	2833.87	71.98	0.03	2733.63	2901.05
		8	2406.85	61.53	0.03	2344.27	2489.67
		24	2397.23	198.86	0.08	2209.28	2690.10
		48	2161.33	77.62	0.04	2037.40	2240.32
		72	2134.92	178.62	0.08	1821.91	2264.01
		96	2144.96	84.92	0.04	2054.39	2276.09
	60.0 ºC	0	2833.87	71.98	0.03	2733.63	2901.05
		8	2236.87	185.55	0.08	2083.67	2535.23
		24	2164.40	201.72	0.09	2001.59	2496.91
		48	2017.46	52.68	0.03	1943.18	2073.35
		72	2054.63	104.92	0.05	1924.38	2207.44
		96	2010.15	91.85	0.05	1867.80	2121.17
Immersed in Alkali Solution	23 ºC	0	2833.87	71.98	0.03	2733.63	2901.05
		8	2170.09	34.02	0.02	2126.32	2209.59
		24	2189.21	90.56	0.04	2039.03	2279.45
		48	2001.43	65.24	0.03	1911.56	2059.18
		72	2079.80	97.91	0.05	1966.29	2191.91
		96	2047.11	57.48	0.03	1951.10	2097.37
Immersed in NaCl Solution	5% NaCl at 23 ºC	0	2833.87	71.98	0.03	2733.63	2901.05
		8	2437.17	222.31	0.09	2204.65	2666.12
		24	2430.91	310.19	0.13	1999.93	2726.75
		48	2335.08	35.97	0.02	2305.67	2376.92
		72	2225.00	150.81	0.07	2061.75	2370.40
		96	2169.99	64.63	0.03	2071.20	2227.86

Table 3-5. Durability Experimental Data for Tensile Modulus for SIKA FRP Strips

Condition	Exposure Level	Time [weeks]	Mean [GPa]	Standard Deviation [GPa]	COV	Minimum [GPa]	Maximum [GPa]
Control	Stored in a controlled humidity chamber at 30% RH and 23ºC	0	168.62	5.98	0.04	161.74	176.33
		8	-	-	-	-	-
		24	168.29	4.50	0.03	160.75	171.38
		48	169.39	3.67	0.02	164.29	173.63
		72	169.85	4.47	0.03	164.12	173.90
		96	169.76	6.57	0.04	159.20	177.37
Immersed in Deionized Water	23 ºC	0	168.62	5.98	0.04	161.74	176.33
		8	167.28	5.27	0.03	160.61	173.03
		24	160.40	14.90	0.09	143.21	169.56
		48	160.32	7.76	0.05	149.18	171.07
		72	159.53	4.74	0.03	152.96	164.87
		96	160.73	6.00	0.04	152.92	166.50
	37.8 ºC	0	168.62	5.98	0.04	161.74	176.33
		8	167.84	4.37	0.03	162.70	171.29
		24	160.84	10.08	0.06	150.98	176.35
		48	159.74	11.79	0.07	140.97	169.86
		72	153.30	3.51	0.02	149.59	158.43
		96	155.47	4.75	0.03	150.24	161.60
	60.0 ºC	0	168.62	5.98	0.04	161.74	176.33
		8	166.14	2.23	0.01	164.00	169.85
		24	157.23	2.24	0.01	155.03	160.01
		48	156.05	16.58	0.11	141.80	181.64
		72	152.04	3.61	0.02	149.23	158.25
		96	154.75	1.88	0.01	151.94	156.75
Immersed in Alkali Solution	23 ºC	0	168.62	5.98	0.04	161.74	176.33
		8	166.15	7.36	0.04	155.87	173.11
		24	161.51	10.35	0.06	151.91	177.61
		48	157.17	20.75	0.13	137.01	180.49
		72	158.53	6.58	0.04	147.37	164.22
		96	156.68	7.98	0.05	146.15	165.83
Immersed in NaCl Solution	5% NaCl at 23 ºC	0	168.62	5.98	0.04	161.74	176.33
		8	167.03	4.29	0.03	162.84	172.84
		24	165.23	8.47	0.05	154.79	178.15
		48	164.64	14.78	0.09	140.70	180.45
		72	158.95	6.75	0.04	152.47	167.68
		96	159.80	4.11	0.03	154.73	163.55

Table 3-6. Durability Experimental Data for Tensile Strain for SIKA FRP Strips

Condition	Exposure Level	Time [weeks]	Mean [mm/mm]	Standard Deviation [mm/mm]	COV	Minimum [mm/mm]	Maximum [mm/mm]
Control	Stored in a controlled humidity chamber at 30% RH and 23ºC	0	0.01683	0.00091	0.05	0.01550	0.01753
		8	-	-	-	-	-
		24	0.01634	0.00086	0.05	0.01510	0.01724
		48	0.01638	0.00043	0.03	0.01566	0.01679
		72	0.01615	0.00050	0.03	0.01565	0.01681
		96	0.01609	0.00080	0.05	0.01489	0.01689
Immersed in Deionized Water	23 ºC	0	0.01683	0.00091	0.05	0.01550	0.01753
		8	0.01611	0.00112	0.07	0.01426	0.01732
		24	0.01682	0.00267	0.16	0.01518	0.01990
		48	0.01533	0.00104	0.07	0.01405	0.01693
		72	0.01426	0.00122	0.09	0.01293	0.01558
		96	0.01413	0.00110	0.08	0.01307	0.01597
	37.8 ºC	0	0.01683	0.00091	0.05	0.01550	0.01753
		8	0.01435	0.00053	0.04	0.01374	0.01507
		24	0.01493	0.00122	0.08	0.01341	0.01629
		48	0.01359	0.00113	0.08	0.01245	0.01525
		72	0.01393	0.00114	0.08	0.01211	0.01513
		96	0.01380	0.00039	0.03	0.01343	0.01429
	60.0 ºC	0	0.01683	0.00091	0.05	0.01550	0.01753
		8	0.01346	0.00098	0.07	0.01263	0.01493
		24	0.01377	0.00134	0.10	0.01265	0.01596
		48	0.01304	0.00136	0.10	0.01128	0.01462
		72	0.01352	0.00079	0.06	0.01282	0.01471
		96	0.01299	0.00054	0.04	0.01210	0.01358
Immersed in Alkali Solution	23 ºC	0	0.01683	0.00091	0.05	0.01550	0.01753
		8	0.01308	0.00053	0.04	0.01247	0.01364
		24	0.01359	0.00094	0.07	0.01234	0.01439
		48	0.01291	0.00184	0.14	0.01129	0.01458
		72	0.01315	0.00101	0.08	0.01222	0.01470
		96	0.01308	0.00053	0.04	0.01231	0.01355
Immersed in NaCl Solution	5% NaCl at 23 ºC	0	0.01683	0.00091	0.05	0.01550	0.01753
		8	0.01462	0.00164	0.11	0.01296	0.01637
		24	0.01468	0.00135	0.09	0.01292	0.01647
		48	0.01427	0.00129	0.09	0.01317	0.01641
		72	0.01402	0.00109	0.08	0.01253	0.01506
		96	0.01359	0.00055	0.04	0.01266	0.01412

Table 3-7. Durability Experimental Data for Tensile Strength for SCCI FRP Strips

Condition	Exposure Level	Time [weeks]	Mean [MPa]	Standard Deviation [MPa]	COV	Minimum [MPa]	Maximum [MPa]
Control	Stored in a controlled humidity chamber at 30% RH and 23ºC	0	2767.57	103.77	0.04	2603.10	2861.06
		8	2625.16	114.08	0.04	2463.94	2732.97
		24	-	-	-	-	-
		48	2637.68	134.72	0.05	2492.07	2757.91
		72	2664.09	137.90	0.05	2504.95	2748.34
		96	2648.15	222.08	0.08	2252.95	2775.69
Immersed in Deionized Water	23 ºC	0	2767.57	103.77	0.04	2603.10	2861.06
		8	2755.70	96.94	0.04	2646.00	2869.08
		24	2589.57	249.81	0.10	2246.46	2799.40
		48	2595.09	108.73	0.04	2437.92	2686.31
		72	2675.04	16.77	0.01	2664.08	2699.90
		96	2671.78	110.65	0.04	2521.93	2788.27
	37.8 ºC	0	2767.57	103.77	0.04	2603.10	2861.06
		8	2793.97	112.22	0.04	2686.33	2947.18
		24	-	-	-	-	-
		48	2597.67	199.80	0.08	2293.55	2777.10
		72	2575.50	109.04	0.04	2469.62	2687.44
		96	2445.63	302.36	0.12	2031.27	2686.55
	60.0 ºC	0	2767.57	103.77	0.04	2603.10	2861.06
		8	2689.11	141.08	0.05	2479.73	2784.80
		24	-	-	-	-	-
		48	2563.93	80.39	0.03	2477.08	2686.00
		72	2282.07	140.47	0.06	2073.43	2446.58
		96	2211.93	161.12	0.07	2025.49	2383.66
Immersed in Alkali Solution	23 ºC	0	2767.57	103.77	0.04	2603.10	2861.06
		8	2562.18	171.94	0.07	2347.77	2759.58
		24	-	-	-	-	-
		48	-	-	-	-	-
		72	2506.78	146.79	0.06	2297.63	2693.08
		96	2507.22	50.38	0.02	2436.71	2572.39
Immersed in NaCl Solution	5% NaCl at 23 ºC	0	2767.57	103.77	0.04	2603.10	2861.06
		8	2698.44	133.76	0.05	2481.17	2821.72
		24	2694.91	231.05	0.09	2309.92	2871.29
		48	2694.05	182.68	0.07	2463.66	2867.87
		72	2651.13	50.28	0.02	2606.14	2711.42
		96	2659.46	66.72	0.03	2568.09	2750.93

Table 3-8. Durability Experimental Data for Tensile Modulus for SCCI FRP Strips

Condition	Exposure Level	Time [weeks]	Mean [GPa]	Standard Deviation [GPa]	COV	Minimum [GPa]	Maximum [GPa]
Control	Stored in a controlled humidity chamber at 30% RH and 23ºC	0	140.79	9.84	0.07	130.45	155.95
		8	142.05	6.92	0.05	133.18	150.09
		24	-	-	-	-	-
		48	140.32	7.78	0.06	131.34	145.14
		72	142.46	2.94	0.02	139.32	145.15
		96	140.90	3.70	0.03	136.98	146.23
Immersed in Deionized Water	23 ºC	0	140.79	9.84	0.07	130.45	155.95
		8	140.53	3.05	0.02	136.94	144.27
		24	135.29	5.11	0.04	129.80	139.93
		48	134.37	4.68	0.03	129.93	141.93
		72	132.95	5.93	0.04	126.67	140.53
		96	134.44	2.30	0.02	132.69	137.67
	37.8 ºC	0	140.79	9.84	0.07	130.45	155.95
		8	141.20	2.15	0.02	139.46	144.70
		24	-	-	-	-	-
		48	135.60	3.08	0.02	131.63	139.91
		72	133.90	5.30	0.04	126.72	141.02
		96	133.91	9.17	0.07	126.19	146.01
	60.0 ºC	0	140.79	9.84	0.07	130.45	155.95
		8	139.47	3.14	0.02	135.99	142.29
		24	-	-	-	-	-
		48	139.99	3.04	0.02	135.33	142.94
		72	133.82	2.71	0.02	129.51	136.70
		96	132.39	2.61	0.02	129.84	135.62
Immersed in Alkali Solution	23 ºC	0	140.79	9.84	0.07	130.45	155.95
		8	141.75	8.19	0.06	136.72	153.98
		24	138.36	24.63	0.18	112.68	179.31
		48	138.08	8.15	0.06	130.25	151.89
		72	131.92	6.35	0.05	126.71	139.45
		96	131.40	4.78	0.04	126.36	137.77
Immersed in NaCl Solution	5% NaCl at 23 ºC	0	140.79	9.84	0.07	130.45	155.95
		8	142.67	1.49	0.01	140.59	144.09
		24	140.29	10.40	0.07	129.10	151.16
		48	134.56	2.48	0.02	131.61	136.79
		72	134.83	1.63	0.01	133.38	136.32
		96	135.48	2.10	0.02	133.09	138.48

Table 3-9. Durability Experimental Data for Tensile Strain for SCCI FRP Strips

Condition	Exposure Level	Time [weeks]	Mean [mm/mm]	Standard Deviation [mm/mm]	COV	Minimum [mm/mm]	Maximum [mm/mm]
Control	Stored in a controlled humidity chamber at 30% RH and 23ºC	0	0.01975	0.00178	0.09	0.01669	0.02123
		8	0.01852	0.00143	0.08	0.01733	0.02052
		24	-	-	-	-	-
		48	0.01887	0.00195	0.10	0.01717	0.02100
		72	0.01872	0.00128	0.07	0.01726	0.01966
		96	0.01878	0.00137	0.07	0.01645	0.01979
Immersed in Deionized Water	23 ºC	0	0.01975	0.00178	0.09	0.01669	0.02123
		8	0.01961	0.00048	0.02	0.01932	0.02033
		24	0.01915	0.00184	0.10	0.01701	0.02117
		48	0.01917	0.00108	0.06	0.01806	0.02012
		72	0.02015	0.00080	0.04	0.01921	0.02105
		96	0.01987	0.00060	0.03	0.01901	0.02030
	37.8 ºC	0	0.01975	0.00178	0.09	0.01669	0.02123
		8	0.01980	0.00052	0.03	0.01922	0.02037
		24	-	-	-	-	-
		48	0.01916	0.00154	0.08	0.01704	0.02110
		72	0.01895	0.00146	0.08	0.01751	0.02044
		96	0.01826	0.00196	0.11	0.01610	0.02083
	60.0 ºC	0	0.01975	0.00178	0.09	0.01669	0.02123
		8	0.01928	0.00082	0.04	0.01823	0.02023
		24	-	-	-	-	-
		48	0.01833	0.00098	0.05	0.01733	0.01985
		72	0.01707	0.00124	0.07	0.01533	0.01835
		96	0.01670	0.00099	0.06	0.01560	0.01802
Immersed in Alkali Solution	23 ºC	0	0.01975	0.00178	0.09	0.01669	0.02123
		8	0.01816	0.00209	0.12	0.01525	0.02018
		24	-	-	-	-	-
		48	-	-	-	-	-
		72	0.01902	0.00111	0.06	0.01775	0.02040
		96	0.01910	0.00074	0.04	0.01806	0.02004
Immersed in NaCl Solution	5% NaCl at 23 ºC	0	0.01975	0.00178	0.09	0.01669	0.02123
		8	0.01891	0.00087	0.05	0.01765	0.01991
		24	0.01937	0.00286	0.15	0.01528	0.02224
		48	0.02005	0.00171	0.09	0.01801	0.02179
		72	0.01966	0.00038	0.02	0.01920	0.02004
		96	0.01963	0.00024	0.01	0.01930	0.01987

Table 3-10. Durability Experimental Data for Tensile Strength for FYFE FRP Strips

Condition	Exposure Level	Time [weeks]	Mean [MPa]	Standard Deviation [MPa]	COV	Minimum [MPa]	Maximum [MPa]
Control	Stored in a controlled humidity chamber at 30% RH and 23ºC	0	2481.65	51.38	0.02	2406.27	2539.54
		8	-	-	-	-	-
		24	2478.14	34.99	0.01	2426.27	2511.29
		48	2538.88	89.85	0.04	2436.35	2670.98
		72	2484.12	74.31	0.03	2412.40	2570.27
		96	2455.12	94.31	0.04	2351.31	2579.46
Immersed in Deionized Water	23 ºC	0	2481.65	51.38	0.02	2406.27	2539.54
		8	-	-	-	-	-
		24	2462.86	71.41	0.03	2393.53	2568.51
		48	2004.54	196.54	0.10	1749.46	2208.69
		72	1717.83	184.41	0.11	1449.00	1865.18
		96	1625.82	77.40	0.05	1562.08	1726.75
	37.8 ºC	0	2481.65	51.38	0.02	2406.27	2539.54
		8	-	-	-	-	-
		24	2446.34	33.48	0.01	2407.15	2487.15
		48	1963.49	17.21	0.01	1942.56	1984.01
		72	1719.70	79.95	0.05	1647.23	1809.94
		96	1567.58	78.98	0.05	1458.78	1637.83
	60.0 ºC	0	2481.65	51.38	0.02	2406.27	2539.54
		8	-	-	-	-	-
		24	2412.71	199.39	0.08	2080.54	2577.32
		48	1960.09	79.16	0.04	1883.27	2070.37
		72	1561.88	34.32	0.02	1515.54	1597.42
		96	1496.47	73.83	0.05	1372.03	1563.30
Immersed in Alkali Solution	23 ºC	0	2481.65	51.38	0.02	2406.27	2539.54
		8	-	-	-	-	-
		24	2414.40	60.84	0.03	2342.97	2505.01
		48	1789.73	88.81	0.05	1703.08	1874.78
		72	1665.71	88.68	0.05	1535.84	1735.93
		96	1688.66	46.74	0.03	1621.83	1728.97
Immersed in NaCl Solution	5% NaCl at 23 ºC	0	2481.65	51.38	0.02	2406.27	2539.54
		8	-	-	-	-	-
		24	2382.15	54.68	0.02	2293.96	2443.51
		48	1837.69	17.24	0.01	1807.98	1851.54
		72	1673.73	89.63	0.05	1566.54	1801.18
		96	1584.49	47.70	0.03	1517.71	1643.90

Table 3-11. Durability Experimental Data for Tensile Modulus for FYFE FRP Strips

Condition	Exposure Level	Time [weeks]	Mean [GPa]	Standard Deviation [GPa]	COV	Minimum [GPa]	Maximum [GPa]
Control	Stored in a controlled humidity chamber at 30% RH and 23ºC	0	126.77	3.37	0.03	121.21	129.87
		8	-	-	-	-	-
		24	125.68	2.10	0.02	123.55	129.11
		48	124.61	1.76	0.01	122.64	126.40
		72	124.82	2.78	0.02	121.50	127.63
		96	124.02	0.70	0.01	123.10	124.82
Immersed in Deionized Water	23 ºC	0	126.77	3.37	0.03	121.21	129.87
		8	-	-	-	-	-
		24	123.49	6.29	0.05	116.19	128.86
		48	125.31	3.35	0.03	121.49	128.71
		72	124.62	6.91	0.06	117.05	133.52
		96	121.81	5.58	0.05	113.73	127.11
	37.8 ºC	0	126.77	3.37	0.03	121.21	129.87
		8	-	-	-	-	-
		24	121.43	5.96	0.05	114.83	127.20
		48	118.54	4.88	0.04	112.30	124.60
		72	118.56	15.71	0.13	100.43	136.32
		96	114.29	4.56	0.04	106.86	119.27
	60.0 ºC	0	126.77	3.37	0.03	121.21	129.87
		8	-	-	-	-	-
		24	110.28	3.78	0.03	104.28	114.50
		48	110.28	5.88	0.05	101.59	114.27
		72	110.05	8.83	0.08	99.28	119.99
		96	110.03	9.53	0.09	93.34	115.53
Immersed in Alkali Solution	23 ºC	0	126.77	3.37	0.03	121.21	129.87
		8	-	-	-	-	-
		24	116.85	2.06	0.02	113.89	119.58
		48	116.06	7.14	0.06	107.59	124.56
		72	115.70	7.48	0.06	108.92	122.24
		96	110.90	3.37	0.03	106.11	113.62
Immersed in NaCl Solution	5% NaCl at 23 ºC	0	126.77	3.37	0.03	121.21	129.87
		8	-	-	-	-	-
		24	120.40	6.44	0.05	112.52	127.38
		48	119.15	2.84	0.02	115.39	123.24
		72	118.81	9.43	0.08	106.54	128.14
		96	116.95	5.59	0.05	107.12	120.81

Table 3-12. Durability Experimental Data for Tensile Strain for FYFE FRP Strips

Condition	Exposure Level	Time [weeks]	Mean [mm/mm]	Standard Deviation [mm/mm]	COV	Minimum [mm/mm]	Maximum [mm/mm]
Control	Stored in a controlled humidity chamber at 30% RH and 23°C	0	0.01959	0.00070	0.04	0.01853	0.02032
		8	-	-	-	-	-
		24	0.01973	0.00059	0.03	0.01879	0.02033
		48	0.02037	0.00059	0.03	0.01980	0.02123
		72	0.01991	0.00072	0.04	0.01903	0.02103
		96	0.01980	0.00072	0.04	0.01910	0.02080
Immersed in Deionized Water	23 °C	0	0.01959	0.00070	0.04	0.01853	0.02032
		8	-	-	-	-	-
		24	0.01998	0.00093	0.05	0.01868	0.02107
		48	0.01601	0.00169	0.11	0.01359	0.01807
		72	0.01386	0.00205	0.15	0.01085	0.01526
		96	0.01339	0.00124	0.09	0.01235	0.01518
	37.8 °C	0	0.01959	0.00070	0.04	0.01853	0.02032
		8	-	-	-	-	-
		24	0.02019	0.00114	0.06	0.01892	0.02122
		48	0.01659	0.00067	0.04	0.01592	0.01757
		72	0.01469	0.00184	0.13	0.01237	0.01647
		96	0.01372	0.00045	0.03	0.01306	0.01433
	60.0 °C	0	0.01959	0.00070	0.04	0.01853	0.02032
		8	-	-	-	-	-
		24	0.02190	0.00197	0.09	0.01897	0.02440
		48	0.01782	0.00126	0.07	0.01648	0.01922
		72	0.01427	0.00134	0.09	0.01263	0.01573
		96	0.01368	0.00137	0.10	0.01238	0.01601
Immersed in Alkali Solution	23 °C	0	0.01959	0.00070	0.04	0.01853	0.02032
		8	-	-	-	-	-
		24	0.02066	0.00031	0.02	0.02015	0.02095
		48	0.01543	0.00040	0.03	0.01505	0.01583
		72	0.01447	0.00154	0.11	0.01258	0.01585
		96	0.01523	0.00025	0.02	0.01502	0.01557
Immersed in NaCl Solution	5% NaCl at 23 °C	0	0.01959	0.00070	0.04	0.01853	0.02032
		8	-	-	-	-	-
		24	0.01983	0.00117	0.06	0.01870	0.02172
		48	0.01543	0.00042	0.03	0.01492	0.01598
		72	0.01416	0.00141	0.10	0.01267	0.01550
		96	0.01358	0.00083	0.06	0.01269	0.01478

3.2.1.2 Normalization of Data

For the purposes of this investigation, it is useful to group the three material systems as a single material class and then compare their tensile properties. This can be done provided that the three materials are fabricated of equivalent constituent materials under equivalent conditions. The tensile properties of interest are fiber-dominated mechanical properties and are dependent on fiber volume fractions (Kaw, 2006). Thus, in order to perform data analysis that compares the tensile properties of materials having different fiber volume fractions, the data must be adjusted to a common fiber volume fraction and this procedure is called data normalization. The purpose of data normalization is to remove or reduce an additional source of variability which can arise when making direct comparisons for fiber-dominated properties between materials having different fiber volume fractions.

In the case of fiber dominated properties in unidirectional composites, this can be done by simple normalization as:

$$\text{Normalized value} = \text{Test value} \times \frac{(V_f)_{\text{normalizing}}}{(V_f)_{\text{specimen}}} \qquad \textbf{Eq. 3-2}$$

where $(V_f)_{\text{normalizing}}$ is a specified common threshold value of fiber volume fraction and $(V_f)_{\text{specimen}}$ is the actual specimen fiber volume fraction measured experimentally. Following the above equation, all test data, based on different fiber volume fractions, as shown in Table 3-14, were normalized with respect to a specified fiber volume fraction of

0.60 (60 %). The specified value was selected to be slightly less than the lowest fiber volume fraction value of the material systems to avoid increases in properties during normalization. A summary of experimental raw data and normalized data are shown in Table 3-15.

Table 3-13. Results of Experimental Determination of Fiber Volume Fraction

	SIKA	SCCI	FYFE
Fiber Volume Fraction	69%	61%	62%

Table 3-14. Summary of Experimental Raw Data and Normalized Data

Property	Material System	Experimental Raw Data					Normalized Data		
		Mean	Standard Deviation	COV [%]	Minimum	Maximum	Mean	Standard Deviation	COV [%]
Ultimate Tensile Strength [MPa]	SIKA	2880.28	95.28	3.31	2665.51	3071.23	2504.59	82.85	3.31
	SCCI	2796.77	63.10	2.26	2679.00	2943.00	2750.92	62.07	2.26
	FYFE	2312.03	85.78	3.71	2105.40	2485.57	2237.42	83.08	3.71
	SIKA+SCCI+FYFE	2663.02	264.67	9.94	2105.00	3071.23	2497.64	223.95	8.97
Tensile Longitudinal Modulus [GPa]	SIKA	158.81	6.00	3.78	146.82	169.26	138.09	5.22	3.78
	SCCI	134.33	5.93	4.42	120.83	146.14	132.13	5.83	4.42
	FYFE	115.18	6.65	5.77	104.23	131.26	111.46	6.43	5.77
	SIKA+SCCI+FYFE	136.11	18.96	13.93	104.23	169.26	127.23	12.85	10.10
Ultimate Tensile Strain [mm/mm]	SIKA	0.01817	0.00097	5.32	0.01607	0.02004	0.01580	0.00084	5.32
	SCCI	0.02086	0.00100	4.79	0.01917	0.02306	0.02052	0.00098	4.79
	FYFE	0.02013	0.00116	5.77	0.01733	0.02194	0.01948	0.00112	5.77
	SIKA+SCCI+FYFE	0.01972	0.00154	7.82	0.01607	0.02306	0.01972	0.00154	7.82

When fiber-dominated properties are normalized, data scatter should decrease compared to the un-normalized values since variability due to fiber volume fraction differences is being reduced. Thus, COVs should be lower after normalization. Decreases in the COVs of the combined data sets for both tensile strength and tensile modulus were observed: from 9.94 % to 8.97% for the combined tensile strength data and from 13.93 % to 10.10 % for the combined tensile modulus data. No change in the COV of the combined tensile strain data set was observed, however this decrease is not always observed and is usually not a cause of concern (HDBK-MIL 17, 2002).

It is noted that the effect of composite thickness on fiber volume fraction is an important factor for fiber-dominated properties. Data normalization with respect to a common composite thickness is often performed in attempt to reduce the source of variability in materials with different thicknesses. However, due to the fact that the thickness of prefabricated composites is a dimensional processing parameter which can be controlled with a high degree of quality assurance, such an effect is not a concern for the materials used herein.

3.2.1.3 Outlier Analysis

An outlier is an observation that is much lower or much higher than most other observations in a data set. Often outliers are erroneous values due to data reporting errors, incorrect testing procedures, or defective test specimens. Data should be routinely investigated for outliers, since these values can have a substantial influence on the

statistical analysis. Each data set and the combined set of the three material systems were analyzed using the T-statistic test following ASTM E178-02 (ASTM, 2000).

Among a number of criteria for testing outliers, the T-statistic test is often considered to be the best and simplest method for the single-outlier case (ASTM E178-02, 2000). The test can only observe one outlier, occurring on either the low or high side, at each repetition. The doubtful observation is included in the calculation of the numerical value of a sample statistic, which is then compared with a critical value to determine whether the doubtful observation is to be retained or rejected. The critical value is that value of the sample criterion which would be exceeded by chance with some specified probability. The specified probability is called the significance level and refers to the risk of erroneously rejecting a good observation. It is generally recommended that a low significance level, such as 1 %, be used and that significance levels greater than 5 % should not be common practice (ASTM E178-02, 2000). For the purposes of this investigation, keeping in mind the scatter in the material characteristic given the immaturity of the technology, the T-statistic test with a 5 % significance level was performed on all sets of data. Details related to the procedures of outlier analysis and the results are discussed below.

The sample of n observations was arranged in order of increasing magnitude and denoted by:

$$x_1 \leq x_2 \leq x_3 \leq \ldots \leq x_n$$

where x_n is the greatest observation. Assuming that either x_1 or x_n is a doubtful outlier, the upper and lower T-statistics can be determined as:

$$T_1 = \frac{\left(\bar{x} - x_1\right)}{s} \qquad \textbf{Eq. 3-3}$$

$$T_n = \frac{\left(x_n - \bar{x}\right)}{s} \qquad \textbf{Eq. 3-4}$$

where s is the standard deviation of the test sample, $\bar{x}$ is the sample mean, x_1 is the smallest sample observation and x_n is the greatest sample observation, and T_1 and T_n are the lower and upper T-statistics, respectively. From the two T-statistics found, the greater one was compared to the corresponding critical T-value from which can be obtained from Table 1 in ASTM E178-02 (ASTM, 2000) with a value of n (number of observations in a set) and the specified significance level. If the test T-statistic is larger than the critical value, the associated test observation can be identified as an outlier and further investigation is required.

All values identified as outliers should be investigated. Those values for which a cause can be determined should be corrected if possible, and otherwise discarded. If no cause can be found for an outlier, it should be retained in the data set. If any observations are corrected or discarded, both the statistical outlier test and the visual inspection should be repeated on the remaining data. These procedures were carefully followed for the

investigation of outliers of the experimental data and a summary of the outlier analysis results is provided in Table 3-16.

Table 3-15. Outlier Analysis Result

Material System	Property	Outlier Observation and Treatment				
		Outlier Check	Number of Samples			Truncated Sample
			Tested	Outlier	Final	
SIKA	Strength	PASS	35	0	35	-
	Modulus	PASS	35	0	35	-
	Strain	PASS	35	0	35	-
SCCI	Strength	FAIL	36	1	35	SCCI2-6
	Modulus	PASS	36	0	35	SCCI2-6
	Strain	PASS	36	0	35	SCCI2-6
FYFE	Strength	PASS	35	0	35	-
	Modulus	PASS	35	0	35	-
	Strain	PASS	35	0	35	-
SCCI+SIKA+FYFE	Strength	PASS	106	1	105	SCCI2-6
	Modulus	PASS	106	0	105	SCCI2-6
	Strain	PASS	106	0	105	SCCI2-6

From a total of 106 observations, there was only one observation, SCCI2-6 from tensile strength property data, found to be an outlier at the 5 % level of significance following the T-statistic test. Further investigation was performed using the laboratory notes to find a possible source of error; however no clear cause was found. However, there are cases where outlier can or should be removed based on judgment. It is assumed that the objective of testing is to characterize the properties of a material when processed, conditioned, and tested in accordance with specified procedures. If this is the case, variability within the test data should ideally reflect only material variability. In reality, there is also unavoidable random variability due to unknown and uncontrollable factors

(HDBK-MIL 17, 2002). For the purposes of this investigation, the outlier was truncated and descriptive statistics of the remaining data were determined.

3.2.1.4 Data Obtained from Statistical Analysis

Experimental data for tensile strength, tensile modulus, and tensile strain properties were subjected to the statistical methods, including normalization and outlier detection and truncation. Mean, standard deviation, COV, minimum, and maximum values of the data were determined for each data set of the material systems as well as for the combined set of all three material systems. These data were later used to determine an appropriate statistical distribution for the characterization of the materials of interest by performing parameter estimation and a series of goodness-of-fit tests. The basic statistical descriptors of the data after the data normalization and outlier truncation are provided in Table 3-17 through Table 3-20.

Table 3-16. Final Experimental Property Data

Property	Material System	Normalized Data				
		Mean	Standard Deviation	COV [%]	Minimum	Maximum
Ultimate Tensile Strength [MPa]	SIKA	2504.59	82.85	3.31	2317.83	2670.63
	SCCI	2750.92	62.07	2.26	2635.08	2894.75
	FYFE	2237.42	83.08	3.71	2037.10	2405.81
	SIKA+SCCI+FYFE	2497.64	223.95	8.97	2037.10	2894.75
Tensile Longitudinal Modulus [GPa]	SIKA	138.09	5.22	3.78	127.67	147.18
	SCCI	132.13	5.83	4.42	118.84	143.74
	FYFE	111.46	6.43	5.77	100.86	127.03
	SIKA+SCCI+FYFE	127.23	12.85	10.10	100.86	147.18
Ultimate Tensile Strain [mm/mm]	SIKA	0.01580	0.00084	5.32	0.01397	0.01743
	SCCI	0.02052	0.00098	4.79	0.01885	0.02268
	FYFE	0.01948	0.00112	5.77	0.01677	0.02123
	SIKA+SCCI+FYFE	0.01972	0.00154	7.82	0.01607	0.02306

From the data in the above table, it is apparent that there is a small spread within a single material system, but a relatively large amount of scatter within the combined set of the material systems for all three properties. This larger range of values was expected for the combined set; however this shows the need to consider possible variations within the three material system properties at the design stage. Detailed experimental results with descriptive statistics of each set of data for the three material systems are provided in Table 3-18 through Table 3-20.

Table 3-17. Detailed Experimental Data for Tensile Strength

Material System	Data Set	Normalized Data				
		Mean [MPa]	Standard Deviation [Mpa]	COV	Minimum [MPa]	Maximum [MPa]
SIKA	SIKA-1	2528.61	88.77	0.04	2386.99	2973.40
	SIKA-2	2499.97	57.05	0.02	2408.91	2583.97
	SIKA-3	2519.23	67.68	0.03	2390.37	2630.76
	SIKA-4	2473.21	111.78	0.05	2317.83	2670.63
SCCI	SCCI-1	2752.02	61.56	0.02	2663.61	2853.44
	SCCI-2	2779.18	56.79	0.02	2695.08	2869.18
	SCCI-3	2743.72	78.84	0.03	2635.08	2894.75
	SCCI-4	2731.91	47.75	0.02	2683.28	2826.89
FYFE	FYFE-1	2229.95	83.61	0.04	2111.61	2364.19
	FYFE-2	2262.30	60.34	0.03	2161.94	2331.29
	FYFE-3	2300.74	95.42	0.04	2140.65	2405.81
	FYFE-4	2196.22	91.56	0.04	2037.10	2314.84
	FYFE-5	2197.88	41.49	0.02	2140.65	2269.35

In considering the normalized strength data, it is clear that different material systems produce significantly different mean properties; therefore the proposed design procedure must be able to account for a range of material property values. The coefficient of variation is seen to range from a low of 0.02 to a high of 0.05.

Table 3-18. Detailed Experimental Data for Tensile Modulus

Material System	Data Set	Normalized Data				
		Mean [GPa]	Standard Deviation [Gpa]	COV	Minimum [GPa]	Maximum [GPa]
SIKA	SIKA-1	136.65	4.86	0.04	127.67	144.70
	SIKA-2	137.96	4.56	0.03	131.61	145.49
	SIKA-3	136.18	6.08	0.04	127.98	146.17
	SIKA-4	141.41	4.31	0.03	135.71	147.18
SCCI	SCCI-1	135.50	4.71	0.03	128.92	143.74
	SCCI-2	133.86	5.09	0.04	126.08	140.44
	SCCI-3	127.39	5.14	0.04	118.84	134.00
	SCCI-4	131.96	5.68	0.04	124.11	140.86
FYFE	FYFE-1	109.00	7.22	0.07	101.67	119.11
	FYFE-2	118.57	4.61	0.04	113.26	127.03
	FYFE-3	109.29	3.08	0.03	105.15	113.46
	FYFE-4	115.24	1.66	0.01	112.85	117.66
	FYFE-5	105.22	3.90	0.04	100.86	111.48

The normalized modulus data shows differences across material systems. The coefficient of variation for the modulus is generally slightly higher than that for strength, ranging from 0.01 to 0.07.

Table 3-19. Detailed Experimental Data for Tensile Strain

Material System	Data Set	Normalized Data				
		Mean [mm/mm]	Standard Deviation [mm/mm]	COV	Minimum [mm/mm]	Maximum [mm/mm]
SIKA	SIKA-1	0.01610	0.00061	0.04	0.01488	0.01674
	SIKA-2	0.01577	0.00068	0.04	0.01480	0.01677
	SIKA-3	0.01612	0.00103	0.06	0.01469	0.01743
	SIKA-4	0.01522	0.00075	0.05	0.01397	0.01605
SCCI	SCCI-1	0.02000	0.00087	0.04	0.01885	0.02177
	SCCI-2	0.02045	0.00084	0.04	0.01935	0.02178
	SCCI-3	0.02121	0.00100	0.05	0.01953	0.02268
	SCCI-4	0.02040	0.00092	0.05	0.01911	0.02175
FYFE	FYFE-1	0.01984	0.00091	0.05	0.01854	0.02123
	FYFE-2	0.01849	0.00085	0.05	0.01677	0.01934
	FYFE-3	0.02037	0.00064	0.03	0.01938	0.02110
	FYFE-4	0.01844	0.00075	0.04	0.01698	0.01904
	FYFE-5	0.02023	0.00069	0.03	0.01897	0.02097

The normalized strain data also shows differences across systems. The coefficient of variation of the strain is within the range of that for either strength or modulus, with a low value of 0.03 and a high of 0.05.

3.2.2 Statistical Distributions for Describing Composite Materials

In composite design, tensile property data for unidirectional composites are obtained from laboratory tests and aid in materials selection and design. When modeling experimental data, statistical distributions are typically used to describe the tensile properties of composite specimens. The selected probability distribution that represents the material property data has a significant effect on the estimated properties and the calculated reliability of a structural component (Ellingwood, 1994). The use of different cumulative probability density functions (CDF) can result in as much as 50% differences in design properties due to the modeling sensitivity in the lower tail regions of the CDFs (Murphy, 1988). Consideration of the sensitivity to the tail behavior is particularly useful in structural engineering applications, where the tail is important in computing the structural reliability (Alqam, 2001).

3.2.2.1 Distributions Considered in this Research

In this study, four statistical distributions, the normal, lognormal, Weibull, and Gamma distributions, were examined. They were selected based on the fact that they have been widely used in engineering and are considered as acceptable for material property characterization. Details related to each distribution are discussed in this section.

The normal distribution has been the most important and widely used distribution in the entire field of probability. An important reason for the wide applicability of the normal distribution is the fact that it is a reasonable model for observations of many

physical processes or properties. The normal distribution has been predominantly used for traditional metallic structural materials, like steel (Bury, 1999). Although this distribution is generally better understood than most other distributions, it has some limitations including the possibility of negative values in its sample space and its symmetric nature while many engineering quantities show some skewness (Bury, 1999). Given that X is a random variable, the probability density function of the normal distribution may be expressed as:

$$f_X(x) = \frac{1}{\sigma\sqrt{2\pi}} \exp\left[-\frac{1}{2}\left(\frac{x-\mu}{\sigma} \right)^2 \right]; \quad \sigma > 0, \quad -\infty < x < +\infty \qquad \textbf{Eq. 3-5}$$

where μ is the mean value and σ is the standard deviation. The cumulative distribution is given by:

$$F_X(x) = \frac{1}{\sigma\sqrt{2\pi}} \int_{-\infty}^{x} \exp\left[-\frac{1}{2}\left(\frac{x-\mu}{\sigma} \right)^2 \right] dx; \quad \sigma > 0, \quad -\infty < x < +\infty \qquad \textbf{Eq. 3-6}$$

The lognormal distribution is widely accepted for modeling material fatigue failures and failure due to crack propagation (Dai, 1992). Many of its properties come directly from the properties of the normal distribution. Its wide applicability comes from its flexibility in matching distribution shape, its being constrained to positive sample space only, and its ease of use. Given that X is a random variable, the lognormal probability density function is:

$$f_X(x) = \frac{1}{\zeta x\sqrt{2\pi}} \exp\left[-\frac{1}{2}\left(\frac{\ln x - \lambda}{\zeta}\right)^2\right]; \quad 0 < x < +\infty \qquad \textbf{Eq. 3-7}$$

where λ is the mean value of the set of natural logs of x and ζ is the standard deviation of the set of natural logs of x. The cumulative probability distribution function is:

$$F_X(x) = \int_{-\infty}^{x} \frac{1}{\zeta x\sqrt{2\pi}} \exp\left[-\frac{1}{2}\left(\frac{\ln x - \lambda}{\zeta}\right)^2\right] dx; \quad 0 < x < +\infty \qquad \textbf{Eq. 3-8}$$

The Weibull distribution is termed as a type III extreme value distribution of minima. The Type III asymptotic form represents a limiting distribution of the extreme values from initial distributions that have finite upper or lower bound values (Haldar, 2000). The Weibull distribution is widely used in a number of statistical models as a means of characterizing the variability of material strength response. Compared to other commonly used distributions, the Weibull distribution is more flexible and suitable and has been used very successfully in describing the strength of composite materials (Bury, 1999). The general form of the Weibull distribution uses three parameters: shape parameter, scale parameter, and location parameter. Often, the location parameter is set to zero and it becomes to the two-parameter Weibull distribution. Although the three-parameter Weibull distribution is considered more robust and may provide more accurate modeling, the two-parameter Weibull distribution is recommended herein for characterization of FRP composite material properties because of its ease of use and small differences in prediction accuracy between the two models (Alqam et al. 2001). In

this work, the two-parameter Weibull distribution was used. The two-parameter Weibull probability density function is given by:

$$f_X(x) = \frac{\alpha}{\beta}\left(\frac{x}{\beta}\right)^{\alpha-1} \exp\left[-\left(\frac{x}{\beta}\right)^{\alpha}\right]; \qquad x \geq 0, \quad \alpha, \beta \geq 0 \qquad \textbf{Eq. 3-9}$$

where X is a random variable, α is the shape parameter, and β is the scale parameter. The cumulative density function is:

$$F_X(x) = 1 - \exp\left[-\left(\frac{x}{\beta}\right)^{\alpha}\right]; \qquad x \geq 0, \quad \alpha, \beta \geq 0 \qquad \textbf{Eq. 3-10}$$

The gamma distribution is a general type of statistical distribution. It has been used as a general model for engineering problems due to its flexible shape and positive sample space (Bury, 1999). The gamma distribution has two parameters, labeled as shape and scale parameters, similar to the Weibull parameters. The probability density function is given by:

$$f_X(x) = \frac{1}{\beta\Gamma(\alpha)}\left(\frac{x}{\beta}\right)^{\alpha-1} \exp\left[-\left(\frac{x}{\beta}\right)\right]; \qquad x \geq 0, \quad \alpha, \beta \geq 0 \qquad \textbf{Eq. 3-11}$$

where X is a random variable, α is the shape parameter, β is the scale parameter, and Γ is the gamma function.

3.2.2.2 Parameter Estimation for Test Distributions

All four of the described distributions were fit to each set of strength, modulus, and strain data. The distribution parameters of both the normal and lognormal distributions were computed for each material property data set using the simple mean and standard deviation formulae. For the Weibull and Gamma distributions, an error minimization procedure was used to determine the distribution parameters. The resulting distribution parameters are shown in Table 3-20.

Table 3-20. Estimated Parameters for Test Distributions

Property	Material System	Normal		Lognormal		Weibull		Gamma	
		μ	σ	λ	ζ	α	β	α	β
Tensile Strength	SIKA	2504.54	82.86	7.825	0.033	33.41	2543.56	936.12	2.68
	SCCI	2750.89	62.06	7.919	0.022	44.10	2781.77	2033.57	1.35
	FYFE	2237.49	83.06	7.712	0.037	29.58	2276.81	744.61	3.00
	SIKA+SCCI+FYFE	2497.64	223.91	7.819	0.091	12.98	2599.14	124.07	20.13
Tensile Modulus	SIKA	138.09	5.22	4.927	0.038	29.49	140.56	718.80	192.12
	SCCI	132.13	5.83	4.883	0.044	25.15	134.86	524.82	0.25
	FYFE	111.46	6.43	4.712	0.058	18.40	114.47	309.14	0.36
	SIKA+SCCI+FYFE	127.23	12.85	4.841	0.104	12.48	132.81	95.00	1.34
Tensile Strain	SIKA	0.01817	0.00097	-4.009	0.054	21.01	0.018618	359.94	5.05E-05
	SCCI	0.02052	0.00098	-3.887	0.047	21.94	0.020993	457.64	4.48E-05
	FYFE	0.01947	0.00112	-3.941	0.058	20.62	0.019976	307.18	6.34E-05
	SIKA+SCCI+FYFE	0.01860	0.00226	-3.992	0.125	10.08	0.019572	65.86	2.82E-04

3.2.2.3 Goodness-of-Fit Testing

In analyzing statistical data, it is important to determine how well the experimental data fit an assumed distribution. A number of methods are available to test how closely a set of data fits an assumed distribution. Three commonly used methods, the Kolmogorov-Smirnov (KS) test, the chi-square test, and the Anderson-Darling (AD) test, and one method from a recent work by Wang et al (Wang et al., 2004) were used to assess the goodness of the four distribution selected previously to model the stochastic variation in composite properties. A MATLAB program was developed to compute the statistics for the methods described above and is provided in Appendix A.4 Details related to each method are described in this section.

The Kolmogorov-Smirnov (KS) test statistic, D, is a measure of the maximum difference between the empirical and an assumed cumulative distribution function. For a random sample of size n, let $X_1 \le X_2 \le,...,\le X_n$ denote those ordered sample values. $F_o(x)$ is the assumed cumulative distribution function and $F_n(x)$ is the empirical cumulative distribution function which can be defined as a step function with n steps as follows:

$$F_n(x) = \begin{cases} 0 & x < X_1 \\ \dfrac{i}{n} & X_i < x < X_{i+1} \\ 1 & x > X_n \end{cases}$$

Then, the KS static, D, can be computed as follows:

$$D = \max\left\{F_o\left(x_i\right) - F_n\left(x_{i-1}\right)\ ,\ F_n\left(x_i\right) - F_o\left(x_i\right)\right\} \qquad \textbf{Eq. 3-12}$$

$F_n\left(x\right)$ has a better goodness-of-fit with $F_o\left(x\right)$ when D is small. This suggests that the lower the KS statistic is, the better the assumed distribution fits the empirical data.

The chi-square test groups the sample data by dividing the sample data into n intervals, or classes, $\left(a_o, a_1\right), \left(a_1, a_o\right), ..., \left(a_{n-1}, a_n\right)$. Although this test is easy to apply to both discrete and continuous distributions, grouping the data into intervals may alter the original sample distribution (Haldar, 2000). To apply this test, an assumed distribution is used to calculate the probability in each of the intervals as follows:

$$p_i = F_o(a_i) - F_o(a_{i-1}) \qquad i = 1, 2, ..., n \qquad \textbf{Eq. 3-13}$$

The chi-square statistic, χ^2, can be computed by:

$$\chi^2 = \sum_{i=1}^{n} \frac{\left(n_i - np_i\right)^2}{np_i} \qquad \textbf{Eq. 3-14}$$

where ni is the actual frequency in the i^{th} interval. It is noted that if the assumed distribution function is a close-fit, χ^2 should be small.

The Anderson-Darling test compares an assumed cumulative distribution function with the empirical cumulative distribution function. The main advantage of this test is that its test statistic is more sensitive to discrepancies in the tail region than other commonly used methods (Lawless, 1982). The sensitivity to the tail behavior is particularly useful in reliability engineering applications, where the tail is important in computing the structural or component reliability. The Anderson-Darling statistic is a measure of the square of the error between the data and the assumed distribution weighted such that the tails of the data are more important than the central portion. For a random sample of size n, the Anderson-Darling test statistic can be obtained as:

$$A^2 = \sum_{i=1}^{n}\left[\frac{1-2i}{n}\left\{\ln F_o\left(x_i\right) + \ln\left[1 - F_o\left(x_{n+1-i}\right)\right]\right\}\right] - n \qquad \textbf{Eq. 3-15}$$

where $F_o(x)$ is the assumed cumulative distribution function and x_i is the i^{th} order statistic of the data set.

The multi-criterion test proposed by Wang et al. (2004) was used in this research. As opposed to the traditional goodness-of-fit tests described above that use a single test criterion, this method considers five different criteria to determine the best fitting distribution, including the KS test statistic, D, the average deviation in cumulative distribution function, the average deviation in probability distribution function, the deviation in skewness and kurtosis, and expert's preference. Due to the absence of information regarding the deviation in skewness and kurtosis and experts' preference,

these two criteria were assumed to be ineffective for the current research and were therefore disregarded. In this method, not only was the KS test used to account for difference between an assumed and empirical cumulative distributions, but also the average deviation in cumulative function distribution and probability distribution function between the assumed and empirical distributions. The average deviation in CDF and PDF are considered to assess the overall goodness-of-fit of an assumed distribution to empirical data rather than a single observed point from the sample data as being done in the KS test. For a random sample of size n, $F_n(x)$ and $F_o(x)$ are considered to be the empirical and an assumed cumulative distribution, respectively. Then, the average deviation between the assumed CDF and the empirical CDF is calculated as:

$$\delta_F = \frac{1}{n}\sum_{i=1}^{n}\left|F_n(x_i) - F_o(x_i)\right| \qquad \textbf{Eq. 3-16}$$

and the average deviation between the assumed PDF and the empirical PDF is determined as:

$$\delta_f = \frac{1}{n}\sum_{i=1}^{n}\left|f_n(x_i) - f_o(x_i)\right| \qquad \textbf{Eq. 3-17}$$

The criteria discussed above are integrated using a performance weighting matrix, W, which in the current case is uniform for all criteria due to lack of experts' preferences, and a performance matrix, R, which consists of normalized statistics of each distribution

against each criteria. If N represents the number of assumed statistical distributions and M represents the number of test criteria to be considered, the weighted average performances of the assumed distributions can be obtained and represented by matrix B as follow:

$$B = W \times R \qquad \textbf{Eq. 3-18}$$

where W, R, and B have dimensions [1x M], [M x N], and [1 x N], respectively. In this test, the smallest value in the matrix, B, represents the best fitting distribution.

3.2.2.4 Results of Best Fitting Distribution Tests

The four goodness-of-fit tests were applied to the strength, modulus, and strain data. The test statistics of each test method were computed for the four test distributions: the normal, lognormal, Weibull, and Gamma. The statistic results were ranked by normalizing the statistics with respect to the smallest value for each data set for ease of comparison. The test statistic with the smallest value and highest ranking, representing the best fitting distributions, is highlighted for each data set. Details related to the results of the four tests are shown in Table 3-21 through Table 3-24.

Table 3-21. KS Test Statistics

Property	Material System	Raw Statistics				Normalized (Ranked) Statistics			
		Normal	Lognormal	Weibull	Gamma	Normal	Lognormal	Weibull	Gamma
Tensile Strength	SIKA	0.097	0.104	0.085	0.102	1.153	1.228	1.000	1.204
	SCCI	0.089	0.089	0.121	0.092	1.004	1.000	1.357	1.038
	FYFE	0.082	0.082	0.121	0.085	1.001	1.000	1.480	1.044
	SIKA+SCCI+FYFE	0.105	0.109	0.089	0.109	1.178	1.223	1.000	1.222
Tensile Modulus	SIKA	0.123	0.118	0.161	0.120	1.043	1.000	1.370	1.018
	SCCI	0.052	0.058	0.090	0.053	1.000	1.110	1.723	1.023
	FYFE	0.115	0.125	0.093	0.123	1.235	1.349	1.000	1.323
	SIKA+SCCI+FYFE	0.126	0.137	0.102	0.132	1.233	1.341	1.000	1.298
Tensile Strain	SIKA	0.094	0.094	0.103	0.097	1.000	1.004	1.097	1.041
	SCCI	0.110	0.106	0.109	0.110	1.030	1.000	1.024	1.039
	FYFE	0.079	0.084	0.101	0.079	1.003	1.065	1.288	1.000
	SIKA+SCCI+FYFE	0.125	0.144	0.121	0.138	1.000	1.155	0.970	1.105

Table 3-22. Chi-Square Test Statistics

Property	Material System	Raw Statistics				Normalized (Ranked) Statistics			
		Normal	Lognormal	Weibull	Gamma	Normal	Lognormal	Weibull	Gamma
Tensile Strength	SIKA	2.103	2.249	1.254	2.153	1.677	1.793	1.000	1.717
	SCCI	1.166	1.147	1.229	1.227	1.017	1.000	1.072	1.070
	FYFE	1.147	1.126	1.053	1.148	1.089	1.069	1.000	1.090
	SIKA+SCCI+FYFE	17.364	20.053	12.100	19.241	1.435	1.657	1.000	1.590
Tensile Modulus	SIKA	2.641	5.179	0.486	5.135	5.432	10.653	1.000	10.562
	SCCI	4.271	4.384	3.251	4.203	1.314	1.349	1.000	1.293
	FYFE	2.234	2.387	1.745	2.305	1.280	1.368	1.000	1.321
	SIKA+SCCI+FYFE	27.743	33.865	17.595	31.694	1.577	1.925	1.000	1.801
Tensile Strain	SIKA	0.439	0.498	1.112	0.425	1.033	1.174	2.620	1.000
	SCCI	2.224	2.187	0.251	2.342	8.868	8.719	1.000	9.339
	FYFE	1.982	1.831	1.735	2.012	1.142	1.055	1.000	1.160
	SIKA+SCCI+FYFE	31.343	37.303	21.299	35.127	1.472	1.751	1.000	1.649

Table 3-23. Anderson-Darling Test Statistics

Property	Material System	Raw Statistics				Normalized (Ranked) Statistics			
		Normal	Lognormal	Weibull	Gamma	Normal	Lognormal	Weibull	Gamma
Tensile Strength	SIKA	34.688	34.729	33.663	35.259	1.030	1.032	1.000	1.047
	SCCI	34.753	34.688	34.385	35.137	1.011	1.009	1.000	1.022
	FYFE	34.182	34.246	33.277	34.778	1.027	1.029	1.000	1.045
	SIKA+SCCI+FYFE	109.166	108.606	111.579	109.285	1.005	1.000	1.027	1.006
Tensile Modulus	SIKA	35.269	35.238	35.438	35.746	1.001	1.000	1.006	1.014
	SCCI	34.564	34.626	33.796	35.150	1.023	1.025	1.000	1.040
	FYFE	36.875	36.743	36.100	37.211	1.021	1.018	1.000	1.031
	SIKA+SCCI+FYFE	111.814	111.530	117.122	112.141	1.003	1.000	1.050	1.005
Tensile Strain	SIKA	34.904	34.898	34.575	35.427	1.009	1.009	1.000	1.025
	SCCI	36.301	36.088	36.479	36.562	1.006	1.000	1.011	1.013
	FYFE	34.862	34.976	35.027	35.515	1.000	1.003	1.005	1.019
	SIKA+SCCI+FYFE	111.060	110.467	115.361	111.149	1.005	1.000	1.044	1.006

Table 3-24. Multi-Criterion Test Statistics

Property	Material System	Raw Statistics				Normalized (Ranked) Statistics			
		Normal	Lognormal	Weibull	Gamma	Normal	Lognormal	Weibull	Gamma
Tensile Strength	SIKA	36.888	37.082	35.001	37.515	1.054	1.059	1.000	1.072
	SCCI	36.009	35.925	35.735	36.457	1.008	1.005	1.000	1.020
	FYFE	35.411	35.453	34.452	36.011	1.028	1.029	1.000	1.045
	SIKA+SCCI+FYFE	126.635	128.768	123.767	128.635	1.023	1.040	1.000	1.039
Tensile Modulus	SIKA	38.032	40.535	36.085	41.001	1.054	1.123	1.000	1.136
	SCCI	38.887	39.068	37.137	39.407	1.047	1.052	1.000	1.061
	FYFE	39.223	39.256	37.938	39.639	1.034	1.035	1.000	1.045
	SIKA+SCCI+FYFE	139.683	145.532	134.818	143.967	1.036	1.079	1.000	1.068
Tensile Strain	SIKA	35.436	35.490	35.790	35.949	1.000	1.002	1.010	1.014
	SCCI	38.634	38.382	36.839	39.015	1.049	1.042	1.000	1.059
	FYFE	36.923	36.891	36.863	37.606	1.002	1.001	1.000	1.020
	SIKA+SCCI+FYFE	142.528	147.914	136.782	146.414	1.042	1.081	1.000	1.070

The results of the KS test and the Anderson-Darling test show that the lognormal and Weibull distributions are the best fitting distributions. For the purposes of this investigation, the Weibull distribution has a slight advantage because it is the best distribution for the combined data sets, SIKA+SCCI+FYFE, for strength and modulus data. According to the results of the chi-square test and the multi-criterion test, it is apparent that the Weibull distribution is the best fitting distribution for both of the single and combined data sets for all material properties.

3.2.2.5 Proposed Distribution for FRP Design Value Determination

The goodness-of-fit test results showed that overall the data was fitted best by the two-parameter Weibull distribution. It should be noted that these tests were conducted based on 35 samples for each material system and 105 samples for the combined material system. It is also possible that the test results may be different if larger number of samples is used. It should also be noted that the use of the two-parameter Weibull distribution is recommended by HDBK-MIL 17 which states that the two-parameter Weibull distribution should be used if it adequately fits the data, even if other distributions apparently fit the data better (HDBK-MIL 17, 2002).

Chapter 4. Determination of Reliability-based FRP Design Value

A "design value" used for a material is generally defined as the minimum value of a material property expected to be used in the design of a structure. The design value can be deterministic or statistically-based. In order to understand the definitions of statistically-based design values, it is important to consider the material property of interest as a random variable, not as a deterministic value. In general, all the parameters of interest in engineering design and analysis have some degree of uncertainty and thus may be considered to be random variables. Statistically-based design values are used in an attempt to account for the stochastic nature of the material properties. In the context of reliability-based design, statistically-based design values must be used in order to make reliability estimates of the material design properties and such a design value used for reliability-based design is the reliability-based design value (MIL-HDBK 17, 2002).

It must be emphasized that this chapter differentiates between material allowable values and design allowable values. Material allowable values, also known as material allowables, are an intrinsic property of a composite material system and are the focus of this chapter. The general approach to determine a material allowable value for composite properties is to define a "characteristic" value. The characteristic value is specified as a certain percentile of test results. Design allowable values, while often based on material allowable values, are application dependent, and account for design specific considerations that may further affect the choice of level of material properties. This chapter focuses on the selection of appropriate characteristic design values by proposing

a new means of determining design values that are appropriate for use with reliability-based design procedures.

4.1 Need for an Improved Reliability-based Approach

The purpose of this research is to develop a methodology to determine reliability-based FRP design values. Such design values can then be used in a reliability-based design procedure for FRP strengthening of concrete that provides a uniform level of reliability across a variety of design situations. Typically, the final design value is expressed as the final product of the characteristic value and any associated factors applied to that value. Nearly, all of the currently available design guidelines mentioned in Chapter 2 use systems of safety factors to account for a variety of design variables, including reinforcement types, environmental effects, time-dependent loading effects, and process specifics. As previously discussed in Chapter 2, due to the presence of the ambiguity in the use of environmental factors in the different guidelines, the need for a more reliable and standardized method of determining the design characteristic value and accounting for time-dependent deterioration behavior of FRPs is apparent.

Using characteristic values such as those recommended by ACI 440 (2002) and TR 55 (2004) where a number of standard deviations are subtracted from the mean ultimate material properties has an undesirable statistical implication. The influence of material variability, expressed as standard deviation, on the characteristic design value often gives a false sense that when composites with high variability are used as part of a

system, the systems have a larger reliability due to the increased amount of material needed to meet requirements while penalizing those with lower material variability, or higher quality controlled products (Atadero, 2006).

The intent of the method used in the existing guidelines is to set the probability of structural failure in an ad-hoc manner by ensuing the probability that the composite falls below the characteristic value. This approach neglects the fact that the reliability of a structure is determined by the interaction of load and resistance, not by its resistance alone. Since the reliability is determined by interaction, the shape of the distribution describing the material property of interest becomes important, rather than just the percentiles of the material property. Therefore, it is important to assess the characteristics of the distribution and to incorporate them in the determination of design values of material properties. In effect, with an appropriately selected distribution, the use of procedures for determining reliability-based design values can enable the description of the material property of interest more accurately and realistically. Thus, more accurate design values can be obtained which are therefore of greater reliability for use in designs that have relatively long periods of anticipated service-life.

4.2 Proposed Approach to Determine Reliability-based Design Values

There are several fundamental elements that are required to determine reliability-based design values. These include basic statistics such as mean and COV, of each set of data, the type of probability distribution which best describes the data set, and the method

of parameter estimation for the distribution. The basic statistics of the test data have already been determined previously and are described in Section 3.2.1.4. The two-parameter Weibull distribution was selected as the distribution for the purposes of the current research. Details related to the selection and application of the two-parameter Weibull distribution and the parameter estimation methods are discussed in this chapter on the basis of which a proposed method for the determination of reliability-based characteristic values using the Weibull distribution and consideration of time-dependent degradation of FRP properties will be presented.

It should be noted that reliability-based materials properties are developed in two steps in the current research. First, a material property is modeled with a probability distribution in order to take into account observed scatter in the property, and determinations of characteristic values in terms of percentiles of this distribution are made. This takes into account uncertainty that exists in the property of interest. However, there is an additional source of uncertainty due to the limited amount of data used in this study. So the characteristic values based on the previous definitions are replaced by estimates of percentiles, also known as confidence intervals, in order to account for the additional uncertainty in a random material property due to limited data (Zureick, 2006). An approach accounting for such uncertainties has already been implemented in aerospace composites design wherein either A-basis values or the B-basis values are often used (HDBK MIL-17, 2002). The A-basis value is the lower tolerance limit associated with 95% confidence for the 1-percentile value of a specified population,

while the B-basis value is the limit associated with 95 % confidence for the 10^{th} percentile value of that population.

4.2.1 Selection of the Two-Parameter Weibull Distribution

The two-parameter Weibull probability density function was defined previously in Eq. 3-9. The parameters of the distribution are α (shape parameter) and β (scale parameter). The probability of failure is given as:

$$F_X(x) = 1 - \exp\left[-\left(\frac{x}{\beta}\right)^{\alpha}\right]; \qquad x \geq 0, \quad \alpha, \beta \geq 0 \qquad \textbf{Eq. 4-1}$$

The scale parameter measures how the distribution spreads out. The larger the value of the scale parameter the more the spread of the distribution. The shape parameter, also known as the Weibull modulus, defines the behavior of the distribution and is a measure of the dispersion of the distribution. The shape parameter gives flexibility to the Weibull distribution as shown in Figure 4-1:

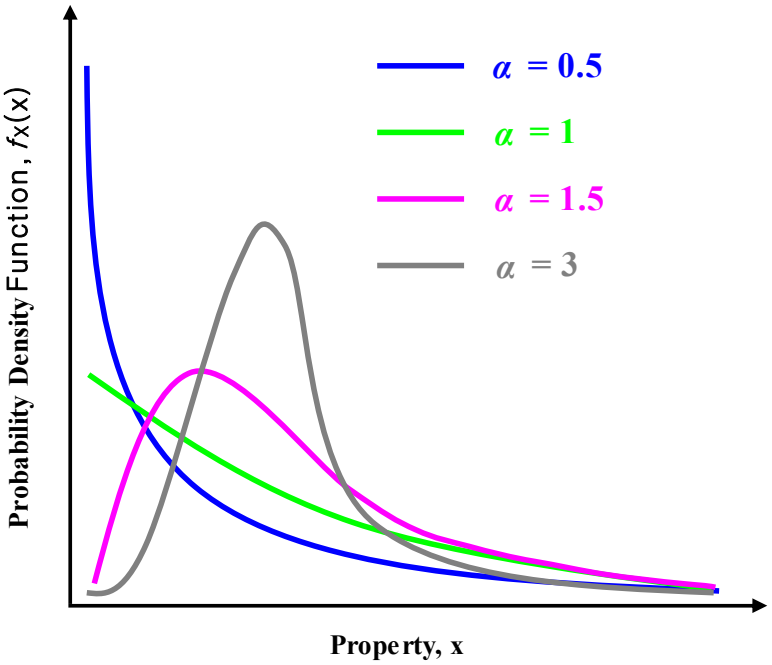

Figure 4-1. The effect of the Weibull shape parameter on the PDF

The shape of the distribution is controlled by the type of probability distribution function chosen to model the variable and by the amount of spread in the data. For a material such as steel, the variation is fairly standard from project to project and thus the shape of its distribution is relatively constant. However, in the case of composites, there is the potential for large change in the degree of variation between material systems (due to manufacturing differences) and between effects of time-based environmental effects. In this case, the shape of the resistance distribution will change as the variation changes. Thus, for design with FRP, there are many possible shapes for the resistance distribution, and statistically each different resistance distribution requires its own distribution parameters to be determined accurately. This leads to a problem that a distribution with a single fixed shape, such as a Normal distribution, may not be adequate to model such

material variability. Compared to the Normal distribution which was predominantly used for traditional metallic structural materials, the Weibull distribution is more flexible and suitable and has been very successful in predicting the strength of composite materials (Bury, 1999).

The Weibull distribution has been the most common probability distribution to be used with FRP material properties (King 1986; Rust et al. 1989). The Weibull distribution was preferred for the characterization of FRP material properties in HDBK MIL-17 (2002) and previous researchers (Zureick et al., 2006; Abanilla and Karbhari, 2006). Based on the fact that the Weibull distribution is well suited for describing the weakest link phenomena, it is often used to describe fracture of brittle materials and strength in composites (Choi et al., 2007). As shown previously in Chapter 3, the Weibull distribution was selected as the best fit to FRP tensile properties in the current research. Although a three-parameter Weibull distribution has sometimes been used, the two-parameter Weibull distribution is generally considered to be adequate (Alqam et al., 2001). For the purposes of this investigation, the tensile properties of prefabricated FRP materials were assumed to follow a two-parameter Weibull distribution.

4.2.2 Methods Used for Parameter Estimation

In order to compute a characteristic value for a two-parameter Weibull distribution, it is first necessary to determine estimates of the shape and scale parameters. The accuracy in estimating these parameters based on the test data determines the success

in modeling the uncertainty in a random variable (Haldar, 2000). For the purposes of this investigation, two methods of parameter estimation of the Weibull distribution were presented and they are the maximum likelihood estimator (MLE) method and the empirical formula method.

The principle behind the MLE method is that for a random variable X, if $x_1, x_{2,}..., x_n$ are the n observations or sample values, and the estimated value of the parameter is the value most likely to produce these observed values, then the estimated value of the parameter is the value most likely to produce these observed values (Bain, 1991). The MLE of parameters α and β are $\hat{\alpha}$ and $\hat{\beta}$, respectively, defined by the expressions

$$\frac{\sum_{i=1}^{n} x_i^{\hat{\alpha}} \ln(x_i)}{\sum_{i=1}^{n} x_i^{\hat{\alpha}}} - \frac{1}{\hat{\alpha}} - \frac{1}{n}\sum_{i=1}^{n} \ln(x_i) = 0 \qquad \textbf{Eq. 4-2}$$

$$\hat{\beta} = \left(\frac{\sum_{i=1}^{n} x_i^{\hat{\alpha}}}{n} \right)^{1/\hat{\alpha}} \qquad \textbf{Eq. 4-3}$$

A MATLAB script was written to compute the MLE parameters for this research listed in Appendix A.4 and the results are provided in Table 4-1.

The empirical formula method is much simpler compared to the MLE method and is preferred for cases when there is a limited amount of data on the basis of which probability distributions may not be accurately derivable. For a two-parameter Weibull distribution, the shape parameter represents the degree of scatter and is a function of only the COV and can be determined as:

$$COV = \frac{\sqrt{\Gamma\left(1+\frac{2}{\alpha}\right) - \Gamma^2\left(1+\frac{1}{\alpha}\right)}}{\Gamma\left(1+\frac{1}{\alpha}\right)} \quad \textbf{Eq. 4-4}$$

where Γ is the gamma function. For the purpose of simplification, two approximations are often used to relate the Weibull shape parameter and the COV with a high degree of accuracy (Haldar, 2000) as follows:

$$COV \approx \alpha^{-0.926} \quad \textbf{Eq. 4-5}$$

and

$$COV \approx \frac{1.2}{\alpha} \quad \textbf{Eq. 4-6}$$

Eq. 4-6 was selected for this research based on the fact that it provides more conservative estimates of the shape parameter than Eq. 4-5. A relation between the mean to the shape parameter and the scale parameter can be expressed by:

$$\text{Mean} = \beta\ \Gamma\left(1+\frac{1}{\alpha}\right) \quad \textbf{Eq. 4-7}$$

Based on the empirical formulae described above, if the mean and COV are known, the Weibull shape and scale parameters can be estimated as the following, respectively:

$$\alpha = \frac{1.2}{COV} \quad \textbf{Eq. 4-8}$$

$$\beta = \frac{\text{Mean}}{\Gamma\left(1+\frac{1}{\alpha}\right)} \quad \textbf{Eq. 4-9}$$

The results of the Weibull parameters estimated using Eq. 4-8 and Eq. 4-9 were compared to the parameters estimated from the MLE method and the results of the comparison are also shown in Table 4-1.

Table 4-1. Weibull Shape Parameter Comparison

Property	Material System	Weibull Parameters			
		MLE Method		Empirical Formula	
		α (Shape)	β (Scale)	α (Shape)	β (Scale)
Tensile Strength [MPa]	SIKA	33.41	2543.56	36.27	2543.19
	SCCI	44.10	2781.77	53.19	2780.14
	FYFE	29.58	2276.81	32.32	2275.97
	SIKA+SCCI+FYFE	12.98	2599.14	13.38	2596.19
Tensile Modulus [GPa]	SIKA	29.49	140.56	31.76	140.51
	SCCI	25.15	134.86	27.18	134.82
	FYFE	18.40	114.47	20.79	114.39
	SIKA+SCCI+FYFE	12.48	132.81	11.89	132.81
Tensile Strain	SIKA	21.01	0.01862	22.55	0.01618
	SCCI	21.94	0.02099	25.08	0.02097
	FYFE	20.62	0.01998	20.79	0.01999
	SIKA+SCCI+FYFE	10.08	0.01957	15.35	0.02040

The parameters estimated using the two methods for each material system for each tensile characteristic of interest are graphically compared for ease of comparison as shown in Table 4-2 through Table 4-5.

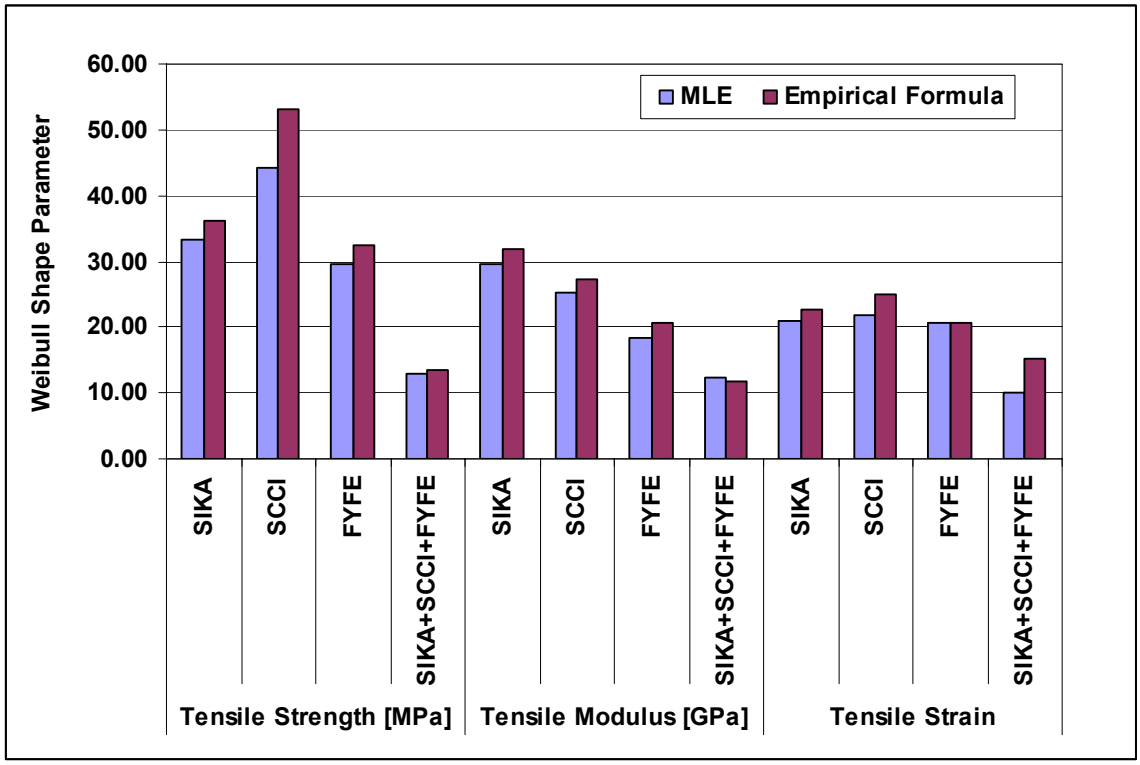

Figure 4-2. Comparison of Weibull Shape Parameters

Figure 4-2 shows that the shape parameters estimated using the empirical formulae are slightly higher than those obtained from the MLE method. The larger shape parameter represents a smaller variation in the data, and therefore lower COVs. It means that the empirical formula method provides less conservative estimates than the MLE method for the shape parameter. However, due to the fact that the MLE method cannot be solved in closed-form, while the empirical formula method can be solved easily based on the given mean and COV, and that the empirical formula method still provides reasonably close estimates, the empirical formula method is preferred over the MLE method as a means of estimating the shape parameter.

In order to select an appropriate method of parameter estimation, the scale parameters estimated based on the two methods for each property for all sets of material systems were compared as shown in Figures 4-3 - 4-5.

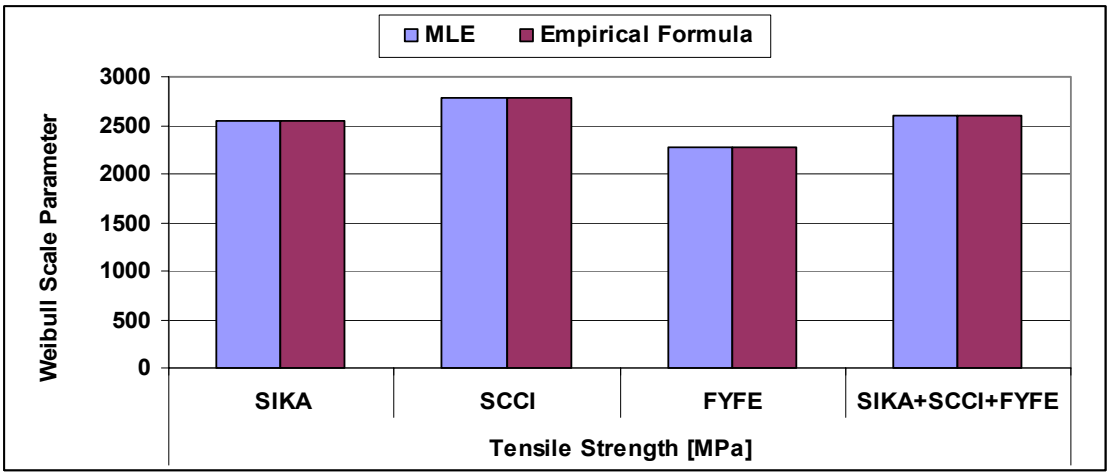

Figure 4-3. Comparison of Weibull Scale Parameters for Tensile Strength

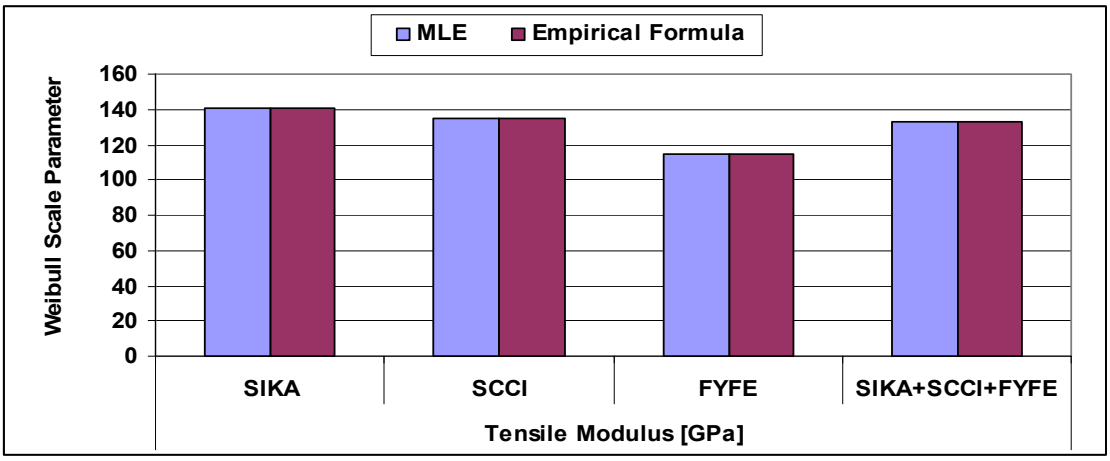

Figure 4-4. Comparison of Weibull Scale Parameters for Tensile Modulus

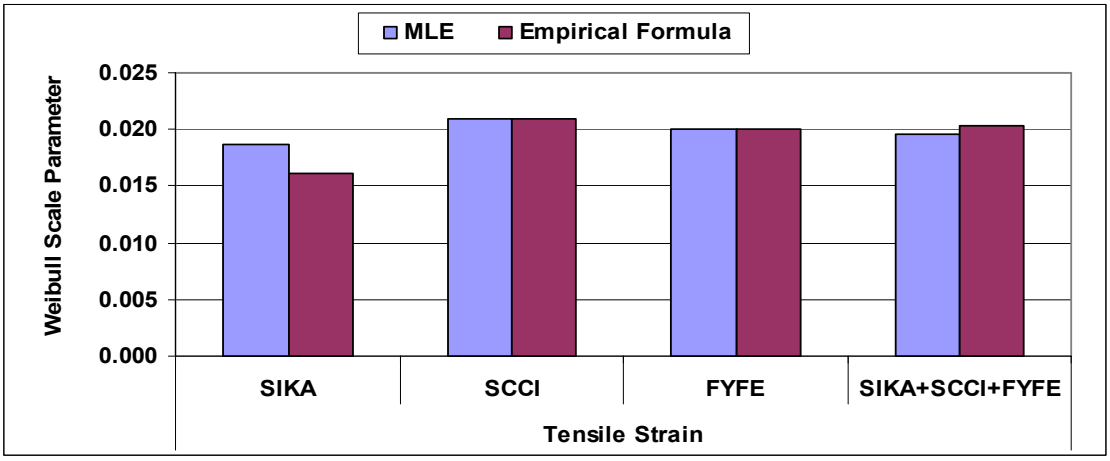

Figure 4-5. Comparison of Weibull Scale Parameters for Tensile Strain

The above comparisons of the estimated scale parameters show that the two methods give almost exactly the same estimates for strength and modulus, and slightly different estimates for strain. Overall, the two methods perform comparably for scale parameter estimation.

For the purpose of selecting an appropriate method of parameter estimation for the current research, it must be emphasized that the method selected should also be applicable to the set of durability data described in Chapter 3. As shown by Eq. 4-3, the accuracy of the MLE estimates for Weibull parameters is dependent on the sample size. The fact that the durability data consists of maximum of 5 samples for each set of data makes it inadequate for use of the MLE method for parameter estimation. Therefore, the empirical formula method was selected as the method of parameter estimation for the purposes of this study. The estimated Weibull parameters using the empirical method for the durability data are summarized in Table 4-2 through Table 4-4.

Table 4-2. Weibull Parameters Estimated Using the Empirical Formula Method for SIKA Strips

Condition	Exposure Level	Time [weeks]	Tensile Strength		Tensile Modulus		Tensile Strain	
			α (Shape)	β (Scale)	α (Shape)	β (Scale)	α (Shape)	β (Scale)
Control	Stored in a controlled humidity chamber at 30% RH and 23ºC	0	53.73	2490.15	37.36	148.82	23.61	0.0174
		8	-	-	-	-	-	-
		24	32.34	2431.22	49.45	148.01	23.98	0.0167
		48	58.79	2435.64	61.69	148.65	51.04	0.0166
		72	81.49	2401.36	51.50	149.32	43.09	0.0164
		96	17.67	2448.39	33.24	150.09	25.57	0.0164
Immersed in Deionized Water	22.8 ºC	0	47.25	2867.66	33.83	171.39	22.30	0.0172
		8	16.31	2782.68	38.12	169.74	17.29	0.0166
		24	20.56	2742.42	12.92	166.94	7.57	0.0179
		48	58.76	2474.83	24.78	163.88	17.75	0.0158
		72	19.64	2334.24	40.35	161.75	14.04	0.0148
		96	23.79	2319.35	32.14	163.51	15.46	0.0146
	37.8 ºC	0	47.25	2867.66	33.83	171.39	22.30	0.0172
		8	46.94	2435.73	46.06	169.89	32.75	0.0146
		24	14.47	2485.35	19.15	165.39	14.70	0.0155
		48	33.41	2197.40	16.25	165.01	14.39	0.0141
		72	14.34	2214.01	52.38	154.95	14.61	0.0144
		96	30.31	2184.27	39.28	157.69	42.52	0.0140
	60.0 ºC	0	47.25	2867.66	33.83	171.39	22.30	0.0172
		8	14.47	2319.08	89.55	167.20	16.42	0.0139
		24	12.88	2252.83	84.32	158.30	12.33	0.0144
		48	45.96	2042.18	11.29	163.22	11.53	0.0136
		72	23.50	2102.66	50.58	153.73	20.52	0.0139
		96	26.26	2052.41	98.93	155.64	28.74	0.0132
Immersed in Alkali Solution	22.8 ºC	0	47.25	2867.66	33.83	171.39	22.30	0.0172
		8	76.54	2186.21	27.07	169.54	29.77	0.0133
		24	29.01	2231.06	18.73	166.19	17.27	0.0140
		48	36.81	2031.85	9.09	165.89	8.41	0.0137
		72	25.49	2124.79	28.90	161.57	15.66	0.0136
		96	42.74	2074.02	23.56	160.33	29.63	0.0133
Immersed in NaCl Solution	5% NaCl at 22.8 ºC	0	47.25	2867.66	33.83	171.39	22.30	0.0172
		8	13.16	2534.84	46.67	169.04	10.71	0.0153
		24	9.40	2562.02	23.41	169.10	13.00	0.0153
		48	77.90	2352.13	13.37	171.14	13.23	0.0148
		72	17.70	2292.87	28.25	162.07	15.47	0.0145
		96	40.29	2200.19	46.69	161.73	29.74	0.0138

Table 4-3. Weibull Parameters Estimated Using the Empirical Formula Method for SCCI Strips

Condition	Exposure Level	Time [weeks]	Tensile Strength		Tensile Modulus		Tensile Strain	
			α (Shape)	β (Scale)	α (Shape)	β (Scale)	α (Shape)	β (Scale)
Control	Stored in a controlled humidity chamber at 30% RH and 23ºC	0	35.18	2765.42	17.67	142.71	13.45	0.0205
		8	29.91	2630.06	25.98	142.68	15.88	0.0191
		24	-	-	-	-	-	-
		48	24.88	2651.88	22.93	141.32	11.60	0.0197
		72	24.36	2679.60	64.86	141.35	18.11	0.0193
		96	14.51	2700.19	51.50	140.11	16.88	0.0194
Immersed in Deionized Water	22.8 ºC	0	32.00	2815.71	17.17	145.21	13.31	0.0205
		8	34.11	2800.77	55.36	141.97	48.96	0.0198
		24	12.44	2698.72	31.78	137.66	12.46	0.0200
		48	28.64	2645.31	34.44	136.54	21.24	0.0197
		72	191.38	2683.06	26.88	135.68	30.41	0.0205
		96	28.98	2722.92	70.00	135.53	39.77	0.0202
	37.8 ºC	0	32.00	2815.71	17.17	145.21	13.31	0.0205
		8	29.88	2845.89	78.79	142.22	45.94	0.0200
		24	-	-	-	-	-	-
		48	15.60	2686.76	52.91	137.05	14.89	0.0198
		72	28.34	2625.85	30.32	136.36	15.53	0.0196
		96	9.71	2573.98	17.51	138.03	11.16	0.0191
	60.0 ºC	0	32.00	2815.71	17.17	145.21	13.31	0.0205
		8	22.87	2753.59	53.35	140.95	28.18	0.0197
		24	-	-	-	-	-	-
		48	38.27	2601.45	55.25	141.42	22.38	0.0188
		72	19.50	2345.69	59.22	135.10	16.56	0.0176
		96	16.47	2284.07	60.78	133.63	20.30	0.0171
Immersed in Alkali Solution	22.8 ºC	0	32.00	2815.71	17.17	145.21	13.31	0.0205
		8	17.88	2639.62	20.77	145.47	10.42	0.0191
		24	-	-	6.74	148.21	-	-
		48	-	-	20.33	141.78	-	-
		72	20.49	2573.46	24.92	134.84	20.64	0.0195
		96	59.72	2530.99	33.01	133.62	31.07	0.0194
Immersed in NaCl Solution	5% NaCl at 22.8 ºC	0	32.00	2815.71	17.17	145.21	13.31	0.0205
		8	24.21	2759.75	115.22	143.38	26.09	0.0193
		24	14.00	2796.99	16.18	144.94	8.14	0.0206
		48	17.70	2776.26	65.00	135.74	14.07	0.0208
		72	63.27	2674.89	99.27	135.60	62.03	0.0198
		96	47.83	2690.79	77.42	136.48	98.67	0.0197

Table 4-4. Weibull Parameters Estimated Using the Empirical Formula Method for FYFE Strips

Condition	Exposure Level	Time [weeks]	Tensile Strength		Tensile Modulus		Tensile Strain	
			α (Shape)	β (Scale)	α (Shape)	β (Scale)	α (Shape)	β (Scale)
Control	Stored in a controlled humidity chamber at 30% RH and 23ºC	0	68.37	2421.53	44.13	124.24	36.54	0.0199
		8	-	-	-	-	-	-
		24	144.54	2407.70	68.37	122.64	44.57	0.0200
		48	32.34	2499.29	144.54	121.07	46.00	0.0206
		72	44.13	2434.62	68.37	121.79	35.81	0.0202
		96	32.34	2416.84	144.54	120.50	36.00	0.0201
Immersed in Deionized Water	22.8 ºC	0	57.96	2505.88	45.15	128.35	33.59	0.0199
		8	-	-	-	-	-	-
		24	41.39	2496.27	23.57	126.37	25.82	0.0204
		48	12.24	2090.27	44.87	126.88	11.38	0.0167
		72	11.18	1797.48	21.64	127.77	8.12	0.0147
		96	25.21	1661.37	26.22	124.37	12.97	0.0139
	37.8 ºC	0	57.96	2505.88	45.15	128.35	33.59	0.0199
		8	-	-	-	-	-	-
		24	87.69	2462.23	24.43	124.16	21.28	0.0207
		48	136.91	1971.70	29.14	120.80	29.49	0.0169
		72	25.81	1756.46	9.05	125.17	9.59	0.0155
		96	23.82	1603.75	30.05	116.41	36.56	0.0139
	60.0 ºC	0	57.96	2505.88	45.15	128.35	33.59	0.0199
		8	-	-	-	-	-	-
		24	14.52	2501.09	35.05	112.03	13.31	0.0228
		48	29.71	1996.71	22.52	112.97	16.90	0.0184
		72	54.61	1578.05	14.95	113.97	12.82	0.0149
		96	24.32	1530.32	13.85	114.23	11.94	0.0143
Immersed in Alkali Solution	22.8 ºC	0	57.96	2505.88	45.15	128.35	33.59	0.0199
		8	-	-	-	-	-	-
		24	47.62	2442.96	68.10	117.82	79.59	0.0208
		48	24.18	1830.43	19.50	119.29	46.61	0.0156
		72	22.54	1706.21	18.57	119.07	11.26	0.0151
		96	43.35	1710.56	39.54	112.47	72.20	0.0153
Immersed in NaCl Solution	5% NaCl at 22.8 ºC	0	57.96	2505.88	45.15	128.35	33.59	0.0199
		8	-	-	-	-	-	-
		24	52.27	2407.88	22.43	123.34	20.26	0.0204
		48	127.91	1845.91	50.37	120.48	44.03	0.0156
		72	22.41	1714.65	15.12	123.01	12.10	0.0148
		96	39.86	1606.78	25.11	119.51	19.60	0.0140

4.2.3 Determination of the Weibull Characteristic Value

As discussed previously, the characteristic value is specified as a certain percentile of test results or manufacturer reported data. With the shape and scale parameters estimated using the empirical formula method discussed in the previous section, the p^{th} percentile of the Weibull distribution, i.e., that value for which $P\left[X < x_p\right] = p$, is defined by

$$x_p = \beta\left[-\ln\left(1-p\right)\right]^{1/\alpha} \qquad \textbf{Eq. 4-10}$$

where p represents the probability that the actual value will be less than the characteristic value.

Based on Eq. 4-10, the Weibull characteristic values that are equivalent to the characteristic values determined based on the approach used by the existing design guidelines for a certain percentile can be computed. As previously discussed in Chapter 2, among the current design guidelines, some use a certain percentile value while others use Eq. 2-1 with different values of the *n* factor to define their characteristic values. To illustrate the method of determining the Weibull characteristic values, three commonly used definitions of the characteristic value used in the current design guidelines were selected and the equivalent Weibull characteristic values for each definition are then determined based on the same percentiles derived from the definitions of the design guidelines. The three definitions selected herein are $\mu - 3\sigma$, as used in ACI 440 (2002);

$\mu - 2\sigma$, as used in TR 55 (2004); and the 5th percentile value, as used in CHBDC (CSA 2006). The corresponding percentiles are 0.0015, 0.025, and 0.05, respectively. A summary of the comparison of the results is provided in Table 4-5, using the value of α and β from Table 4-1 in Eq. 4-10.

Table 4-5. Comparisons of Equivalent Weibull Characteristic Values to Current Guideline Characteristic Values

Property	Material System	*p*=0.0015			*p*=0.025			*p*=0.05		
		μ - 3σ [ACI 440] [1]	Weibull	P.D.[%]	μ - 2σ [TR 55] [2]	Weibull	P.D.[%]	μ - 1.64σ [CHBDC] [3]	Weibull	P.D.[%]
Tensile Strength [MPa]	SIKA	2256.03	2125.89	-6.12	2338.88	2298.09	-1.78	2368.71	2343.25	-1.09
	SCCI	2564.73	2460.25	-4.25	2626.79	2594.47	-1.25	2649.13	2629.14	-0.76
	FYFE	1988.19	1861.22	-6.82	2071.26	2031.26	-1.97	2101.17	2076.12	-1.21
	SIKA+SCCI+FYFE	1825.79	1597.19	-14.31	2049.74	1972.60	-3.91	2130.36	2079.46	-2.45
Tensile Modulus [GPa]	SIKA	122.44	114.50	-6.93	127.66	125.15	-2.00	129.54	127.97	-1.23
	SCCI	114.63	106.13	-8.00	120.46	117.76	-2.29	122.56	120.86	-1.41
	FYFE	92.16	83.67	-10.15	98.60	95.85	-2.87	100.91	99.16	-1.77
	SIKA+SCCI+FYFE	88.69	76.86	-15.40	101.54	97.48	-4.16	106.16	103.45	-2.63
Tensile Strain	SIKA	0.01327	0.01213	-9.46	0.01411	0.01375	-2.68	0.01442	0.01418	-1.65
	SCCI	0.01757	0.01618	-8.61	0.01855	0.01811	-2.46	0.01891	0.01862	-1.51
	FYFE	0.01610	0.01462	-10.15	0.01723	0.01675	-2.87	0.01763	0.01733	-1.77
	SIKA+SCCI+FYFE	0.01509	0.01336	-12.99	0.01663	0.01606	-3.59	0.01719	0.01681	-2.23

Notes:

[1]American Concrete Institute (ACI). (2002). "Guide for the design and construction of externally bonded FRP systems for strengthening concrete structures." ACI Committee 440, Report 440.2R-02, ACI, Farmington Hills, MI.

[2]Technical Report (TR) 55. (2004). "Design guidance for strengthening concrete structures using fibre composite materials (2nd Ed.)." The Concrete Society, UK.

[3]Canadian Highway Bridge Design Code (CHBDC). (2006). CAN/CSA-S6-06, Canadian Standards Association (CSA), Ontario,Canada.

***p* represents the percentile value.**

P.D. = Percent Difference = $\left(\frac{\text{Weibull - Guideline}}{\text{Guideline}}\right)\times 100\%$

As shown in Table 4-5, it is apparent that the equivalent Weibull characteristic values are lower than the corresponding design guideline characteristic values for the same percentiles. For reliability purposes, using the design guideline characteristic values is inadequate due to the fact that the definitions of their characteristic values are not based on the type of distribution which best describes the data of interest. Therefore, the proposed method of determining the Weibull characteristic values is more suitable for reliability-based design and provides more appropriate and reliable material properties especially since time-dependent effects need to be included based on these values.

4.2.4 Proposed Method for Consideration of Time-Dependent Degradation of FRP Properties

The proposed method to consider the material degradation for the current research is based on an estimated service life of the FRP materials. With a known value of intended service life, the mean value of the predicted material property at that point in time can be calculated using predictive equations of material deterioration determined based on data from accelerated degradation tests. With this approach of using the degradation predictive equations, environmental effects can be determined on a continuum basis. Application of the environmental deterioration determined from the accelerated degradation tests allows the material property values to be calculated accurately for reasonable levels of expected service life. The factors developed in this method consider the reliability, exposure environment, and intended service life of the

FRP strengthening. Details related to the development of the predictive equations and the environmental factors will be discussed in Chapter 5.

The reliability of a material system over a given time period can be evaluated using the distribution of the maximum load during that period and the distribution of minimum material resistance. Assuming that the information of the maximum load distribution is the same as that used with other conventional materials, such as steel and concrete, and therefore is already known, only the information of the distribution of material resistance at any given time needs to be defined. The information required includes the distribution describing the degraded state and the distribution parameters specific to the time step of interest. For the purposes of this investigation, it is assumed that the distribution form does not change as the composite degrades over time. Therefore, for the two-parameter Weibull distribution, the shape parameter at time zero is assumed to be constant throughout the time period. To illustrate the method for consideration of time-dependent degradation behavior, a simplified schematic is provided in Figure 4-6.

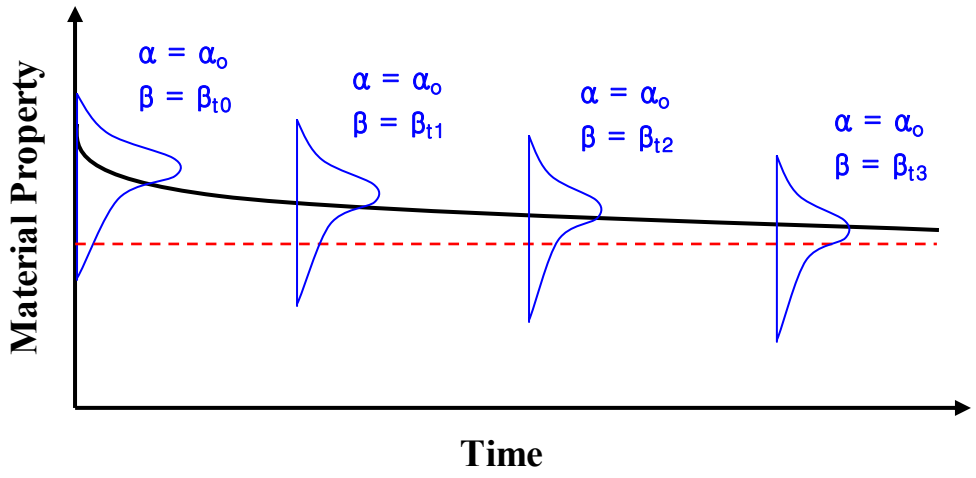

Figure 4-6. Schematic of Reliability Assessment of Time-Dependent Degradation Behavior

The solid curve line represents the degradation of the FRP material property of interest while the red dotted line represents a prescribed threshold of the design value. The distributions with a constant shape parameter but varying scale parameters are represented in the schematic.

To illustrate the application procedure of this method, it is assumed that a set of mean and COV values for a material system is provided by a manufacture or through standardized qualification testing. The Weibull shape parameter can be estimated using Eq. 4-8 and is assumed to be constant with time. In order to further describe the distribution of degraded properties, only the mean at the degraded state is needed. The implementation of predictive equations allows the determination of the mean values at any given time within the service life of the FRP strengthened structure. For a specific time step, with the shape parameter and the mean value known, the corresponding Weibull scale parameter can be calculated using Eq. 4-9. Then, all the information required to assess the reliability at a given time is attained. The reliability can be determined by calculating the probability of failure of the material system at a given time step. This method allows the determination of the change in probability of failure as a function of time and type of exposure and therefore provides a better perspective of the time-dependent degradation behavior. The design values determined based on this method can be used in design with sufficient confidence that the value of the material will not fall below the expected threshold during the service life of the FRP strengthened component or structure. Details related to the application of this method will be further discussed in Chapter 6 thorough the demonstration of design examples.

4.2.5 Consideration of Statistical Uncertainty due to Limited Data

The empirical formula method of parameter estimation discussed in Section 4.3.2 does not account for statistical uncertainty that arises from the fact that the Weibull shape and scale parameters are estimated from a sample of limited size. In order to accurately determine the Weibull characteristic value, this source of uncertainty due to limited data must be considered. Bain (1991) presents a method for determining the confidence interval for the p - percentile value of the Weibull distribution, as shown in Eq. 4-10, that only depends on the desired probability percentile, p, the confidence level desired, γ, and the sample size. The fact that the confidence interval is only a function of the sample size for a given set of p and γ makes this method attractive (Zureick et al., 2006). The use of confidence intervals provides information on the accuracy of the parameter estimates. The equation for this method is given by:

$$x_{p,\gamma} = x_p \exp\left(-\frac{U_\gamma}{\sqrt{n}\cdot\alpha}\right) \qquad \textbf{Eq. 4-11}$$

where α is the estimate of the shape parameter, n is the sample size, x_p is the p - percentile value, $x_{p,\gamma}$ is the lower tolerance limit of x_p with a confidence level of γ, and U_γ is a parameter depending the sample size and the desired confidence level. The parameter U_γ is tabulated as a function of sample size and confidence level and can be taken from Table 4A of Bain (1991) which is reproduced for purposes of reference in Appendix C. As an example of this method of calculating the design strength with a

confidence factor, the 90th percent confidence of the 5th percentile of the sample size of 35 tensile specimens for the combined material system, SIKA+SCCI+FYFE, is shown here as an example. The estimated shape and scale parameters based on the empirical formula method are 13.38 and 2596.19 MPa, respectively as listed in Table 4-1. From Eq. 4-10, the 5th percentile value is determined as

$$x_{0.05} = 2596.19\left[-\ln\left(1-0.05\right)\right]^{1/13.38} = 2079.35MPa\,.$$

The factor $U_\gamma = 1.393$ is taken from Table 4A of Bain (1991) and the term $\exp\left(-\frac{U_\gamma}{\sqrt{n}\cdot\alpha}\right)$ is determined to be

$$\exp\left(-\frac{1.393}{\sqrt{35}\times 13.38}\right) = 0.983\,.$$

Then, from Eq. 4-11, the value of tensile strength for which there is 90% confidence that 95% of the population is above this value can be computed as

$$x_{0.05,0.90} = \left(0.983\right)\left(2079.35\right) = 2044.00MPa\,.$$

This method of considering the statistical uncertainty due to a sample of limited size will be used when incorporating the durability data with a small sample size $\left(\approx 5\right)$ into the current data with a larger sample size $\left(\geq 35\right)$ for the investigation in Chapter 5.

4.2.6 Assessment of Material Reliability

The reliability of a material system rather than a structure, where the interaction between the load and resistance variables is more complicated than that of a material system, is the focus of this section. The reliability of a material system is the probability that the material will not fail, or more accurately, reach a limit state (Melchers, 1999). In order to accurately assess the reliability of the material for a prescribed limit state, it is important to use an appropriate method for the determination of reliability. Due to the difficulties in computing the exact probability of failure, and the typically small numbers involved, the reliability index, β, has been developed as a measure of structural or material reliability (Madsen, 1986). Among many different methods that are currently available for determining β, β is conventionally related to the probability of failure through the standard normal distribution through Eq. 4-12 (Atadero, 2005).

$$p_f = \Phi(-\beta) \qquad \textbf{Eq. 4-12}$$

where Φ is the cumulative standard normal distribution. This relation is valid only if all the associated random variables are normal and the limit state function is linear. Often, it is used for nonnormal variables as a means of defining a generalized reliability index when only the probability of failure is known (Atadero and Karbhari, 2005). However, using Eq. 4-12 for nonnormal variables will not accurately describe a relation between β and p_f and therefore results in misleading estimates of the reliability of the material system for a given probability of failure. Since the tensile properties of the FRP material

systems considered in the current research were modeled as the Weibull variables, it is necessary to use a more suitable, reliable method for reliability computation. To this end, the use of the Mean Value First Order Second Moment (MVFOSM) method was proposed herein.

The MVFOSM method defines the reliability index, β, as (Madsen, 1986):

$$\beta = \frac{\mu_z}{\sigma_z} \qquad \textbf{Eq. 4-13}$$

where μ_z and σ_z are the mean and standard deviation of a limit state function, Z, respectively. To illustrate the definition of β, a schematic is provided in Figure 4-7.

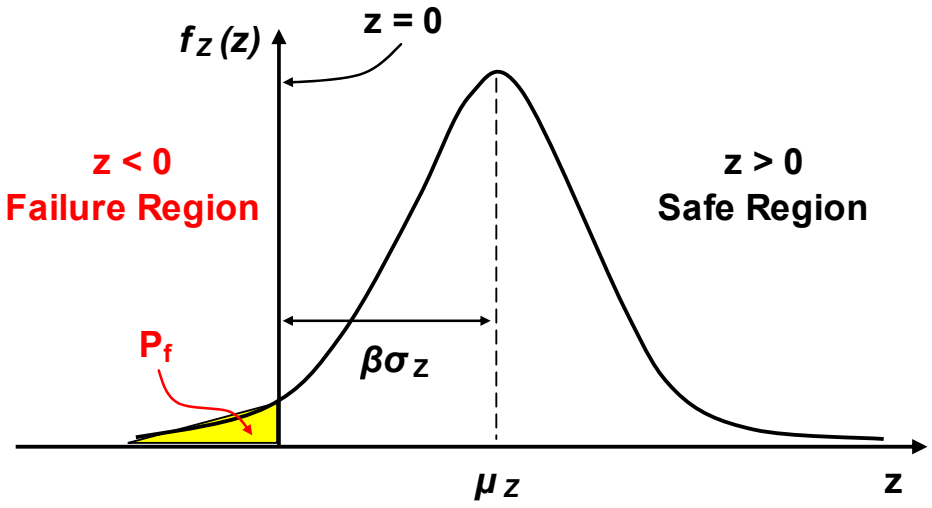

Figure 4-7. Schematic of Definition of Reliability Index, β , for Limit-state function Z (Madsen, 1986)

For a two-variable problem, such as variables of strength, R, and stress, S, the limit state function, Z, is linear as given by

$$Z = (R - S) \quad \textbf{Eq. 4-14}$$

and

$$\mu_z = \mu_R - \mu_S \quad \textbf{Eq. 4-15}$$

$$\sigma_z = \sqrt{\sigma_R^2 + \sigma_S^2} \quad \textbf{Eq. 4-16}$$

where R and S represents the resistance of the material system and the load demand placed of the material, respectively. Eq. 4-13 can be expressed as:

$$\beta = \frac{\mu_R - \mu_S}{\sqrt{\sigma_R^2 + \sigma_S^2}} \quad \textbf{Eq. 4-17}$$

In this derivation, the probability distributions have not been specified and thus can be either normal or nonnormal distributions; the reliability index β depends only on measures of mean, μ_z, and standard deviation, σ_z, in the limit state function. However, to compute reliability or probability of failure, a relation between β and p_f must be established, and thus the probability distribution of the variables in the limit state equation should be known (Madsen, 1986). It must be noted that this method can introduce significant errors under two conditions: (1) when the limit state function is nonlinear, and (2) when multiple load variables counteract one another (Ellingwood,

1982). However, these two conditions are ineffective to the current investigation because the limit state function considered is linear and it involves with a single tensile load case. Therefore, the use of the MVFOSM is validated herein.

To illustrate the application of this method for Weibull variables, the two-parameter Weibull distribution is used to derive a relation between β_{R} and p_f. Note that the subscript R is used to differentiate the reliability index, β_{R}, from the Weibull scale parameter, β_{w}, for this example. Given that R is the FRP tensile strength and S represents the tensile stress placed on the FRP material, it is logical to assume that all variables of R and S are uncorrelated and thus statistically independent (Haldar, 2000). Provided that R can be described by the two-parameter Weibull distribution as determined in Chapter 3, it is also assumed that all variables of S follow the Weibull distribution. Then, the reliability index of this relation can be expressed as:

$$\beta_{\mathrm{R}} = \frac{\mu_{\mathrm{R}}^{\mathrm{w}} - \mu_{\mathrm{S}}^{\mathrm{w}}}{\sqrt{\left(\sigma_{\mathrm{R}}^{\mathrm{w}}\right)^2 + \left(\sigma_{\mathrm{S}}^{\mathrm{w}}\right)^2}} \qquad \textbf{Eq. 4-18}$$

where $\mu_{\mathrm{R}}^{\mathrm{w}}$ and $\mu_{\mathrm{S}}^{\mathrm{w}}$ are the corresponding mean values of the Weibull variables of R and S, respectively, and $\sigma_{\mathrm{R}}^{\mathrm{w}}$ and $\sigma_{\mathrm{S}}^{\mathrm{w}}$ are the standard deviations of the Weibull variables of R and S, respectively. Assuming that the applied tensile stress is controlled with high accuracy and therefore the load is a constant, the standard deviation of the tensile stress variable is negligible ($\sigma_{\mathrm{S}}^{\mathrm{w}} = 0$) (Haldar, 2000). Thus, the constant value of the tensile

stress can be considered to be the material threshold value below which the material will be considered to have failed as:

$$S_o = \mu_S^w \quad \textbf{Eq. 4-19}$$

Eq. 4-18 can be simplified and rewritten in terms of the material threshold value, S_o, as:

$$S_o = \mu_R^w - \beta_R \sigma_R^w \quad \textbf{Eq. 4-20}$$

From the definitions of the Weibull COV and mean, as shown in Eq. 4-4 and Eq. 4-7, respectively, the Weibull standard deviation, σ_R^w, can be derived as:

$$\sigma_R^w = \beta_w \sqrt{\Gamma\left(\frac{2}{\alpha_w}+1\right) - \Gamma\left(\frac{1}{\alpha_w}+1\right)^2} \quad \textbf{Eq. 4-21}$$

where α_w and β_w represent the Weibull shape and scale parameters, respectively.

Based on the definition of the probability of failure of the Weibull distribution (See Eq. 4-1), a relation between β_R and p_f can be established as:

$$P_f = 1 - \exp\left\{-\left(\frac{\mu_R^w - \beta_R \sigma_R^w}{\beta_w}\right)^{\alpha_w}\right\} \quad \textbf{Eq. 4-22}$$

Reliability-based design is based on achieving a certain reliability level, often expressed as a target reliability index, β_T (Zureick, 2004). As discussed previously in Chapter 2, the target reliability index depends on the mode and the consequences of approaching various limit states. Ellingwood suggested that, for FRP materials, the target reliability index be set to approximately 3.5 because they exhibit little ductility while the reliability index for other construction materials, such as hot-rolled steel, cold-formed steel, reinforced or prestressed concrete, and engineered wood elements designed by LRFD specifications fall in the range of 2.2 – 3.0 (Ellingwood, 2003). Details related to the investigation of target reliability index for FRP materials can be found in previous research (Ellingwood, 2003; Zureick; 2004; Atadero, 2006).

For the purposes of this investigation, the two equations relating β_R and p_f, as shown in Eq. 4-12 and Eq. 4-22, are compared by determining the probabilities of failure for three different target reliabilities, β_R=2.5, 3.0, and 3.5, for the tensile strength data of all material systems considered in the current research. A summary of the input parameters used for this comparison is provided in Table 4-6, and the results are shown in Table 4-7.

Table 4-6. Input Parameters Derived from the Tensile Strength Data

Experimental Data	
Mean [MPa]	2497.64
Standard Deviation [MPa]	223.95
Weibull Parameter Estimates	
α (shape)	13.38
β (scale)	2596.19
Equivalent Weibull Parameter	
Mean [MPa]	2497.62
Standard Deviation [MPa]	227.88

Table 4-7. Comparison of the Probabilities of Failure Computed from the Conventional Method and the Mean Value FOSM Method

β_T	**Conventional Method Using the Standard Normal Relation (See Eq. 4-12)**	**Mean Value FOSM Method (See Eq. 4-22)**
2.5	0.00621	0.01848
3.0	0.00135	0.00822
3.5	0.00023	0.00346

It must be noted here that the conventional method using Eq. 4-12 is based on assumption that all variables of R and S are described by a Normal distribution while in fact the variables can be better described by the Weibull distribution. It is clear from Table 4-7 that the computation of the probability of failure for a given target reliability significantly depends on the method of reliability computation. The fact that the MVFOSM method considers the type of distribution used to model the material property of interest instead of blindly assuming a Normal distribution and gives more accurate and thus accurate

estimates of the probability of failure makes it more attractive for reliability computation. With using Eq. 4-21, the Weibull material design value for a given target reliability can be obtained. The application of the MVFOSM for determining the Weibull design values will be demonstrated in Chapter 6.

Chapter 5. Predictive Analysis of FRP Material Degradation

In order to accurately determine the reliability-based design values of FRP materials, it is critical to consider the time-dependent degradation behavior of the materials. To this end, it is essential to define the limits of use of the FRP materials. These limits can be used to define the extent of allowable degradation of material performance characteristics beyond which the originally intended reliability of the material can no longer be guaranteed. Due to lack of an extensive validated database regarding long-term durability, degradation, and service life for FRP materials, long-term safety is often accounted for through the use of empirically selected high factors of safety (Abanilla and Karbhari, 2006). The use of these empirical factors often results in inefficient, unreliable design due to inaccurate representation of the material performance characteristics over time. Therefore, a more reliable approach that is suitable for reliability-based design is desired.

This chapter discusses a predictive approach which can accurately estimate the time-dependent performance characteristics of FRP materials and thus is more suitable to reliability-based design than the empirical factor based approach. The predictive approach discussed herein is developed based on the use of the Arrhenius rate relationship which provides a basis for the use of results from an accelerated aging model to convert short-term experimental results into long-term predictions of material properties. In this approach, the rates of material degradation are assumed to be a function of exposure condition and time. The implementation of this approach facilitates

the determination of long-term durability of the material systems considered in the current research and the correlation of their degradation to levels of service life and capacity of FRP strengthened structures. Service life predictions of material properties are made incrementally to a maximum of 50 years. This chapter provides the background to the use of the Arrhenius rate relationship and its implementation for the development of predictive equations. Description of the input data obtained from the aforementioned durability tests is presented. The degraded properties predicted by the theoretical predictive equations are compared to the experimental durability data obtained over a 96 week period of exposure and also to the factored values recommended by ACI 440 (2002) to illustrate the differences between current guideline assumptions and realistic material values for common environmental exposures. The predictive analysis is extended further to determine environmental factors to consider the effects of various exposure conditions of FRP strengthening applications.

5.1 The Arrhenius Degradation Model

The fundamental step to predictive analysis is to select an appropriate model to describe the relationship between the material property of interest and the parameter representing the material degradation characteristics. Among many available degradation models, the Arrhenius model which is based on the use of the Arrhenius rate relationship is widely used to characterize rates of degradation due to increases in temperature as a means of achieving acceleration (Nelson, 2004). It is commonly accepted for FRP materials (Abanilla and Karbhari, 2006) and thus is selected as the basis for the following

degradation analysis of prefabricated FRP materials. It must be noted that this model is based on several assumptions: (1) degradation is not reversible, (2) the model only applies to a single degradation process (i.e. mechanism or failure mode), and (3) degradation of specimen performance before the initiation of exposure is negligible.

In the Arrhenius rate relationship, the degradation rate is expressed as follows (Nelson, 2004):

$$k = Ae^{-\frac{E_a}{RT}} \quad \textbf{Eq. 5-1}$$

where k is the rate of degradation (1 / time), A is a reaction constant dependent on the material and degradation process, E_a is the activation energy, R is the universal gas constant ($1.38\times10^{-23}\frac{J}{K}$), and T is the absolute temperature in Kelvin. As mentioned previously, this model assumes that the single dominant degradation mechanism of the material will not change with time and temperature during the exposure, but the rate of degradation will be accelerated with an increase in temperature. Eq. 5-1 can be transformed into

$$\frac{1}{k} = \frac{1}{A}e^{\frac{E_a}{RT}} \quad \textbf{Eq. 5-2}$$

$$\ln\left(\frac{1}{k}\right) = \frac{E_a}{R}\frac{1}{T} - \ln(A) \quad \textbf{Eq. 5-3}$$

From Eq. 5-2, the degradation rate k can be expressed as the inverse of time needed for a material property to reach a given value. It is observed in Eq. 5-3 that the logarithm of time required for a material property to reach a given value is a linear function of $\frac{1}{T}$ with the slope of $\frac{E_a}{R}$. The relationship shown in Eq. 5-3 describes a time-temperature superposition method and provides a basis for the development of predictive equations of performance properties in the form

$$P(t) = \frac{P_0}{100}\left[B \ln(t) + C\right] \qquad \textbf{Eq. 5-4}$$

where $P(t)$ is the predicted degraded property at time t (in days), P_0 is the initial material property at time zero (i.e. in the unexposed condition), B is a constant denoting degradation rate, and C is a material constant. The constant B determines the behavior of the degradation trend line and therefore controls the property retention values determined by each predictive equation. Details related to the development of the predictive equations will be discussed in Section 5.3.

5.2 Experimental Durability Testing and Data

As discussed previously in Section 3.2.1.1, the durability data from previous research (Yang and Karbhari, 2008) were used for this predictive analysis. In this test, tensile properties of specimens were measured before and after the exposures, since changes in tensile property values can be used as a measure of the durability performance.

The durability tensile specimens were immersed in five different exposure conditions: (1) deionized water at 23 °C, (2) deionized water at 37.8 °C, (3) deionized water at 60 °C, (4) 5% NaCl solution at 23 °C , and (5) concrete based alkali solution with a pH of 12 at 23 °C. An additional set of specimens was stored in a controlled environment at 30 % relative humidity and at 23 °C and served as the control (baseline) condition.

It should be noted that only the data from the three test cases of immersion in deionized water at 23 °C, 37.8 °C, and 60 °C were used for the derivation of predictive equations based on the fact that predictions of long-term material behavior can be determined from the extrapolation of elevated temperature response using the Arrhenius model. The other two cases will later be used for the considerations of other environmental effects, such as alkali and sea-water conditions. For the purposes of this predictive analysis, the durability specimens were tested prior to the initiation of exposure and then at periods of 8, 24, 48, 72, and 96 weeks to obtain time-dependent degradation trends. Details related to the durability test results can be found in Section 3.2.1.1 (See Table 3-4 through Table 3-12). For the input data of the predictive analysis, the durability data were used in the form of percentage retention following Eq. 5-5:

$$\% \text{ Property Retention} = \frac{P(t)}{P_0} \times 100 \qquad \textbf{Eq. 5-5}$$

where $P(t)$ is the degraded material property at time t and P_0 is the initial property at time zero. A summary of the percent retention values is provided in Table 5-1.

Table 5-1. Percent Retentions of Experimental Tensile Property Data

Material System	Time [weeks]	Tensile Strength Retention [%]				Tensile Modulus Retention [%]				Tensile Strain Retention [%]			
		Control	23 ºC	37.8 ºC	60 ºC	Control	23 ºC	37.8 ºC	60 ºC	Control	23 ºC	37.8 ºC	60 ºC
SIKA	0	100	100	100	100	100	100	100	100	100	100	100	100
	8	-	95	85	79	-	99	100	99	-	96	85	80
	24	97	94	85	76	100	95	95	93	97	100	89	82
	48	98	86	76	71	100	95	95	93	97	91	81	77
	72	97	80	75	73	101	95	91	90	96	85	83	80
	96	96	80	76	71	101	95	92	92	96	84	82	77
SCCI	0	100	100	100	100	100	100	100	100	100	100	100	100
	8	95	100	101	97	101	100	100	99	94	99	100	98
	24	-	94	-	-	-	96	-	-	-	97	-	-
	48	95	94	94	93	100	95	96	99	96	97	97	93
	72	96	97	93	82	101	94	95	95	95	102	96	86
	96	96	97	88	80	100	95	95	94	95	101	92	85
FYFE	0	100	100	100	100	100	100	100	100	100	100	100	100
	8	-	-	-	-	-	-	-	-	-	-	-	-
	24	100	99	99	97	99	97	96	87	101	102	103	112
	48	102	81	79	79	98	99	94	87	104	82	85	91
	72	100	69	69	63	98	98	94	87	102	71	75	73
	96	99	66	63	60	98	96	90	87	101	68	70	70
SIKA+SCCI+FYFE	0	100	100	100	100	100	100	100	100	100	100	100	100
	8	-	-	-	-	-	-	-	-	-	-	-	-
	24	-	96	-	-	-	95	-	-	-	100	-	-
	48	98	86	83	82	100	97	95	95	98	88	87	86
	72	97	82	77	74	100	97	93	92	96	85	82	80
	96	97	80	75	71	101	96	93	92	96	82	80	77

5.3 Procedure for Prediction of Material Degradation

To illustrate the determination of predictive equations for time-dependent degradation, an example of the procedure as applied to the analysis of strength data related to SIKA system is presented in this section.

The experimental data for the strength of system SIKA is shown in Table 5-2.

Table 5-2. Experimental Results of Strength Retention for SIKA Strip

Time [weeks]	23 °C	37.8 °C	60 °C
0	100.0	100.0	100.0
8	95.1	84.9	78.9
24	94.3	84.6	76.4
48	86.5	76.3	71.2
72	80.2	75.3	72.5
96	80.0	75.7	70.9

Note: Units for retention are in %.

The resulting relationship between strength retention and time for each test temperature is given in Figure 5-1.

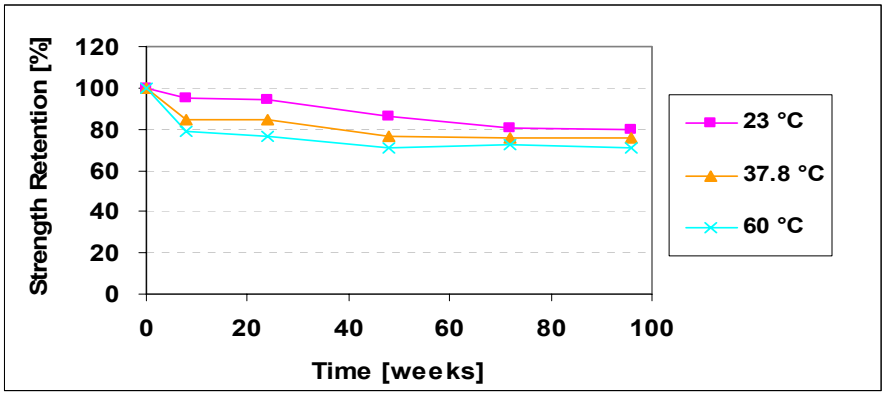

Figure 5-1. Strength Retention vs. Time for SIKA

Using the Arrhenius relationship model, this system can be linearized by taking the natural log of the time. This results in the relationships shown in Figure 5-2, with time being expressed in days.

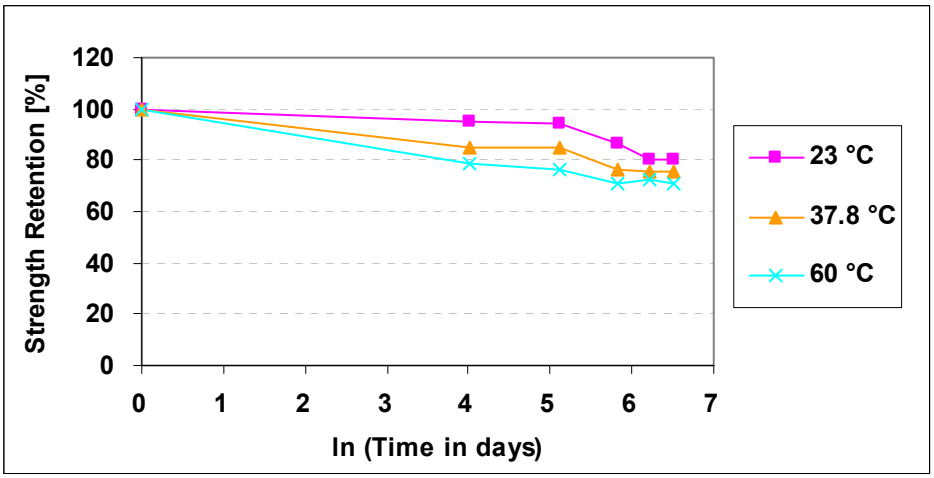

Note: Initial time is assumed at 1day.

Figure 5-2. Strength Retention vs. ln (Time) for SIKA

Assuming a linear relationship between strength retention and the natural log of time in days, a curve fit may be applied to the data shown in Figure 5-2 to obtain idealized relationships. The use of a least squares curve fit on the previous relationships results in idealized linear relationships between strength and the natural log of time as given below in Table 5-3.

Table 5-3. Linear Relationship between Strength and Natural Log of Time

Temperature	Equation	R^2
23 ˚C	$\sigma(t) = \sigma_i \left(1.0513 - 0.0334 \ln(t)\right)$	0.7484
37.8 ˚C	$\sigma(t) = \sigma_i \left(1.0314 - 0.0430 \ln(t)\right)$	0.9606
60 ˚C	$\sigma(t) = \sigma_i \left(1.0212 - 0.0503 \ln(t)\right)$	0.9698

Note: R^2 represents the least square test statistic.

These equations can then be used for extrapolation of material response to longer time periods.

With the strength retention versus time relation linearized, the retention versus temperature relation is considered. The relation between strength retention and temperature varies with each time step. As mentioned previously, it is also a function of the inverse temperature and can therefore be plotted as shown in Figure 5-3.

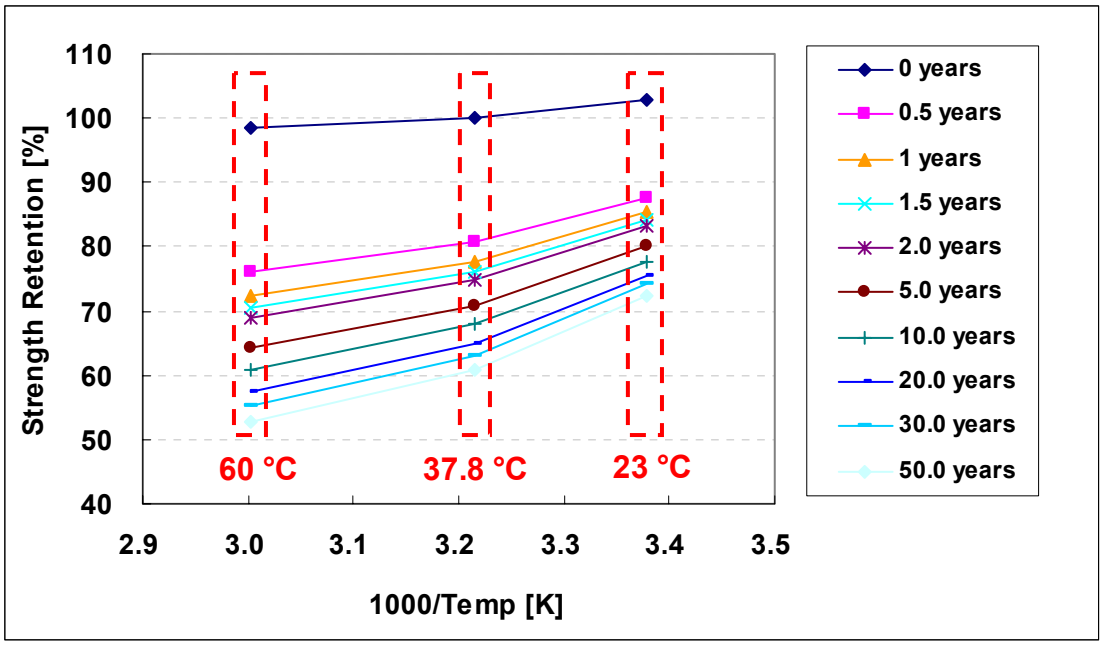

Note: Initial time is assumed at 1day.

Figure 5-3. Strength Retention vs. Inverse Temperature for SIKA

The use of a least squares curve fit on the previous relationships results in idealized linear relationships between strength and the inverse of temperature as given below in Table 5-4.

Table 5-4. Linear Relationship between Strength and the Inverse of Temperature

Time [years]	Equation	R^2
0.0	$\sigma(T) = \sigma_i \left(0.6574 + 0.1088\left(1000/T\right)\right)$	0.9467
0.5	$\sigma(T) = \sigma_i \left(-0.1716 + 0.3084\left(1000/T\right)\right)$	0.9666
1.0	$\sigma(T) = \sigma_i \left(-29.89 + 0.3390\left(1000/T\right)\right)$	0.9675
1.5	$\sigma(T) = \sigma_i \left(-37.34 + 0.3569\left(1000/T\right)\right)$	0.9679
2.0	$\sigma(T) = \sigma_i \left(-0.4262 + 0.3697\left(1000/T\right)\right)$	0.9682
5.0	$\sigma(T) = \sigma_i \left(-0.5945 + 0.4102\left(1000/T\right)\right)$	0.9690
10.0	$\sigma(T) = \sigma_i \left(-0.7218 + 0.4408\left(1000/T\right)\right)$	0.9695
20.0	$\sigma(T) = \sigma_i \left(-0.8491 + 0.4715\left(1000/T\right)\right)$	0.9699
30.0	$\sigma(T) = \sigma_i \left(-0.9236 + 0.4894\left(1000/T\right)\right)$	0.9701
50.0	$\sigma(T) = \sigma_i \left(-1.0174 + 0.5120\left(1000/T\right)\right)$	0.9704

Note: R^2 represents the least square test statistic.

The linear relationships determined by the curve fit of the strength retention and inverse temperature relationships evaluated for each time step at normal stress are used as the theoretical predictions of strength retention. The predictions for each time step can be combined to form a single theoretical relationship between strength retention and time at normal stress. This theoretical relationship is compared to the experimental results measured at normal stress. The difference between the theoretical and experimental relationship as shown in Figure 5-4 demonstrates the accuracy of the prediction of time-dependent degradation. The quantitative comparison is also provided in Table 5-5.

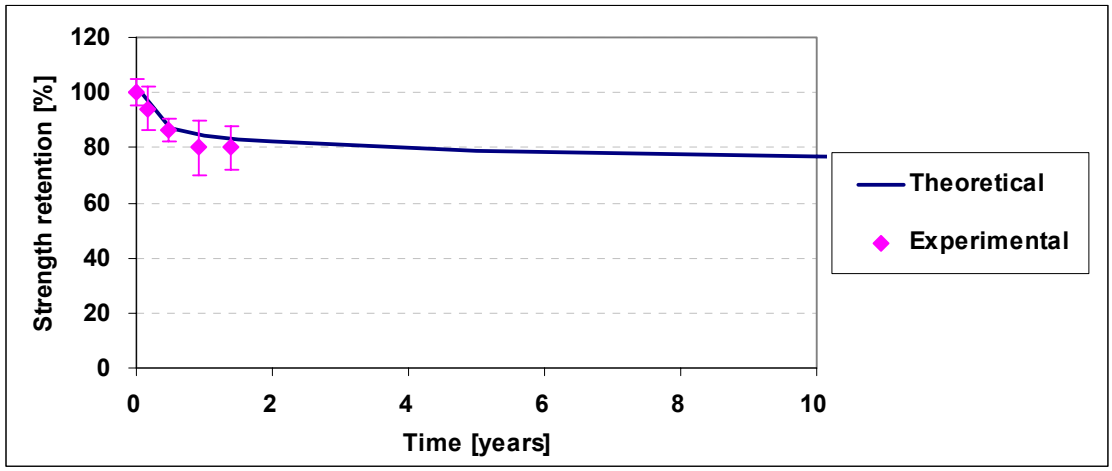

Figure 5-4. Comparison of Theoretical Prediction and Experimental Results for SIKA Strength Data

Table 5-5. Comparison of Theoretical Prediction and Experimental Results for SIKA Strength Data

Time [years]	Theoretical Strength Retention [%]	Experimental Strength Retention [%]	Percent Difference [%]
0.0	102.5	100.0	2.5
0.5	87.0	94.3	-7.8
1.0	84.6	86.5	-2.2
1.5	83.2	80.2	3.8
2.0	82.2	80.0	2.8
5.0	79.1	-	-
10.0	76.7	-	-
20.0	74.3	-	-
30.0	72.9	-	-
50.0	71.1	-	-

For this example procedure, the difference between the theoretical prediction and experimental relationships, as shown in Table 5-5, is reasonably small with a maximum percent difference of 7.8%. This result indicates good prediction of the degradation of the

strength over time. Finally, the strength retention versus time relationship shown in Figure 5-4 can be linearized by taking the natural log of the time and using the linear curve fit of the strength retention and the natural log of the time relationship. Then, the theoretical relationship can be derived as:

$$\sigma(t) = \sigma_i \left(1.0485 - 0.0344 \ln(t)\right) \quad \textbf{Eq. 5-6}$$

where σ_i is the initial FRP strip tensile strength and t is the time in days.

5.4 Proposed Predictive Equations

The procedure illustrated in Section 5.3 is applied to all material systems considered in the current research. The resulting predictive equations are provided in Table 5-6 and they may be used to more accurately design FRP rehabilitation systems considering their service life. As discussed in Section 3.2.1.1, it must be noted that the durability data from the previous research (Yang and Karbhari, 2008) are only used to characterize time-dependent degradation trends of the FRP material systems. The tensile properties obtained from the current research, as listed in Table 3-16, will be used as initial material properties at the zero time step and then incorporated into the theoretical predictive equations. A summary of the results of the theoretical predictive equations is provided in Table 5-6.

Table 5-6. Theoretical Predictive Equations

Data	Property	Theoretical Equation (at 23˚C)
SIKA	**Strength [MPa]**	$\sigma(t) = \sigma_i\left(1 - 0.03\ln(t)\right)$
	Modulus [GPa]	$E(t) = E_i\left(1 - 0.01\ln(t)\right)$
	Strain [mm/mm]	$\varepsilon(t) = \varepsilon_i\left(1 - 0.03\ln(t)\right)$
SCCI	**Strength [MPa]**	$\sigma(t) = \sigma_i\left(1 - 0.01\ln(t)\right)$
	Modulus [GPa]	$E(t) = E_i\left(1 - 0.01\ln(t)\right)$
	Strain [mm/mm]	$\varepsilon(t) = \varepsilon_i\left(1 - 0.01\ln(t)\right)$
FYFE	**Strength [MPa]**	$\sigma(t) = \sigma_i\left(1 - 0.05\ln(t)\right)$
	Modulus [GPa]	$E(t) = E_i\left(1 - 0.01\ln(t)\right)$
	Strain [mm/mm]	$\varepsilon(t) = \varepsilon_i\left(1 - 0.05\ln(t)\right)$
SIKA+SCCI+FYFE	**Strength [MPa]**	$\sigma(t) = \sigma_i\left(1 - 0.03\ln(t)\right)$
	Modulus [GPa]	$E(t) = E_i\left(1 - 0.01\ln(t)\right)$
	Strain [mm/mm]	$\varepsilon(t) = \varepsilon_i\left(1 - 0.03\ln(t)\right)$

Note: t is the time in days.

It should be noted that the coefficients in the theoretical equations were rounded such that the percent differences of the degraded properties predicted by the resulting equations with respect to those predicted by the original equations were less than 10%. This was done in an attempt to simplify the predictive equations in a more realistic and practical format to be used by design engineers in practice. The theoretical equations listed in Table 5-6 were transformed into the tensile property retention equations (i.e. $\sigma(t)/\sigma_i$, $E(t)/E_i$, and $\varepsilon(t)/\varepsilon_i$) and then were plotted to show the differences of the predictive degradation trends between the material systems (See Figure 5-5 through Figure 5-7).

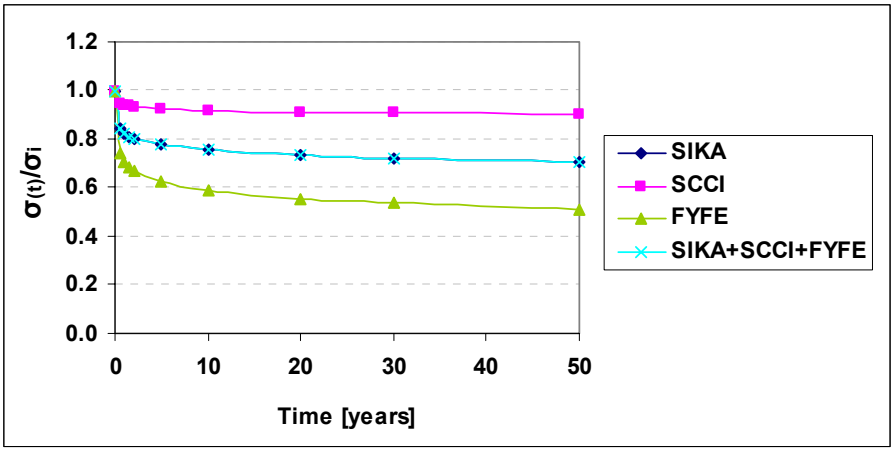

Figure 5-5. Theoretical Predictive Degradation of Tensile Strength

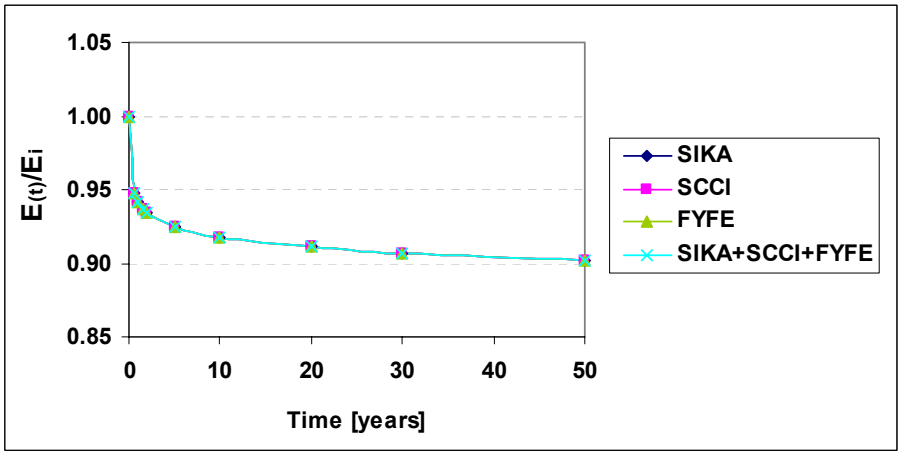

Figure 5-6. Theoretical Predictive Degradation of Tensile Modulus

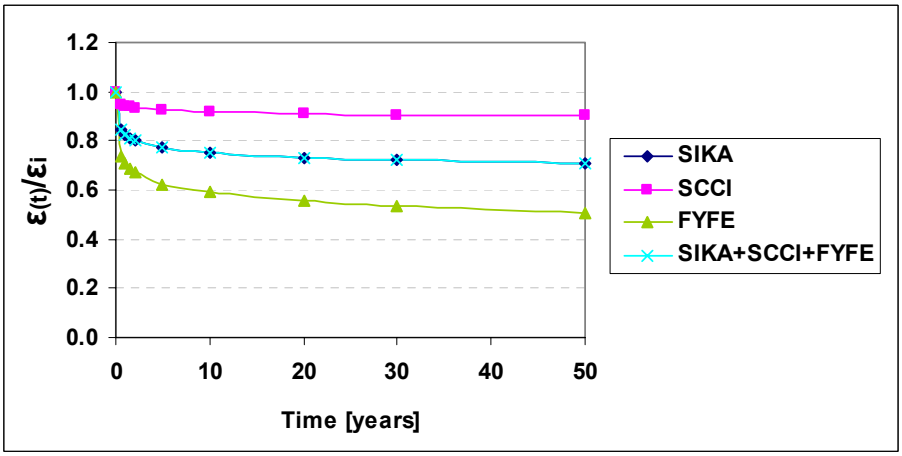

Figure 5-7. Theoretical Predictive Degradation of Tensile Strain

It is clearly shown in the above figures that there exists a large degree of variation within the predicted material properties for tensile strength and tensile strain, especially between SIKA and FYFE. This variation can be attributed to the intrinsic material variability and process details among the different material systems, such as different constitutive material properties and fiber volume fractions. This emphasizes the importance of using the reliability-based approach to more reliably characterize the time-dependent degradation behavior of different material systems and also the need to develop a standard procedure for manufacturing and testing of prefabricated FRP strips in order to produce more uniform products. As shown in Figure 5-6, no variation between the material systems is observed for the tensile modulus predictions since the theoretical equations for tensile modulus for all material systems were simplified to be identical as listed in Table 5-6. It must also be noted that unlike the recommendation specified by ACI 440 (2002), the degradation of tensile modulus over time is apparent and thus needs to be considered as well.

5.5 Consideration of Other Immersion Environments

The environments likely to be faced in the strengthening of concrete structures with externally bonded FRP include water, humidity, sea-water, alkaline solutions from moisture transport through the concrete, temperature excursions and cycling, and ultra-violet (UV) radiation (Abanilla and Karbhari, 2006). A methodology to account for these environmental effects when considering the time-dependent degradation of the FRP materials is discussed in this section. This approach is based on the use of partial safety

factors which can be applied to the already derived theoretical predictive equations for immersion in deionized water at 23 °C, which is considered to be a severe, but base environment for exposure of civil infrastructure. For the purposes of the current investigation, two exposure conditions are considered: (1) alkaline environment and (2) sea-water environment.

The environmental factors considered for FRP exposure to alkali and sea-water environments are denoted as F_{ALKALI} and F_{SALT}, respectively, and determined based on the experimental data obtained from the durability tests. These factors can then be directly applied to the derived predictive equations as:

$$P_E(t) = \frac{F_{ENV} \cdot P_0}{100}\left[B \ln(t) + C\right] \qquad \textbf{Eq. 5-7}$$

where $P_E(t)$ is the degraded material property at time t due to an exposure condition and F_{ENV} is the empirically derived environmental factor (F_{ALKALI} or F_{SALT}). To illustrate the derivation of the environmental factors, an example procedure to determine F_{ALKALI} for the tensile strength of material system SIKA is demonstrated herein.

The experimental data for the strength of system SIKA is shown in Table 5-7 and the relationship between strength retention and time for each exposure is plotted as shown in Figure 5-8.

Table 5-7. Experimental Results of Strength Data of SIKA for Immersion Environments

Time		Deionized water at 23 ºC		Alkali Solution at 23 ºC	
[weeks]	[days]	Strength [MPa]	Percent Strength Retention [%]	Strength [MPa]	Percent Strength Retention [%]
0	**0**	2833.87	100	2833.87	100
8	**56**	2693.99	95	2170.09	77
24	**168**	2671.56	94	2189.21	77
48	**336**	2451.22	86	2001.43	71
72	**504**	2271.35	80	2079.80	73
96	**672**	2266.99	80	2047.11	72

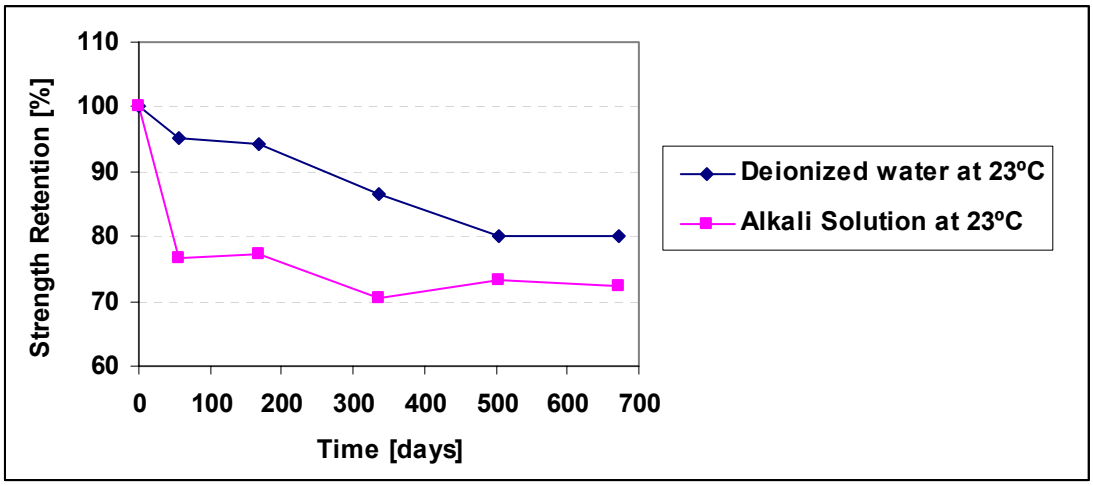

Figure 5-8. Strength Retention vs. Time for SIKA

When analyzing the two curves shown in Figure 5-8, it is important to determine the time period at which asymptotic response with an almost constant level of moisture gain is observed (Abanilla and Karbhari, 2006). For the current research, it was observed that such asymptotic response appeared after about 24 weeks (168 days) of immersion in most cases and thus only the data after this time period were used to determine the environmental factors.

The remaining data from the deionized and alkali conditions are then plotted and the resulting relationships are linearized by using a first order linear regression method as shown in Figure 5-9.

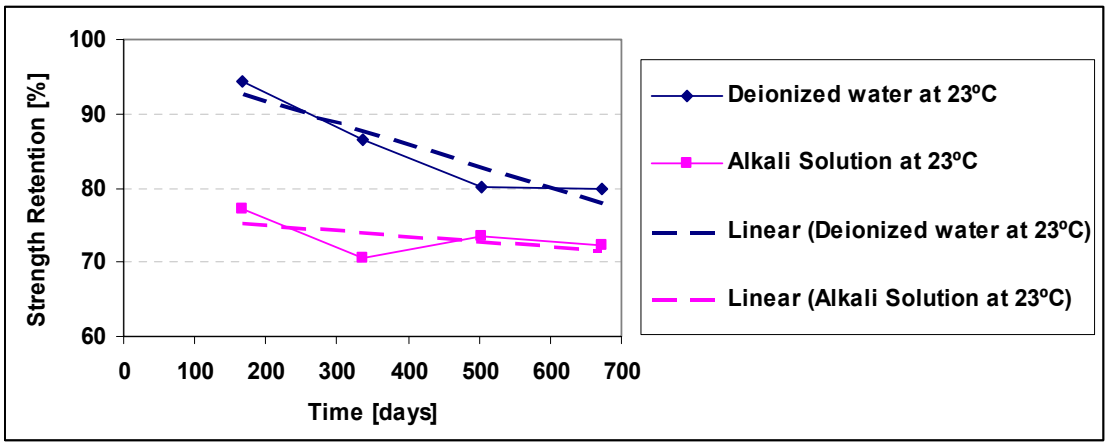

Figure 5-9. Linearized Curves of Deionized and Alkali Conditions

The resulting linearlized functions are:

$$\text{Deionized Condition: } \frac{\sigma(t)}{\sigma_0}\times 100\% = -0.0293(t) + 97.523 \qquad \textbf{Eq. 5-8}$$

$$\text{Alkali Condition: } \frac{\sigma(t)}{\sigma_0}\times 100\% = -0.0073(t) + 76.446 \qquad \textbf{Eq. 5-9}$$

Based on Eq. 5-8 and Eq. 5-9, a new set of data for each condition following the linearly approximated function is obtained and ratios of alkali condition to deionized condition are determined for each data point. Then, the environmental factor for the condition of interest is determined via error minimization of the original experimental data and the predicted data for a period of 96 weeks. For this example case, the environmental factor

for alkali condition, F_{ALKALI}, was determined to be 0.84. The difference between the original experimental data and the predicted data, as shown in Figure 5-10, demonstrates the accuracy of this approach.

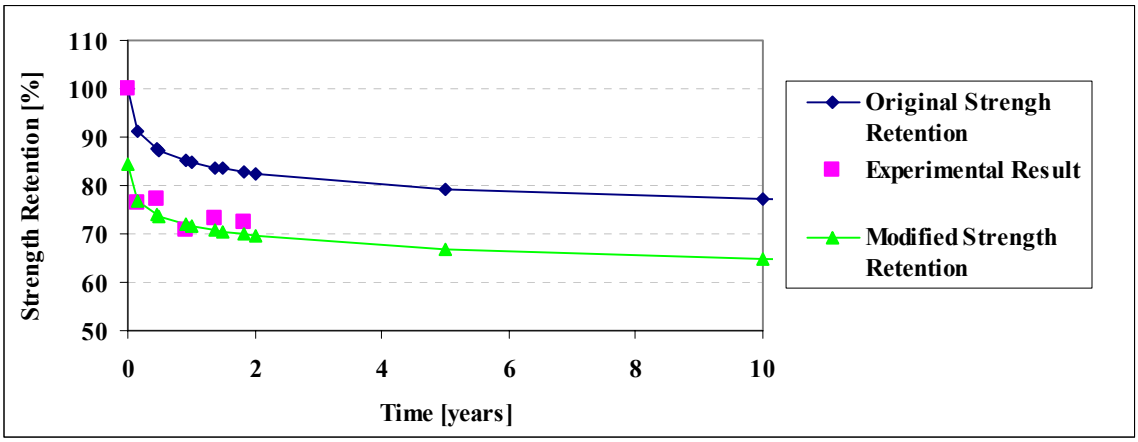

Figure 5-10. Comparison of Prediction and Experimental Results for SIKA Strength Data

The procedure presented in this section is applied to all material systems and a summary of the results of the environment factors, F_{ALKALI} and F_{SALT}, is provided in Table 5-8.

Table 5-8. Results of Environmental Factors for All Material Systems

Property	Material Systems	F_{ENV} [Exposure Condition]	
		F_{ALKALI} [Alkali Environment]	F_{SALT} [Sea-water Environment]
Tensile Strength	SIKA	0.84	0.96
	SCCI	0.96	1.00
	FYFE	0.84	0.82
	SIKA+SCCI+FYFE	0.88	0.97
Tensile Modulus	SIKA	0.99	1.00
	SCCI	0.99	1.00
	FYFE	0.94	0.97
	SIKA+SCCI+FYFE	0.97	0.99
Tensile Strain	SIKA	0.87	0.95
	SCCI	0.96	1.00
	FYFE	0.89	0.87
	SIKA+SCCI+FYFE	0.91	0.96

The differences of the environmental factors observed in Table 5-8 can be attributed to the differences in the constitutive material properties and the inherent material variability of the material systems considered herein. In most cases, the effects of exposure to alkaline solution are the most severe and this trend is the same as that from the previous durability study (Abanilla and Karbhari, 2006).

5.6 Application of Prediction Analysis to Determine Reliability-based Design Values

As discussed in Chapter 2, the use of safety factors in approaches recommended by the existing design guidelines, for example ACI 400 (2002) and TR 55 (2004), provides a means of assessing safety of performance. However, they are based on

empirical safety factors rather than on estimates of reliability. This empirical factor approach as a means of considering the time-dependent degradation behavior may provide an undesirable misconception to design engineers that there is a zero probability of failure until the prescribed threshold design value is reached. In the context of reliability engineering, this is not true since as the material degrades with time, the reliability of the material decreases accordingly. To accurately characterize the relationship between the material degradation behavior and the time-dependent reliability of the material, a predictive approach incorporating the predictive analysis discussed in this chapter with the use of the two-parameter Weibull distribution as a time-dependent performance distribution is proposed herein. This approach considers the change in probability of failure as a function of time and type of exposure and thus provides a more accurate, reliable means of assessing the reliability over time.

5.6.1 Issues with Current Guideline Approach

To address the issue of the empirical factor approach recommended by the aforementioned existing design guidelines and demonstrate use of the proposed predictive approach, two approaches, including the approach as prescribed by ACI 440 (2002), $C_E(\mu - 3\sigma)$, using $C_E = 0.85$ and the predictive approach as discussed in this section, are compared. This comparison is made for the tensile strength data for two cases, material system SIKA alone and the combined system, SIKA+SCCI+FYFE, and is graphically shown in Figures 5-11 and 5-12. The input data can be found in Table 3-16

for the tensile properties of the material systems considered and the predictive equation used herein is provided in Table 5-6.

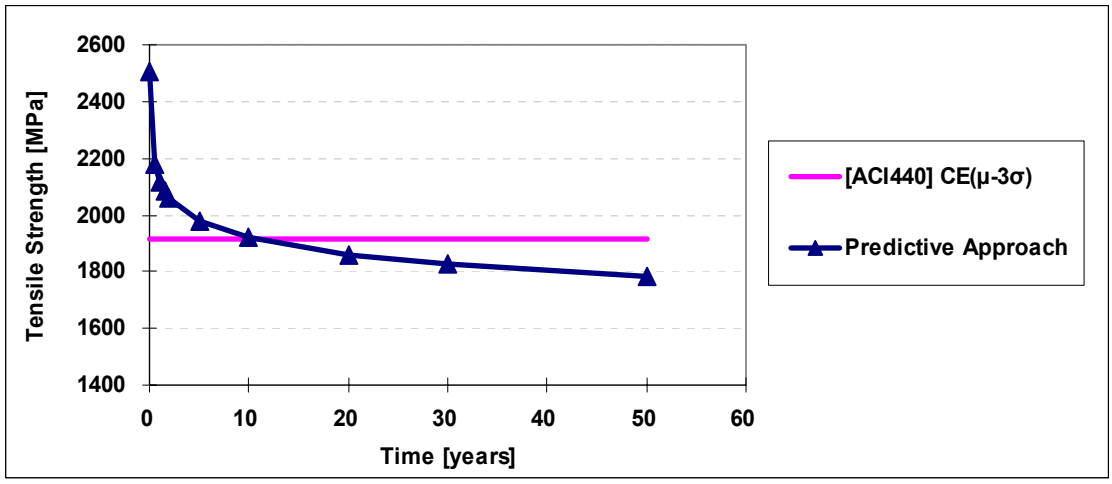

Figure 5-11. Graphical comparison of the predictive approach and guideline approach for SIKA Strength Data

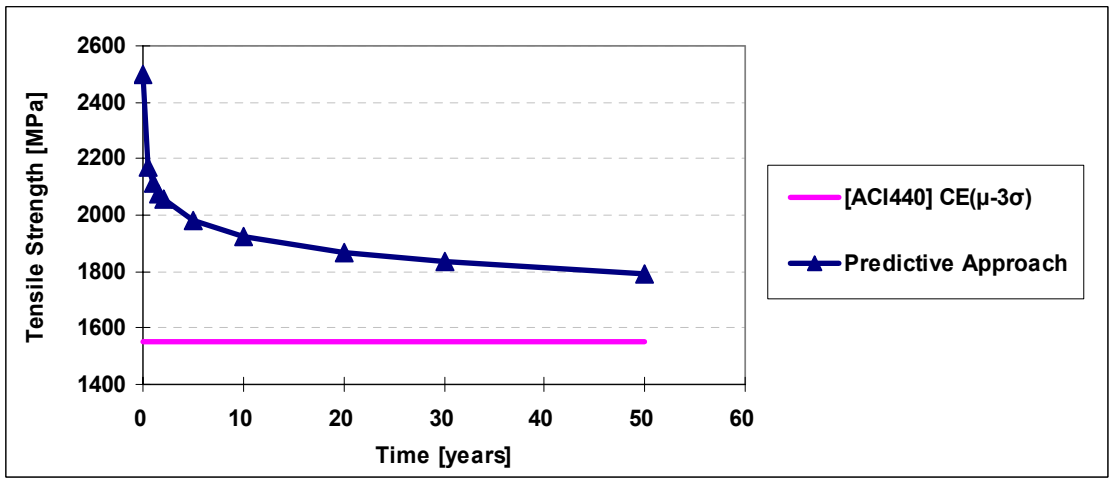

Figure 5-12. Graphical comparison of the predictive approach and guideline approach for SIKA+SCCI+FYFE Strength Data

As clearly shown in Figure 5-11, the predictive approach indicates that the mean capacity of the SIKA material will be exceeded by the guideline design value within less than 15 years. On the other hand, in the case shown in Figure 5-12, the guideline design value

will not be exceeded for over 100 years and is extremely conservative. This can be attributed to the fact that the empirical factor approach used by the design guidelines is generally based on the lack of detailed knowledge regarding degradation behavior and service life and therefore safety over extended periods of time is often assured through the use of exceedingly high and unrealistic factors of safety.

5.6.2 Incorporation of the Weibull Distribution into Predictive Analysis

The preceding predictive analysis described in Section 5.3 can be extended to include the distribution of data used in this current analysis and thus the two-parameter Weibull distribution is considered herein. As listed in Table 4-1, the parameters of the Weibull distribution for the current data have already been estimated from the experimental data based on Eq. 4-8 and Eq. 4-9. For the purposes of this study, the material properties of the durability data at time zero will be replaced by those of the current data based on the fact that the base-line data consists of larger sample size and thus are more representative and reliable. To this end, it is necessary to check the validity of the incorporation of the resulting Weibull parameters derived from the base-line data into the existing set of the parameters in the durability data. The Weibull parameters of the durability data for the initial time step were determined by the empirical formula method as discussed in Section 4.3.2 and the parameters estimated for the both test data are provided in Table 5-9. Graphical comparisons are made between the base-line data and the durability data for the estimated shape and scale parameters and the results are shown in Figures 5-13 – 5-16.

Table 5-9. Results of Weibull Parameters at Time Zero for the Base-Line Data and Durability Data

Property	Manufacturer	Base-Line Data		Durability Data	
		α (Shape)	β (Scale)	α (Shape)	β (Scale)
Tensile Strength	SIKA	36.27	2543.19	47.25	2493.61
	SCCI	53.19	2780.14	32.00	2769.55
	FYFE	32.32	2275.97	57.95	2425.04
	SIKA+SCCI+FYFE	13.38	2596.19	18.60	2607.83
Tensile Modulus	SIKA	31.76	140.51	33.83	149.04
	SCCI	27.18	134.82	17.17	142.83
	FYFE	20.79	114.39	45.16	124.21
	SIKA+SCCI+FYFE	11.89	132.81	13.57	140.43
Tensile Strain	SIKA	22.55	0.01618	22.42	0.01742
	SCCI	25.08	0.02097	13.31	0.02054
	FYFE	20.79	0.01999	33.59	0.01991
	SIKA+SCCI+FYFE	15.35	0.02040	15.86	0.01963

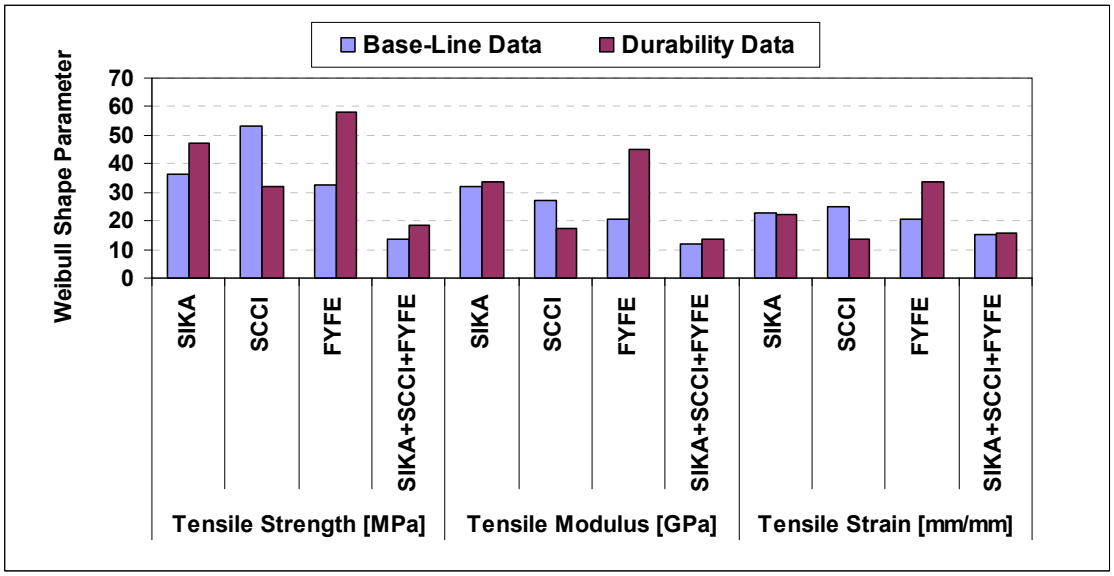

Figure 5-13. Graphical Comparison of the Base-Line Data and Durability Data for Weibull Shape Parameter Estimation

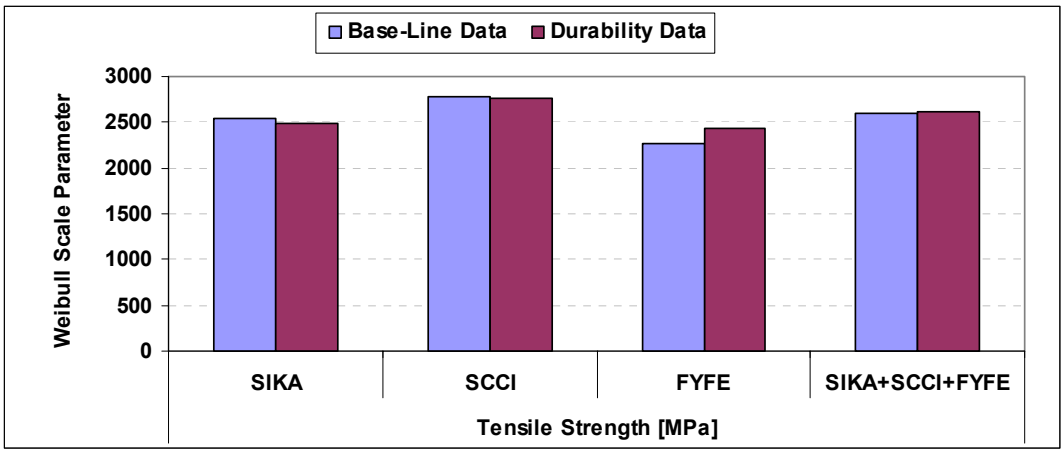

Figure 5-14. Graphical Comparison of the Base-Line Data and Durability Data for Weibull Scale Parameter Estimation for Tensile Strength

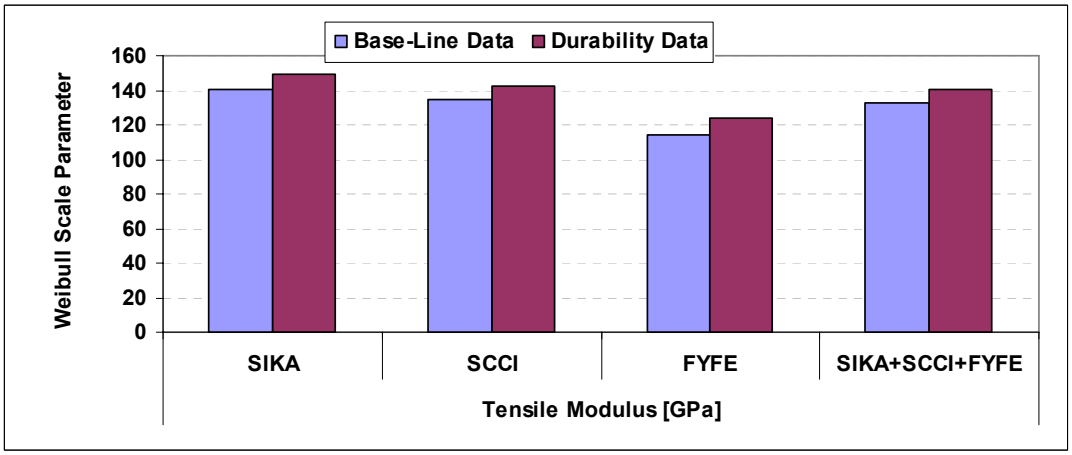

Figure 5-15. Graphical Comparison of the Base-Line Data and Durability Data for Weibull Scale Parameter Estimation for Tensile Modulus

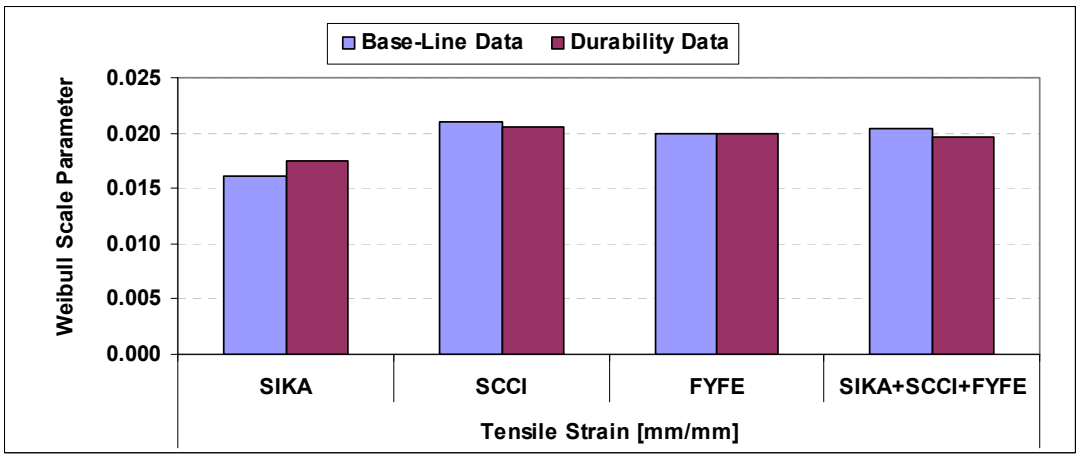

Figure 5-16. Graphical Comparison of the Base-Line Data and Durability Data for Weibull Scale Parameter Estimation for Tensile Strain

Figure 5-13 shows that the shape parameters of the base-line data for all material systems, except for SCCI, are lower than those of the durability data. The larger shape parameter represents a smaller variation in the data. It means that overall the shape parameters of the durability data are less conservative estimates than those of the base-line data. The above comparisons of the estimated scale parameters show that the two tests give only slightly different estimates for all tensile properties. Overall, the estimated scale parameters for the two tests are considered to be comparable. Based on the fact that the current data provides more conservative estimates of the shape parameters and are more accurate and representative due to larger sample size, the incorporation of the current data into the durability data for the initial time step can be validated.

As already mentioned in Section 4.3.4, the shape parameters of the zero time data are assumed to remain constant with time for the purpose of this study. This results in a common two-parameter Weibull distribution with a constant shape parameter, but with varying scale parameters over time. Applying this distribution to a derived predictive equation gives the following relationship:

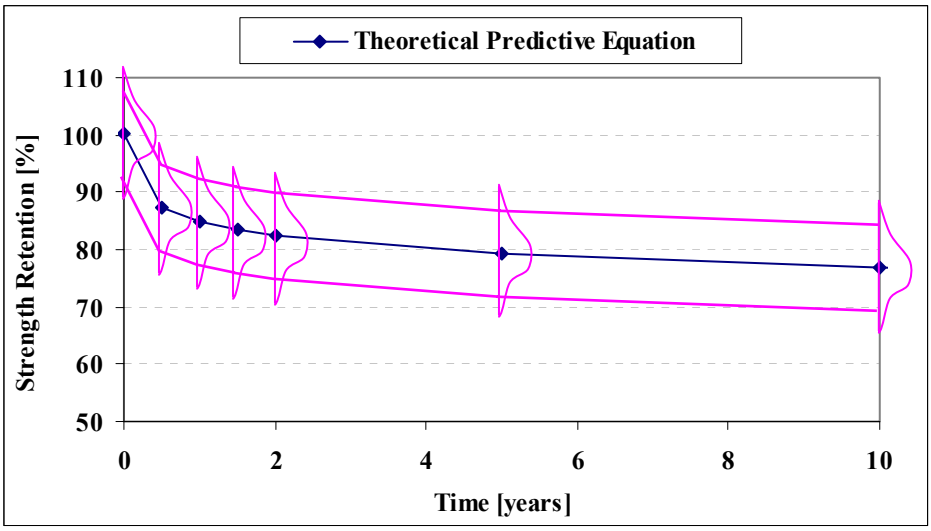

Figure 5-17. Theoretical predictive equation with time-based Weibull distribution

Figure 5-17 shows that all the theoretical relationships provided in Table 5-6 can be extended to include the two-parameter Weibull distribution along the degradation functions. The mean values of these distributions are described by the equations while retaining a constant shape parameter. This means that the mean value and the two Weibull parameters, shape and scale, at any given time can be obtained using the relationships presented in Section 4.3.2. With the information of these distribution parameters, it is possible to determine the actual range of property values and to accurately assess the probability of failure at any give time. Details related to the application of this predictive approach using the Weibull distribution will be further discussed in the following section .

5.6.3 Procedure for Assessment of Time-Dependent Material Reliability

The predictive analysis discussed in this chapter provides a means to assess the probability of failure of the material property of interest with respect to a prescribed design value at any given time. The effects of environmental exposure and time-dependent FRP material degradation behavior are considered based on approaches that are suitable for use with reliability-based design procedures. The change in probability of failure as a function of time and type of exposure provides a better understanding of reliability of the material for design than just knowing whether a value meets or exceeds an arbitrarily prescribed threshold. The predictive approach provides a means of determining the FRP design values such that the probability of failure of the material at the time of the expected service life remains within a tolerable range of design safety. In this approach, the performance characteristics of the material of interest can be more accurately and realistically predicted and thus more efficient and reliable design values can be achieved.

To illustrate the implementation of this predictive approach using the Weibull distribution as a time-based performance distribution, an example procedure to assess the time-dependent probability of failure is presented herein. Two cases of FRP design values are compared for this procedure. Case 1 is based on the empirical factor approach as prescribed by ACI 440 (2002) using the characteristic value with the environmental factor included, $C_{\mathrm{E}}\left(\mu - 3\sigma\right)$, as described in Chapter 2. The type of exposure is assumed as "exterior exposure" to simulate a typical FRP strengthening for concrete girders and

thus the environmental factor, C_E, is assumed to be 0.85. Case 2 is based on the predictive approach using the Weibull design value as discussed in Section 4.3. To illustrate the determination of the Weibull design value, a step-by-step procedure is provided herein.

(i) Assume the expected service life of the FRP strengthened structure. In this example, it is assumed to be 50 years ($t = 50 \text{ years} = 18250 \text{ days}$).

(ii) Predict the mean property of interest using a predictive equation at the expected service life. For the tensile strength property of material system SIKA, the mean strength at $t = 50 \text{ years}$ is predicted with the initial strength of 2504.59 MPa (as listed in Table 3-16) as:

$$\sigma_{t=50 \text{ years}} = 2504.59 \text{ MPa} \cdot \left(1 - 0.03 \ln(18250)\right) = 1767.34 \text{ MPa}$$

(iii) Select an appropriate environmental factor and apply it to the determined mean property value (See Eq. 5-7). To simulate a similar effect as ACI 440 assumes, $F_{\text{ALKALI}} = 0.84$ is selected from the Table 5-8 for the SIKA tensile strength and the factor is multiplied to the predicted property in step (ii) as:

$$\sigma_E(t) = F_{\text{ALKALI}} \cdot \sigma(t) = 0.84 \times 1767.34 \text{ MPa} = 1484.57 \text{ MPa}$$

(iv) Estimate the Weibull scale parameter at the time of interest from the modified mean and an assumed constant shape parameter. For the SIKA strength data, the estimated shape parameter is 36.27 as listed in Table 4-1. The scale parameter can be estimated by Eq. 4-9:

$$\beta = \frac{1484.57 \text{ MPa}}{\Gamma\left(1+\frac{1}{36.27}\right)} = 1507.45 \text{ MPa}$$

(v) Determine the FRP design value for a specific probability of failure which will be expected at the end of the service life. In this example, the FRP strength design value for SIKA is determined such that 30% probability of failure can be expected at $t = 50$ years. The Weibull design value can be determined using Eq. 4-10 with the assumed shape parameter and the estimated scale parameter as:

$$\text{Weibull Design Strength Value} = 1507.45 \text{ MPa}\left[-\ln\left(1-0.3\right)\right]^{1/36.27} = 1465.21 \text{ MPa}$$

Based on the above procedure, the determination of the Weibull design value can be simplified into an equation as:

$$\text{Weibull Design Value} = \frac{F_{\text{ENV}} \cdot \mu \cdot \left(1 - C \cdot \ln(365 \cdot t)\right)}{\Gamma\left(1+\frac{1}{\alpha}\right)}\left[-\ln\left(1-P_{\text{T}}\right)\right]^{1/\alpha} \qquad \textbf{Eq. 5-10}$$

where μ is the mean of the experimental results or manufacturer reported data, α is the Weibull shape parameter, which can be estimated from the COV using Eq. 4-6, C is a constant dependent on property and material system and is the same as the coefficient of the predictive equation as listed in Table 5-6, t is the expected service life, expressed in years, and P_T is the target probability of failure at the expected service life.

The above procedure is applied to all material systems for all tensile properties to determine the Weibull design values. The ACI 400 design values are also determined from the input properties as provided in Table 3-16. The results of the design values are shown in Table 5-10.

Table 5-10. Comparison of Weibull Design Values and ACI 440 Design Values

Material System	Strength [MPa]		Modulus [GPa]		Strain [mm/mm]	
	ACI 440	Weibull	ACI 440	Weibull	ACI 440	Weibull
SIKA	1917.63	1465.21	122.43	121.45	0.0157	0.0095
SCCI	2180.00	2360.85	114.64	115.89	0.0190	0.0174
FYFE	1689.95	943.31	92.17	92.28	0.0183	0.0086
SIKA+SCCI+FYFE	1551.92	1492.60	88.68	106.54	0.0175	0.0123

It must be noted here that the Weibull design values shown in Table 5-10 were determined based on a probability of failure expectancy of 30% at the end of the assumed service life. It should also be noted that the ACI 440 modulus design values were determined based on assuming no degradation over time ($C_E = 1$) and the ACI 440 strain

design values were determined based on the relationship of Hooke's law. As shown in Table 5-10, the differences of the derived design values between the two approaches are apparent and can be explained by the results of the comparisons of the time-dependent probabilities of failure determined based on the two cases of design values.

For each tensile property of each material system, using a predictive equation and an assumed Weibull shape parameter, the resulting time-varying Weibull shape parameter at a given time step can be determined. Then, the probability of failure of the material property of interest with respect to a selected design value at any given time can be calculated as:

$$P_{\mathrm{f}}(t) = 1 - \exp\left[-\left(\frac{x}{\beta(t)} \right)^{\alpha} \right]; \qquad \alpha, \beta \geq 0 \qquad \textbf{Eq. 5-11}$$

where α is the Weibull shape parameter which remains constant throughout the time, $\beta(t)$ is the time-varying Weibull shape parameter, and x is the selected design value of interest. This procedure is applied to the two design values considered in this section to determine the time-dependent probabilities of failure and the results are provided in Tables 5-11 – 5-14.

Table 5-11. Comparison Results of Time-Dependent Probaility of Failure of Case 1 and Case 2 for Material System SIKA

Property	Time [years]	Predicted Mean, P(t)	Modified Mean, P_{ENV}*P(t)	Weibull Parameters		Probabilty of Failure, $P_F(t)$	
				α (Shape)	β (Scale)	Case 1	Case 2
Tensile Strength [MPa]	**0.0**	2504.59	2103.86	36.27	2136.29	0.020	0.000
	0.5	2113.37	1775.23	36.27	1802.59	1.000	0.001
	1.0	2061.29	1731.48	36.27	1758.17	1.000	0.001
	1.5	2030.82	1705.89	36.27	1732.18	1.000	0.002
	2.0	2009.20	1687.73	36.27	1713.75	1.000	0.003
	3.0	1978.74	1662.14	36.27	1687.76	1.000	0.006
	5.0	1940.36	1629.90	36.27	1655.02	1.000	0.012
	10.0	1888.27	1586.15	36.27	1610.60	1.000	0.032
	15.0	1857.81	1560.56	36.27	1584.62	1.000	0.057
	20.0	1836.19	1542.40	36.27	1566.18	1.000	0.085
	30.0	1805.73	1516.81	36.27	1540.19	1.000	0.151
	50.0	1767.34	1484.57	36.27	1507.45	1.000	0.300
Tensile Modulus [GPa]	**0.0**	138.09	136.71	31.76	139.10	0.017	0.013
	0.5	130.90	129.59	31.76	131.86	0.090	0.071
	1.0	129.94	128.64	31.76	130.90	0.113	0.088
	1.5	129.38	128.09	31.76	130.33	0.128	0.101
	2.0	128.99	127.70	31.76	129.93	0.140	0.111
	3.0	128.43	127.14	31.76	129.37	0.159	0.126
	5.0	127.72	126.44	31.76	128.66	0.187	0.148
	10.0	126.76	125.50	31.76	127.69	0.231	0.184
	15.0	126.20	124.94	31.76	127.13	0.261	0.209
	20.0	125.81	124.55	31.76	126.73	0.284	0.228
	30.0	125.25	123.99	31.76	126.17	0.319	0.258
	50.0	124.54	123.30	31.76	125.46	0.369	0.300
Tensile Strain [mm/mm]	**0.0**	0.0158	0.0137	22.55	0.0141	1.000	0.000
	0.5	0.0133	0.0116	22.55	0.0119	1.000	0.006
	1.0	0.0130	0.0113	22.55	0.0116	1.000	0.011
	1.5	0.0128	0.0111	22.55	0.0114	1.000	0.015
	2.0	0.0127	0.0110	22.55	0.0113	1.000	0.020
	3.0	0.0125	0.0109	22.55	0.0111	1.000	0.028
	5.0	0.0122	0.0106	22.55	0.0109	1.000	0.042
	10.0	0.0119	0.0104	22.55	0.0106	1.000	0.077
	15.0	0.0117	0.0102	22.55	0.0104	1.000	0.109
	20.0	0.0116	0.0101	22.55	0.0103	1.000	0.140
	30.0	0.0114	0.0099	22.55	0.0102	1.000	0.197
	50.0	0.0111	0.0097	22.55	0.0099	1.000	0.300

Table 5-12. Comparison Results of Time-Dependent Probaility of Failure of Case 1 and Case 2 for Material System SCCI

Property	Time [years]	Predicted Mean, P(t)	Modified Mean, P_{ENV}*P(t)	Weibull Parameters		Probabilty of Failure, $P_F(t)$	
				α (Shape)	β (Scale)	Case 1	Case 2
Tensile Strength [MPa]	**0.0**	2750.92	2640.88	53.19	2668.93	0.000	0.001
	0.5	2607.69	2503.38	53.19	2529.96	0.000	0.025
	1.0	2588.62	2485.07	53.19	2511.46	0.001	0.037
	1.5	2577.46	2474.37	53.19	2500.64	0.001	0.046
	2.0	2569.55	2466.77	53.19	2492.97	0.001	0.054
	3.0	2558.40	2456.06	53.19	2482.14	0.001	0.067
	5.0	2544.34	2442.57	53.19	2468.51	0.001	0.089
	10.0	2525.28	2424.27	53.19	2450.01	0.002	0.130
	15.0	2514.12	2413.56	53.19	2439.19	0.003	0.162
	20.0	2506.21	2405.96	53.19	2431.51	0.003	0.188
	30.0	2495.05	2395.25	53.19	2420.69	0.004	0.232
	50.0	2481.00	2381.76	53.19	2407.06	0.005	0.300
Tensile Modulus [GPa]	**0.0**	132.13	130.81	27.18	133.47	0.016	0.021
	0.5	125.25	124.00	27.18	126.52	0.066	0.088
	1.0	124.33	123.09	27.18	125.60	0.080	0.106
	1.5	123.80	122.56	27.18	125.05	0.090	0.119
	2.0	123.42	122.18	27.18	124.67	0.097	0.128
	3.0	122.88	121.65	27.18	124.13	0.109	0.143
	5.0	122.21	120.99	27.18	123.45	0.125	0.165
	10.0	121.29	120.08	27.18	122.52	0.151	0.198
	15.0	120.76	119.55	27.18	121.98	0.169	0.220
	20.0	120.38	119.17	27.18	121.60	0.183	0.237
	30.0	119.84	118.64	27.18	121.06	0.204	0.264
	50.0	119.17	117.97	27.18	120.37	0.233	0.300
Tensile Strain [mm/mm]	**0.0**	0.0205	0.0197	25.08	0.0201	0.213	0.026
	0.5	0.0195	0.0187	25.08	0.0191	0.599	0.097
	1.0	0.0193	0.0185	25.08	0.0189	0.667	0.116
	1.5	0.0192	0.0185	25.08	0.0189	0.706	0.128
	2.0	0.0192	0.0184	25.08	0.0188	0.734	0.138
	3.0	0.0191	0.0183	25.08	0.0187	0.771	0.152
	5.0	0.0190	0.0182	25.08	0.0186	0.816	0.173
	10.0	0.0188	0.0181	25.08	0.0185	0.871	0.205
	15.0	0.0188	0.0180	25.08	0.0184	0.898	0.226
	20.0	0.0187	0.0179	25.08	0.0183	0.916	0.242
	30.0	0.0186	0.0179	25.08	0.0183	0.937	0.266
	50.0	0.0185	0.0178	25.08	0.0182	0.959	0.300

Table 5-13. Comparison Results of Time-Dependent Probaility of Failure of Case 1 and Case 2 for Material System FYFE

Property	Time [years]	Predicted Mean, P(t)	Modified Mean, P_{ENV}*P(t)	Weibull Parameters		Probabilty of Failure, $P_F(t)$	
				α (Shape)	β (Scale)	Case 1	Case 2
Tensile Strength [MPa]	**0.0**	2237.42	1879.43	32.32	1911.82	0.018	0.000
	0.5	1654.94	1390.15	32.32	1414.10	1.000	0.000
	1.0	1577.39	1325.01	32.32	1347.84	1.000	0.000
	1.5	1532.03	1286.91	32.32	1309.08	1.000	0.000
	2.0	1499.85	1259.87	32.32	1281.58	1.000	0.000
	3.0	1454.49	1221.77	32.32	1242.82	1.000	0.000
	5.0	1397.34	1173.77	32.32	1193.99	1.000	0.000
	10.0	1319.80	1108.63	32.32	1127.73	1.000	0.003
	15.0	1274.44	1070.53	32.32	1088.98	1.000	0.010
	20.0	1242.26	1043.50	32.32	1061.48	1.000	0.022
	30.0	1196.90	1005.39	32.32	1022.72	1.000	0.071
	50.0	1139.75	957.39	32.32	973.89	1.000	0.300
Tensile Modulus [GPa]	**0.0**	111.46	104.77	20.79	107.52	0.040	0.041
	0.5	105.66	99.32	20.79	101.92	0.116	0.119
	1.0	104.88	98.59	20.79	101.18	0.134	0.137
	1.5	104.43	98.17	20.79	100.74	0.146	0.149
	2.0	104.11	97.86	20.79	100.43	0.154	0.158
	3.0	103.66	97.44	20.79	100.00	0.168	0.172
	5.0	103.09	96.90	20.79	99.45	0.186	0.190
	10.0	102.32	96.18	20.79	98.70	0.214	0.219
	15.0	101.87	95.75	20.79	98.27	0.232	0.237
	20.0	101.54	95.45	20.79	97.96	0.246	0.251
	30.0	101.09	95.03	20.79	97.52	0.266	0.272
	50.0	100.52	94.49	20.79	96.97	0.294	0.300
Tensile Strain [mm/mm]	**0.0**	0.0195	0.0173	20.79	0.0178	0.846	0.000
	0.5	0.0144	0.0128	20.79	0.0132	1.000	0.000
	1.0	0.0137	0.0122	20.79	0.0125	1.000	0.000
	1.5	0.0133	0.0119	20.79	0.0122	1.000	0.001
	2.0	0.0131	0.0116	20.79	0.0119	1.000	0.001
	3.0	0.0127	0.0113	20.79	0.0116	1.000	0.002
	5.0	0.0122	0.0108	20.79	0.0111	1.000	0.005
	10.0	0.0115	0.0102	20.79	0.0105	1.000	0.017
	15.0	0.0111	0.0099	20.79	0.0101	1.000	0.034
	20.0	0.0108	0.0096	20.79	0.0099	1.000	0.058
	30.0	0.0104	0.0093	20.79	0.0095	1.000	0.121
	50.0	0.0099	0.0088	20.79	0.0091	1.000	0.300

Table 5-14. Comparison Results of Time-Dependent Probaility of Failure of Case 1 and Case 2 for Material System SIKA+SCCI+FYFE

Property	Time [years]	Predicted Mean, P(t)	Modified Mean, P_{ENV}*P(t)	Weibull Parameters		Probabilty of Failure, $P_F(t)$	
				α (Shape)	β (Scale)	Case 1	Case 2
Tensile Strength [MPa]	**0.0**	2497.64	2197.92	13.38	2284.66	0.006	0.003
	0.5	2107.50	1854.60	13.38	1927.79	0.053	0.032
	1.0	2055.57	1808.90	13.38	1880.28	0.074	0.045
	1.5	2025.18	1782.16	13.38	1852.49	0.089	0.054
	2.0	2003.63	1763.19	13.38	1832.78	0.102	0.062
	3.0	1973.25	1736.46	13.38	1804.99	0.124	0.076
	5.0	1934.97	1702.77	13.38	1769.97	0.158	0.097
	10.0	1883.03	1657.07	13.38	1722.47	0.220	0.137
	15.0	1852.65	1630.33	13.38	1694.67	0.265	0.167
	20.0	1831.10	1611.37	13.38	1674.96	0.303	0.193
	30.0	1800.72	1584.63	13.38	1647.17	0.363	0.235
	50.0	1762.44	1550.95	13.38	1612.15	0.452	0.300
Tensile Modulus [GPa]	**0.0**	127.23	123.41	11.89	128.83	0.012	0.099
	0.5	120.61	116.99	11.89	122.12	0.022	0.179
	1.0	119.72	116.13	11.89	121.23	0.024	0.194
	1.5	119.21	115.63	11.89	120.71	0.025	0.203
	2.0	118.84	115.28	11.89	120.34	0.026	0.209
	3.0	118.33	114.78	11.89	119.81	0.028	0.219
	5.0	117.68	114.15	11.89	119.16	0.029	0.232
	10.0	116.79	113.29	11.89	118.26	0.032	0.251
	15.0	116.28	112.79	11.89	117.74	0.034	0.263
	20.0	115.91	112.43	11.89	117.37	0.035	0.271
	30.0	115.40	111.93	11.89	116.85	0.037	0.284
	50.0	114.75	111.30	11.89	116.19	0.039	0.300
Tensile Strain [mm/mm]	**0.0**	0.0197	0.0179	15.35	0.0186	0.331	0.002
	0.5	0.0166	0.0151	15.35	0.0157	0.996	0.023
	1.0	0.0162	0.0148	15.35	0.0153	1.000	0.033
	1.5	0.0160	0.0146	15.35	0.0151	1.000	0.041
	2.0	0.0158	0.0144	15.35	0.0149	1.000	0.049
	3.0	0.0156	0.0142	15.35	0.0147	1.000	0.061
	5.0	0.0153	0.0139	15.35	0.0144	1.000	0.082
	10.0	0.0149	0.0135	15.35	0.0140	1.000	0.121
	15.0	0.0146	0.0133	15.35	0.0138	1.000	0.153
	20.0	0.0145	0.0132	15.35	0.0136	1.000	0.180
	30.0	0.0142	0.0129	15.35	0.0134	1.000	0.226
	50.0	0.0139	0.0127	15.35	0.0131	1.000	0.300

As Table 5-11 through Table 5-14 illustrate, the probability of failure predicted at the expected service life of the FRP material systems from the design values prescribed by the ACI design guideline is inconsistent and extreme in nature. These results exemplify a shortcoming in the ACI 440 design guidelines as previously noted that the design values are based on somewhat arbitrary safety factors to account for time-dependent performance characteristics and therefore cannot guarantee the safety of the material performance at the time of interest. Graphically, the difference between the two approaches compared can be clearly observed as shown in Figures 5-18 – 5-19.

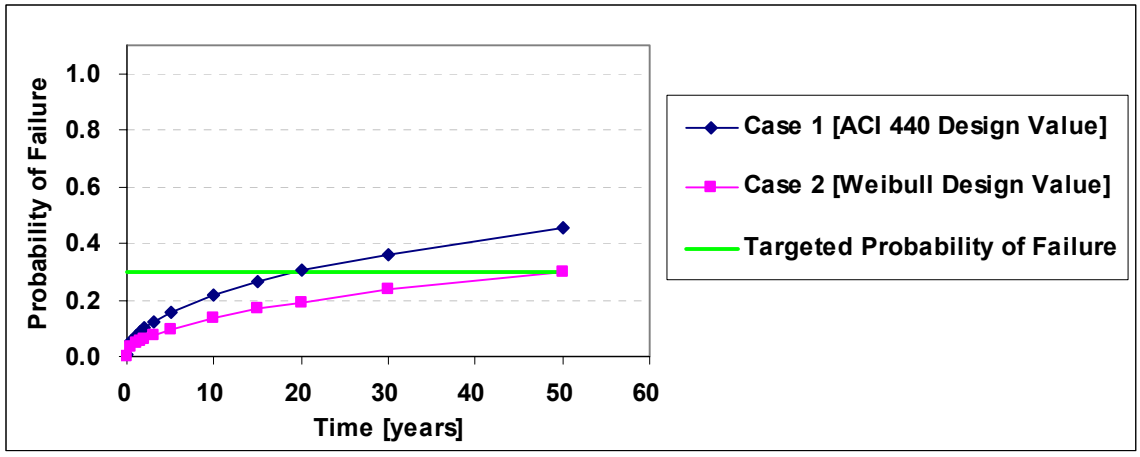

Figure 5-18. Graphical Comparison of Case 1 and Case 2 for Tensile Strength Data of SIKA+SCCI+FYFE

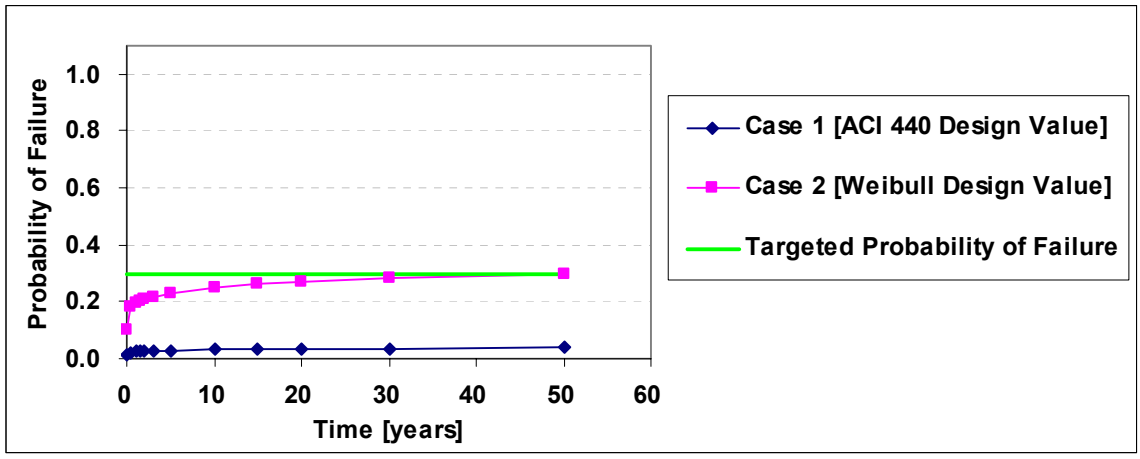

Figure 5-19. Graphical Comparison of Case 1 and Case 2 for Tensile Modulus Data of SIKA+SCCI+FYFE

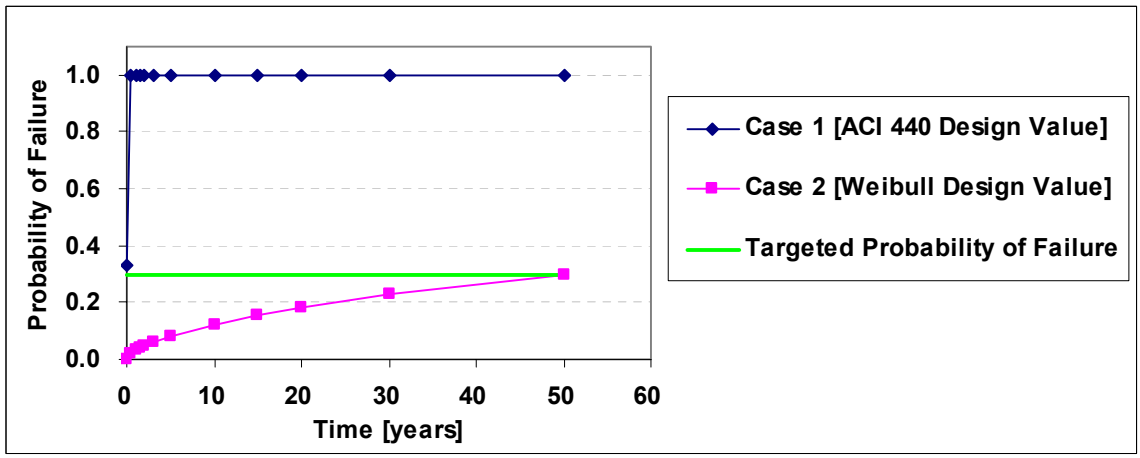

Figure 5-20. Graphical Comparison of Case 1 and Case 2 for Tensile Strain Data of SIKA+SCCI+FYFE

As clearly shown in the above figures, the Weibull design values derived based on the predictive approach guarantee the targeted reliability at the expected service life, which was a probability of failure expectancy of 30% for this example. Therefore, the use of the proposed predictive approach, incorporating degradation effects on material properties and time-dependent performance distribution, can provide a more accurate assessment of the safety of the material performance at the time of the expected service life.

Chapter 6. Design Example

This chapter illustrates a reliability-based design procedure for FRP strengthening of concrete bridge girders through design examples. Two T-beam bridge girder systems were chosen from numerous girder systems considered in previous research by Atadero (2006). For FRP prefabricated strips used for strengthening, two sets of material characteristics considered in the current research, SIKA and SIKA+SCCI+FYFE, will be used herein. The two design approaches discussed throughout this research, (1) using ACI 440 recommended FRP material design values and (2) using the Weibull design values that incorporate time-dependent FRP degradation serving as part of the ongoing development of a LRFD based approach, will be compared based on results from two types of analysis. The sectional analysis prescribed by ACI 440 (2002) is performed to determine the resistance of the strengthened girder and the required number of FRP prefabricated strips to meet the design load is determined analytically. Then, a reliability analysis is performed through considerations of variation of selected load and resistance variables in the girder systems of interest to determine the reliability index, β, on the basis of which comparisons of strengthened girders can be made. In order to illustrate the differences of the aforementioned two design approaches for FRP strengthening design and consideration of time-dependent degradation of FRP and steel reinforcement, four design cases are chosen for both sectional and reliability analysis, as listed in Table 6-1.

Table 6-1. Design Cases Considered for Sectional Analysis and Reliability Analysis

Case 1	➢ ACI 440 characteristic design value $(\mu - 3\sigma)$ ➢ ACI environmental factor $(C_E = 0.85)$ ➢ 10 % initial reinforcing steel loss
Case 2	➢ Proposed Weibull design value, See Section 5.6.2 ➢ Environmental factor, F_{ENV}, See Table 5.8 ➢ 10 % initial reinforcing steel loss ➢ Continuous FRP degradation
Case 3	➢ ACI 440 characteristic design value $(\mu - 3\sigma)$ ➢ ACI environmental factor $(C_E = 0.85)$ ➢ 10 % initial reinforcing steel loss ➢ Continuous reinforcing steel degradation
Case 4	➢ Proposed Weibull design value, See Section 5.6.2 ➢ Environmental factor, F_{ENV}, See Table 5.8 ➢ 10 % initial reinforcing steel loss ➢ Continuous reinforcing steel and FRP degradation

To show the effects of environmental aging on reinforced concrete structures, the amount of steel reinforcement was reduced by a lump sum initial steel loss of 10 % assuming the full design quantity of steel reinforcement was present before initiation of degradation for all cases. In addition, a corrosion model used in previous research (Atadero, 2006) was used to account for the effect of continued steel degradation over time. Prefabricated FRP strips are also considered to degrade over time in Case 2 and Case 4, using the degradation predictive equations discussed in Chapter 5, to provide comprehensive insight of the effect of materials level degradation on behavior at the systems level.

6.1 Structural Assessment

The two bridge girders chosen as design examples for the current research are labeled as Girder 5 and 20 as described in Chapter 4 of previous research (Atadero, 2006). The dimensions and material properties of these girders are described in Table 6-2.

Table 6-2. Dimensions and Material Properties of Girder 5 and 20

	Girder 5	**Girder 20**
Span Length, L [m]	16.76	22.86
Girder Spacing [m]	2.23	2.59
Slab Depth, t_{slab} [mm]	177.8	168.2
Web Width, t_w [mm]	304.8	406.4
Web Depth, h [m]	1.07	1.52
Effective Flange Width, b_f [m]	2.23	2.43
Cover at Bottom of Girder [mm]	50.8	50.8
Steel Reinforcement	Six 35.8 mm diameter (#36) bars	Nine 35.8 mm diameter (#36) bars
Steel Yield Strength, f_y [MPa]	275.8	275.8
Steel Elastic Modulus, E_s [GPa]	200	200
Concrete Compressive Strength, f'_c [MPa]	22.4	22.4
Concrete Elastic Modulus, E_c [GPa]	22	22

It should be noted that the both girders represent singly reinforced sections such that no steel reinforcing bars are found near the top of the girders and that the steel reinforcement existing in the deck slab and shear stirrups are not considered in these examples and thus are not described in Table 6-2 (Atadero, 2006). It will be assumed for the two girders that

corrosion of steel reinforcement has been inspected and it is estimated that approximately ten percent of the initial reinforcement area has been lost to corrosion. For the purposes of this investigation, a flexural limit state is the primary mode of structural deficiency and thus only the reliability of their flexural performance of the girders will be evaluated in this study.

6.2 Design Load for FRP Strengthening

The main objective of FRP strengthening of a bridge girder is to recover or reinforce flexural load carrying capacity and therefore to increase the safety of the structure under normal traffic loads. Thus, strengthening projects are often based on the Load and Resistance Factor Rating (LRFR) factored load (Atadero, 2006). The LRFR factored load can be determined as shown in Eq. 6-1

$$\sum \gamma_i Q_i = 1.25D + 1.5W + 1.35 \cdot DF\left(L + IM\right) \qquad \textbf{Eq. 6-1}$$

where D is the dead load, W is the load due to the wearing surface, DF is the distribution factor, L is the live load, and IM is the impact load. It is noted that the loads considered herein represent the maximum bending moments acting on the girder of interest. Details related to the descriptions of load components and the procedure of the determination of the LRFR factored load combinations were originally studied by Nowak (1999) and can be found in Chapter 4 of Atadero (2006). A summary of the load components and design factored loads for girder 5 and girder 20 is shown in Table 6-3.

Table 6-3. Load Components and LRFR Factored Load for Design

Girder	Dead Load [kN-m]	Wearing Load [kN-m]	Live+Impact Load [kN-m]	Distribution Factor	LRFD Factored Load [kN-m]
5	228.5	54	930.1	0.64	1168.1
20	515.9	83.4	1994.6	0.74	2754.5

6.3 Prefabricated FRP Design Values

As mentioned previously, two sets of material characteristics pertaining to the earlier considered SIKA and SIKA+SCCI+FYFE sets are considered in these design examples. Based on experimental tensile tests as described in Table 3-16, the properties of the two material systems are summarized in Table 6-4.

Table 6-4. Experimental Tensile Properties Used for Design Examples

Material System	Property	Mean	Standard Deviation	COV
SIKA	**Tensile Strength [MPa]**	2504.59	82.85	0.03
	Tensile Modulus [Gpa]	138.09	5.22	0.04
	Tensile Strain [mm/mm]	0.01580	0.00084	0.05
SIKA+SCCI+FYFE	**Tensile Strength [MPa]**	2497.64	223.95	0.09
	Tensile Modulus [Gpa]	127.23	12.85	0.10
	Tensile Strain [mm/mm]	0.01972	0.00154	0.08

As shown in Table 6-1, case 1 and 3 are based on the ACI 440 guideline design values whereas case 2 and 4 are based on the Weibull design values. The ACI 440 prescribed

design values can be determined by $C_E(\mu - 3\sigma)$ with $C_E = 0.85$ as listed in Table 6-1 with the experimental mean and standard deviation values provided in Table 6-4. In order to determine the Weibull design values of the two material systems, as described in Section 5.6.3, the expected service life of FRP materials is assumed to be 50 years which is the same as the expected design life of girder strengthening. It is also assumed that the probability of failure of the material systems at the end of the expected design life is 0.30 as previously used in the example procedure in Section 5.6.3. Then, following the procedure illustrated in Section 5.6.3 with the properties listed in Table 6-4 and the environmental factors described in Table 5-8, the Weibull design values were determined. A summary of the resulting FRP design values for all cases considered in the design examples are shown in Table 6-5.

Table 6-5. Summary of Prefabricated FRP Design Values Used for Analysis

Material System	Case 1 & 3 [ACI 440 Design Value]			Case 2 & 4 [Weibull Design Value]		
	Tensile Strength [MPa]	Tensile Modulus [GPa]	Tensile Strain [mm/mm]	Tensile Strength [MPa]	Tensile Modulus [GPa]	Tensile Strain [mm/mm]
SIKA	1917.62	138.09	0.0133	1465.21	121.45	0.0095
SIKA+SCCI+FYFE	1551.92	127.23	0.0128	1492.6	106.54	0.0123

It must be noted that the derived Weibull design values shown in Table 6-5 were based on the environmental modification factors, as described in Section 5.5, for the alkaline environment, which affected the material systems considered in this study most severely. These selected factors are thus the most severe from the set and are hence considered to

be comparable to the ACI 440 specified factor, $C_E = 0.85$, for the most aggressive environment.

6.4 Girder Resistance and Resistance Factors

In typical FRP strengthening applications, the girders are strengthened by externally bonding prefabricated FRP strips to the concrete substrate in the longitudinal direction. A primary goal of strengthening design is to obtain the desired flexural design strength by applying a sufficient number of strips. As mentioned previously, sectional analysis is performed to determine the resistance of strengthened girders for design purposes. Sectional analysis of a concrete bridge girder strengthened with FRP is described by ACI 440 (2002) and details related to the analysis procedure to determine the resistance and the required number of required FRP strips can be found from Appendix D in Atadero (2006). The nominal moment capacity of a strengthened girder can be determined using Eq. 6-2.

$$M_n = A_s f_y \left(d - \frac{\beta_1 c}{2} \right) + \psi_f A_f f_{fe} \left(h - \frac{\beta_1 c}{2} \right) \qquad \textbf{Eq. 6-2}$$

where:
A_s is the area of steel reinforcement
A_f is the area of FRP composite
f_y is the steel yield strength
f_{fe} is the effective stress in FRP
$\beta_1 c$ is the depth of the compressive stress block, and
ψ_f is the safety factor specific to FRP material

A limit-state specific resistance factor, ϕ, is multiplied to M_n as shown in Eq. 6-2 to determine the factored moment capacity specific to a limit state as:

$$\phi M_n = \phi\left[A_s f_y\left(d - \frac{\beta_1 c}{2}\right) + \psi_f A_f f_{fe}\left(h - \frac{\beta_1 c}{2}\right)\right] \quad \textbf{Eq. 6-3}$$

For the purposes of the design examples, the resistance factor, ϕ, equal to 0.90 is used in all design cases and the FRP specific resistance factor, ψ_f, is assumed to be 0.85 for the material systems of interest. It should be noted that these factors are determined based on the assumed initial steel deficiency of 20 %, the expected design life of strengthening of 50 years, and the target reliability index of 3.5, which is comparable to that used for the current research. Details related to the calibration of these factors are discussed in Chapter 5 of Atadero (2006).

Table 6-6. Resistance Factors for Design Example

ϕ	**0.9**
ψ_f	**0.85**

6.5 Example of Girder Strengthening

After determining the design load, FRP material design values, and the resistance factors, the amount of FRP required to satisfy the design load demand can be determined following the sectional analysis procedure as described in ACI 440 (2002). This section provides an example procedure to determine the moment capacity and the required

number of prefabricated FRP strips for the aforementioned Case 2, as listed in Table 6-1. Girder 5 with material system SIKA is used for this example. The design procedure is shown below.

1. **Obtain the geometric and material properties for the girder and the FRP material applied**. These properties are summarized in Table 6-7 and Table 6-8.

Table 6-7. FRP Properties for SIKA Strips Used for Design Example

Property	Value
Strip Thickness, t_f	1.31 mm
Strip Width, w_f	50.8 mm
Experimental Mean Tensile Strength	2504.59 MPa
Experimental Mean Tensile Modulus	138.09 GPa

Table 6-8. Girder Properties of Girder 5 Used for Design Example

Property	Value
Web Width, b_w	304.8 mm
Flange Width, b_f	2235.2 mm
Girder Depth, h	1066.8 mm
Effective Depth, d	922.1 mm
Deck Thickness, t_s	177.8 mm
Area of Steel, A_s	$6107\,mm^2$
Corroded Steel Area, $A^*_s = 0.2A_s$ (20% Initial Steel Loss)	$4886\,mm^2$
Steel Tensile Strength, f_y	275.8 MPa
Steel Tensile Modulus, E_s	200 GPa
Concrete Strength, f'_c	22.4 MPa
Concrete Modulus, E_c	22.7 GPa

2. **Determine the FRP material design values.** The Weibull design values for strength, modulus, and strain were already determined from the experimental tensile properties obtained from the current research following the procedure described in Section 5.6.3. It is noted here that these design values were determined based on considering time-dependent FRP degradation for a design life of 50 years and a probability of failure expectancy of 30%. The results are summarized in Table 6-9.

Table 6-9. Weibull Design Material Properties for SIKA Strip

Design Strength, f_{fu}	1465.21 MPa
Design Modulus, E_f	121.45 GPa
Design Strain, ε_{fu}	0.0095 mm/mm

3. **Choose a trial quantity of FRP by specifying the number of strips,** n**.** It is noted that the FRP strips in this example are applied directly to the concrete girder rather than being applied on top of each other. Thus, the maximum number of strips is limited by the width of the girder of interest and can be determined from dividing the web width by the strip width. The maximum number of strips that can be applied for girder 5 and girder 20 are 6 and 8, respectively. The trial quantity for this example is $n = 2$ (strips).

4. **Determine whether the example girder acts as a T-beam section or rectangular section.** This step is important since the resulting geometry significantly affects the analysis. The depth of the compressive block, a, is used as a measure to determine the analytical girder geometry.

$$\text{Analytical Section} = \begin{cases} \text{Rectangular Section} & \text{if } a \le t_s \\ \text{T-Beam Section} & \text{if } a > t_s \end{cases}$$

The depth of compressive block, a, is calculated as:

$$a = \frac{A_s^* f_y}{f_c' b_f} = \frac{4886 \times 275.8}{22.4 \times 2235} = 26.9mm \quad < \quad t_s = 177.8mm \qquad \textbf{Eq. 6-4}$$

$$\Rightarrow \text{ Rectangular beam analysis}$$

5. **Determine the reinforcement ratio of steel and FRP.** First, the total girder section area, A_t, and the FRP reinforcement area, A_f, are determined. Then, the steel ratio and FRP ratio are determined using Eq. 6-5 and Eq. 6-6, respectively, as:

$$A_t = b_f t_s + b_w \left(d - t_s\right) = 2235.2 \times 177.8 + 304.8\left(922.1 - 177.8\right) = 624,296 \text{ mm}^2$$

$$A_f = n t_f w_f = 2 \times 1.31 \times 50.8 = 133.1 \text{ mm}^2$$

$$\rho_s = \frac{A_s}{A_t} = \frac{4,886}{624,296} = 0.00783 \qquad \textbf{Eq. 6-5}$$

$$\rho_f = \frac{A_f}{A_t} = \frac{133.1}{624,296} = 0.000213 \qquad \textbf{Eq. 6-6}$$

6. Determine the existing strain at the bottom soffit of the girder, ε_{bi}.

$$\varepsilon_{bi} = \frac{M_{DL}\left(h - kd\right)}{I_{cr}E_c} \qquad \textbf{Eq. 6-7}$$

$$k = \sqrt{\left(\rho_s \frac{E_s}{E_c} + \rho_f \frac{E_f}{E_c}\right)^2 + 2\left(\rho_s \frac{E_s}{E_c} + \rho_f \frac{E_f}{E_c}\left(\frac{h}{d}\right)\right)} - \left(\rho_s \frac{E_s}{E_c} + \rho_f \frac{E_f}{E_c}\right) = 0.311$$

$$I_{cr} = \frac{b\left(kd\right)^3}{3} + nA_s^*\left(d - kd\right)^2 = 1.98\times10^{10} \text{ mm}^4$$

$$M_{DL} = M_D + M_W = 228,500 + 54,000 = 282,500 \text{ N-m}$$

$$\varepsilon_{bi} = \frac{282,500\left(1066.8 - 0.311\times922.1\right)\times1000}{1.98\times10^{10}\times22,700} = 0.000491 \text{ mm/mm}$$

where M_{DL} is the total dead load moment demand, including the wearing load, as listed in Table 6-2, k is the distance factor to the neutral axis of the section, and I_{cr} is the cracked moment of inertia.

7. Determine the bond coefficient, κ_m.

$$\kappa_m = \begin{cases} \dfrac{1}{60\varepsilon_{fu}}\left(1-\dfrac{nE_f t_f}{360,000}\right) \le 0.90, & for \quad nE_f t_f \le 180,000 \\ \dfrac{1}{60\varepsilon_{fu}}\left(\dfrac{90,000}{nE_f t_f}\right) \le 0.90, & for \quad nE_f t_f > 180,000 \end{cases} \qquad \textbf{Eq. 6-8}$$

$$nE_f t_f = 1 \times 121,450 \times 1.31 = 159,100 \quad < \quad 180,000$$

$$\kappa_m = 0.90$$

It should be noted that the term, n, used in Eq. 6-8 is different from that representing the number of strips used as determined from Step 3 of this example. This n represents the number of FRP strips applied on top of each other. As discussed previously in Step 3, the FRP strips are only directly applied to the concrete and thus n is assumed to be 1 for Eq. 6-8.

8. Estimate a trial value for the neutral axis depth, c_0. Assume $c_0 = 41$ mm.

9. Determine the effective strain in the FRP, ε_{fe}.

$$\varepsilon_{fe} = \varepsilon_{cu}\left(\frac{h-c}{c}\right) - \varepsilon_{bi} < \kappa_m \varepsilon_{fu} \qquad \textbf{Eq. 6-9}$$

$$\varepsilon_{fe} = 0.003\left(\frac{1066.8-41.0}{41.0}\right) - 0.000491 = 0.07468 \text{ mm/mm}$$

$\kappa_m \varepsilon_{fu} = 0.9 \times 0.0095 = 0.00855$ mm/mm $\quad \Rightarrow$ FRP bond failure governs

$$\varepsilon_{fe} = 0.00855 \text{ mm/mm}$$

10. Determine the strain in the reinforcing steel.

$$\varepsilon_s = \left(\varepsilon_{fe} + \varepsilon_{bi}\right)\left(\frac{d-c}{h-c}\right) \qquad \textbf{Eq. 6-10}$$

$$\varepsilon_s = \left(0.00855 + 0.000491\right)\left(\frac{922.1-41.0}{1066.8-41.0}\right) = 0.00777 \text{ mm/mm}$$

11. Determine the stresses in the steel reinforcement and FRP. These calculations are provided in Eq. 6-13 and Eq. 6-14 for the steel and FRP, respectively.

$$f_s = E_s \varepsilon_s \le f_y \qquad \textbf{Eq. 6-11}$$

$E_s \varepsilon_s = 200{,}000 \times 0.00777 = 1554$ MPa $\qquad f_y = 275.8$ MPa

$$f_s = f_y = 275.8 \text{ MPa}$$

$$f_{fe} = E_f \varepsilon_{fe} \qquad \textbf{Eq. 6-12}$$

$$f_{fe} = 121{,}450 \times 0.00855 = 1038.4 \text{ MPa}$$

12. Estimate the Whitney compressive stress block constant, β_1.

$$\beta_1 = \begin{cases} 0.65 & \text{if} \quad \left(1.09 - 0.008 f_c'\right) < 0.65 \\ 0.85 & \text{if} \quad \left(1.09 - 0.008 f_c'\right) > 0.85 \\ 1.09 - 0.008 f_c' \left[N/mm^2\right] & \text{if} \quad \text{otherwise} \end{cases} \qquad \textbf{Eq. 6-13}$$

$$1.09 - 0.008 \cdot 22.4 = 0.91 \quad > \quad 0.85$$

$$\beta_1 = 0.85$$

13. Use equilibrium to calculate a new estimate of the neutral axis depth, c.

$$c = \frac{A_s^* f_s + A_f f_{fe}}{\gamma f_c' \beta_1 b_f} \qquad \textbf{Eq. 6-14}$$

$$\gamma = 0.85$$

$$c = \frac{4886 \times 275.8 + 133.1 \times 1038.4}{0.85 \times 22.4 \times 0.85 \times 2235.2} = 41.05 \text{ mm}$$

14. Iterate to find the neutral axis. For this example, since the assumed neutral axis depth of $c_0 = 41$ mm is reasonably close to the actual neutral axis depth as shown in Eq. 6-15. No iteration is required and thus the resulting neutral axis depth is

found to be $c_0 = 41$ mm . However, if the assumed value and the actual value do not converge, a new value must be assumed as a trial value and the procedure from Step 8 to Step 13 should be iterated until they converge.

15. Determine the factored moment capacity of the section.

$$\phi M_n = \phi\left[A_s f_s \left(d - \frac{\beta_1 c}{2} \right) + \psi A_f f_{fe} \left(h - \frac{\beta_1 c}{2} \right) \right] \qquad \textbf{Eq. 6-15}$$

$$\phi = 0.9 \quad \& \quad \psi = 0.85$$

$$\phi M_n = 0.9\left[4886 \times 275.8 \left(922.1 - \frac{0.85 \times 41}{2} \right) + 0.85 \times 133.1 \times 1038.4 \left(1066.8 - \frac{0.85 \times 41}{2} \right) \right]$$

$$\phi M_n = 1.208 \times 10^9 \text{ N-mm } = 1,208 \text{ kN-m}$$

16. Check the service stress in the steel as prescribed by ACI 440 (2002).

$$f_{s,s} = \frac{\left[M_s + \varepsilon_{bi} A_f E_f \left(h - \frac{kd}{3} \right) \right] (d - kd) E_s}{A_s E_s \left(d - \frac{kd}{3} \right)(d - kd) + A_f E_f \left(h - \frac{kd}{3} \right)(h - kd)} \le 0.9 f_y \qquad \textbf{Eq. 6-16}$$

$$f_{s,s} = \frac{\left[M_s + \varepsilon_{bi} A_f E_f \left(h - \frac{kd}{3} \right) \right] (d - kd) E_s}{A_s E_s \left(d - \frac{kd}{3} \right)(d - kd) + A_f E_f \left(h - \frac{kd}{3} \right)(h - kd)} = 213.93 \text{ MPa} \quad \le \quad 248.21 \text{ MPa}$$

$\Rightarrow$ Service stress check is satisfied.

17. **Check if the factored moment capacity is larger than the factored moment demand.** The factored moment demand for girder 5 is 1168.1 kN-m as provided in Table 6-3. Since the factored moment capacity is determined to be 1208.1 kN-m for this example, this design is satisfied. Thus, the final design is to apply two 50.8 mm wide layers of prefabricated FRP strips to the girder.

The implementation of the above procedure of the sectional analysis is facilitated by a program written in EXCEL, which is available in Appendix B. This procedure is applied to all design cases of the two girders for two material systems, SIKA and SIKA+SCCI+FYFE. The results from sectional analysis consisting of the number of FRP strips required to meet the LRFR factored loads is provided in Table 6-13 in Section 6.7.

6.6 Evaluation of Structural Reliability

As mentioned in Chapter 2, the reliability method chosen for the current research is a hybrid reliability approach using a first-order reliability method (FORM) and Monte Carlo Simulation (MCS). This method is described in the National Cooperative Highway Research Program (NCHRP) Report 368 by Nowak (1999) and was used for the calibration of the ASSHTO LRFD code for bridges (AASHTO, 2004). Therefore, it is appropriate for use in assessing the structural reliability for FRP strengthening of concrete bridge girders (Nowak, 1999; Atadero, 2006; Wilcox, 2008). The procedure of this reliability method is illustrated in the flow chart described in Figure 6-1.

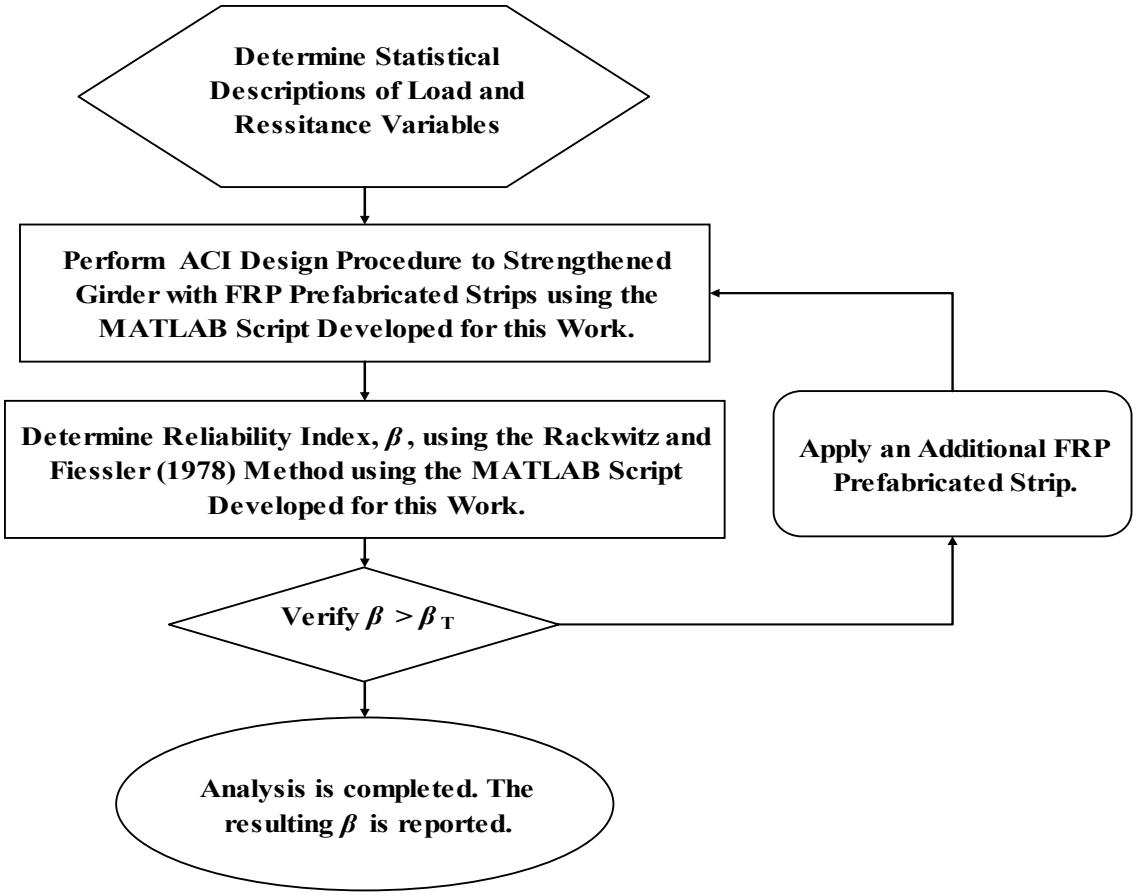

Figure 6-1. Flowchart of Reliability Analysis Used For this Research

In order to assess the structural reliability of the strengthened girders considered in this study via MCS, the statistical descriptions of load and resistance variables related to the girder systems must be obtained. An extensive study for characterization of the load variables related to bridges was conducted by Nowak (1999) and details related this information can be found from Chapter 2 in Atadero (2006). The statistical descriptions of the load variables that are applicable to the two example girder systems considered in this study were obtained and a summary of the means and standard deviations of the selected design load variables used for reliability analysis is provided in Table 6-10.

Table 6-10. Distribution Parameters of Load Considered for Reliability Analysis

Load	Girder 5		Girder 20	
	Mean	**STD**	**Mean**	**STD**
Dead Load [kN-m]	239.9	24.0	541.7	54.2
Wearing Load [kN-m]	63.0	15.8	97.3	24.3
Live+Impact Load [kN-m]	691.2	124.4	1723.3	310.2
Total Load [kN-m]	994.1	127.7	2362.3	315.8

It must be noted that, according to NCHRP Report 368, a Normal distribution was determined as the best fit to describe the load variables (Nowak, 1999) and therefore the load effect considered for reliability analysis in this study is considered as a Normal random variable.

To determine the structural reliability index of a strengthened girder, MCS is utilized to determine the mean and standard deviation of the moment capacity of the girder. To perform MCS, the statistical descriptions of the variables associated with the resistance capacity of the girder must be available. In this study, variability of many resistance variables characterized by previous researchers (Mirza and MacGregor, 1976; Nowak, 1999; Atadero, 2006) were included in MCS, including steel strength and rebar size, concrete strength, geometric dimensions of girders, and FRP tensile properties. The statistical variation in the prefabricated FRP strips was determined using the two-parameter Weibull distribution as discussed in Chapter 3. The descriptions of the remaining variables involved in the resistance of the strengthened girder can be found in previous studies (Atadero, 2006; Wilcox, 2008). A summary of the statistical descriptions of the resistance variables used for reliability analysis in this study is shown in Table 6-11.

Table 6-11. Statistical Distribution and Distribution Parameters of Resistance Variables Considered for Reliability Analysis (Atadero, 2006; Wilcox, 2008)

Variable	Statistical Distribution	Mean	COV
FRP Strength, f_f	Weibull	Depends on Material System, See Table 3.16	Depends on Material System, See Table 3.16
FRP Modulus, E_f	Weibull	Depends on Material System, See Table 3.16	Depends on Material System, See Table 3.16
FRP Strain, ε_f	Weibull	Depends on Material System, See Table 3.16	Depends on Material System, See Table 3.16
Error in Girder Effective Flange Width, b_f	Normal	0.80 mm (1/32 in)	15
Error in Girder Height, h	Normal	-3.2 mm (-1/8 in)	2
Error in Effective depth of Girder, d	Normal	-4.8 mm (-3/16 in)	2.667
Error in Slab Thickness, t_s	Normal	0.80 mm (1/32 in)	15
Error in Concrete Bottom Cover	Normal	1.6 mm (1/16 in)	5
Water Cement Ratio, w_c	Normal	0.45	0.05
Concrete Compressive Strength, f'_c	Normal	Depends on Nominal f'_c in psi,	0.15
Concrete Modulus, E_c	Depends on f'_c	Depends on f'_c, See Section 6.2.3 (Wilcox, 2008)	-
Initial Steel Bar Area, A_{si}	Normal (Truncated at 94% and 106% of the stated A_s)	0.99	0.024
Steel Strength, f_y	Beta	Depends on Strength Grade of Steel, See Section 6.2.4 (Wilcox, 2008)	Depends on Strength Grade of Steel, See Section 6.2.4 (Wilcox, 2008)
Steel Modulus, E_s	Normal	201.3 GPa (29,200 ksi)	0.024

With these statistical descriptions of the selected load and resistance variables for reliability analysis determined, as described in Tables 6-10 and 6-11, a MATLAB script written by Wilcox (2008) was modified and utilized for this study. An example of this MATLAB script used for reliability analysis for design case 1 for material system SIKA is provided in Appendix A. The results constituting of the number of FRP strips required to meet the LRFR factored loads and the resulting reliability indices are shown in Section 6.7. The results from both sectional analysis and reliability analysis will be compared in Table 6-14.

6.7 Results and Discussion

As mentioned previously, four design cases were used to show the effects of different approaches to determine FRP design values and of different approaches to consider time-dependent degradation of FRP and steel reinforcement to the resulting reliability of the strengthened girders. The design cases considered in this study are summarized in Table 6-1. The sectional analysis as prescribed by ACI 440 (2002) was performed in this study. The results of the sectional analysis consist of the factored moment capacity of the strengthened girders and the number of required FRP strips to meet the LRFR factored load demands. Details related to the results of the sectional analysis are shown in Tables 6-12 and 6-13. The aforementioned reliability procedure, as described in Chapter 2, was used to assess the reliability indices of the two girders for all design cases. Then, effects of design values are illustrated by comparing the reliability indices determined from reliability analysis between the design cases and the proximity

of the resulting reliability to the target reliability for each design case. The results from the reliability analysis are shown in Tables 6-14.

Table 6-12. Results of Sectional Analysis Performed in Microsoft Excel Using the ACI 440 (2002) Procedure

Case	Girder ID	Material System	FRP Degradation Time [years]	Steel Degradation Time [years]	Initial Steel Loss [%]	Environmental Factors				FRP Design Values			Steel Area Used for Design, A^*_s [mm^2]
						C_E	F_{ENV}			Strength [MPa]	Modulus [GPa]	Strain [mm/mm]	
							Strength	Modulus	Strain				
1	5	SIKA	-	-	10	0.85	-	-	-	1917.6	138.1	0.0133	5496.5
	20	SIKA	-	-	10	0.85	-	-	-	1917.6	138.1	0.0133	8244.8
	5	ALL	-	-	10	0.85	-	-	-	1551.9	127.2	0.0128	5496.5
	20	ALL	-	-	10	0.85	-	-	-	1551.9	127.2	0.0128	8244.8
2	5	SIKA	50	-	10	-	0.84	0.99	0.87	1465.2	121.5	0.0095	5496.5
	20	SIKA	50	-	10	-	0.84	0.99	0.87	1465.2	121.5	0.0095	8244.8
	5	ALL	50	-	10	-	0.88	0.97	0.91	1492.6	106.5	0.0123	5496.5
	20	ALL	50	-	10	-	0.88	0.97	0.91	1492.6	106.5	0.0123	8244.8
3	5	SIKA	-	50	10	0.85	-	-	-	1917.63	138.1	0.0133	4739.3
	20	SIKA	-	50	10	0.85	-	-	-	1917.63	138.1	0.0133	7108.9
	5	ALL	-	50	10	0.85	-	-	-	1551.9	127.2	0.0128	4739.3
	20	ALL	-	50	10	0.85	-	-	-	1551.9	127.2	0.0128	7108.9
4	5	SIKA	50	50	10	-	0.84	0.99	0.87	1465.21	121.5	0.0095	4739.3
	20	SIKA	50	50	10	-	0.84	0.99	0.87	1465.21	121.5	0.0095	7108.9
	5	ALL	50	50	10	-	0.88	0.97	0.91	1492.6	106.5	0.0123	4739.3
	20	ALL	50	50	10	-	0.88	0.97	0.91	1492.6	106.5	0.0123	7108.9

Table 6-13. (Continued) Results of Sectional Analysis Performed in Microsoft Excel Using the ACI 440 (2002) Procedure

Case	Girder ID	Material System	Number of FRP Strips Applied	Soffit Strain ε_{bi} [mm/mm]	Bond Coeff. K_m	Effective FRP Strain ε_{fe} [mm/mm]	Strain in Steel ε_s [mm/mm]	Stress in FRP σ_{fe} [MPa]	Stress in Steel σ_s [MPa]	Neutral Axis Depth [mm]	Factored Moment Capacity φMn, φ=0.9 (kN-m)	LRFR Factored Design Moment Mu, (kN-m)	Design Check Mu≤φMn	ACI 440 Service Stress Check
1	5	SIKA	1	0.00044	0.63	0.00829	0.00750	1145.0	275.8	44	1293.67	1168.1	OK	OK
	20	SIKA	1	0.00038	0.63	0.00829	0.00777	1145.0	275.8	60	2839.51	2754.5	OK	OK
	5	ALL	1	0.00044	0.70	0.00895	0.00807	1138.8	275.8	44	1293.34	1168.1	OK	OK
	20	ALL	1	0.00038	0.70	0.00895	0.00835	1138.8	275.8	60	2839.03	2754.5	OK	OK
2	5	SIKA	1	0.00044	0.90	0.00855	0.00772	1038.4	275.8	44	1287.98	1168.1	OK	OK
	20	SIKA	1	0.00038	0.90	0.00855	0.00800	1038.4	275.8	60	2831.37	2754.5	OK	OK
	5	ALL	1	0.00044	0.83	0.01021	0.00914	1087.3	275.8	44	1290.59	1168.1	OK	OK
	20	ALL	1	0.00038	0.83	0.01021	0.00948	1087.3	275.8	60	2835.1	2754.5	OK	OK
3	5	SIKA	2	0.00050	0.63	0.00829	0.00756	1145.0	275.8	40	1187.15	1168.1	OK	OK
	20	SIKA	5	0.00044	0.63	0.00829	0.00781	1145.0	275.8	59	2810.62	2754.5	OK	OK
	5	ALL	2	0.00050	0.70	0.00895	0.00812	1138.8	275.8	40	1186.48	1168.1	OK	OK
	20	ALL	5	0.00044	0.70	0.00895	0.00840	1138.8	275.8	60	2807.35	2754.5	OK	OK
4	5	SIKA	2	0.00050	0.90	0.00855	0.00778	1038.4	275.8	40	1175.75	1168.1	OK	OK
	20	SIKA	5	0.00044	0.90	0.00855	0.00805	1038.4	275.8	58	2770.8	2754.5	OK	OK
	5	ALL	2	0.00050	0.83	0.01021	0.00920	1087.3	275.8	40	1180.98	1168.1	OK	OK
	20	ALL	5	0.00044	0.83	0.01021	0.00953	1087.3	275.8	59	2788.58	2754.5	OK	OK

It should be noted that reliability indices were not determined for the examples of sectional analysis since the selected reliability procedure in this study requires statistical descriptions of load and resistance variables which were not available for some of the parameters used for the sectional analysis procedure. As shown in Tables 6-12 and 6-13, design cases 1 and 3 using the ACI 440 design values and design cases 2 and 4 using the Weibull design values provide the same results of the number of FRP prefabricated strips required to meet the LRFR factored loads. However, these results do not provide any information regarding the structural reliability of the girders strengthened with the FRP strips and therefore cannot guarantee that the target reliability has been met. For this reason, reliability analysis was also performed to assess the structural reliability indices of the girder systems and to evaluate the adequacy of the results obtained from the sectional analysis for reliability-based design purposes. The results of reliability analysis are provided in Table 6-14 and the results of the previous sectional analysis are also included for the purpose of illustrating the differences of the results between the two analyses.

Table 6-14. Comparisons Between the Results of Sectional Analysis and Reliability Analysis

Case	Girder ID	Material System	FRP Degradation Time [years]	Steel Degradation Time [years]	Initial Steel Loss [%]	Sectional Analysis		Reliability Analysis			
						Number of Strips Required	LRFR Design Check Mu≤φMn	Number of Strips Required	LRFR Design Check Mu≤φMn	Reliability Index	Reliability Design Check $B \geq B_T$
1	5	SIKA	-	-	10	1	OK	2	OK	3.96	OK
	20	SIKA	-	-	10	1	OK	4	OK	3.58	OK
	5	ALL	-	-	10	1	OK	1	OK	3.66	OK
	20	ALL	-	-	10	1	OK	4	OK	3.66	OK
2	5	SIKA	50	-	10	1	OK	2	OK	3.90	OK
	20	SIKA	50	-	10	1	OK	4	OK	3.60	OK
	5	ALL	50	-	10	1	OK	2	OK	3.85	OK
	20	ALL	50	-	10	1	OK	5	OK	3.81	OK
3	5	SIKA	-	50	10	2	OK	4	OK	3.62	OK
	20	SIKA	-	50	10	5	OK	8 (Max)	OK	3.09	FAIL
	5	ALL	-	50	10	2	OK	4	OK	3.60	OK
	20	ALL	-	50	10	5	OK	8 (Max)	OK	3.18	FAIL
4	5	SIKA	50	50	10	2	OK	4	OK	3.55	OK
	20	SIKA	50	50	10	5	OK	8 (Max)	OK	3.16	FAIL
	5	ALL	50	50	10	2	OK	5	OK	3.81	OK
	20	ALL	50	50	10	5	OK	8 (Max)	OK	3.03	FAIL

As clearly shown in Table 6-14, the differences in the required number of FRP strips determined from the sectional analysis and reliability analysis are apparent. It is noted that the required amount of FRP strips obtained from the reliability analysis are greater than those determined from the sectional analysis. These results can be attributed to the fact that the reliability analysis takes into account the statistical variation inherent in the component properties. More importantly, the reliability analysis determines the minimum number of FRP strips required to meet both the LRFR load demands and the target reliability, whereas the sectional analysis only considers the LRFR factored load requirement. This implies that, although the strengthened girders designed based on the sectional analysis do meet the LRFR factored load demands, as shown in Table 6-14, the resulting reliability indices of the girders do not meet the target reliability selected for these design examples. Therefore, the sectional analysis prescribed by ACI 440 (2002) provides non-conservative and inaccurate results. This investigation suggests that the ACI 440 sectional analysis based design procedure should incorporate reliability criteria in its design procedure to account for the structural reliability of the structure of interest.

In order to illustrate the differences between the ACI 440 design values and the Weibull design values and their effects on the reliability-based design procedures, the resulting reliability indices of all design cases considered in this study were compared. Effects of design values are illustrated by the proximity of the resulting reliability indices to the target reliability, $\beta_T = 3.5$, and by the differences in the number of FRP strips required to meet the design requirements between the design cases. Additional

reliability analyses were conducted for cases of incremental expected design life periods of 10, 25, and 35 years to show the time-dependent characteristics of the reliability-based design procedures. A summary of the computed reliability indices for SIKA system is provided in Table 6-15 followed by the graphical comparisons of the resulting reliability indices and the required number of FRP strips for ease of comparison, as shown in Figures 6-2 to 6-5.

Table 6-15. Results of Reliability Analysis for Design Life Periods of 10, 25, 35, and 50 years

Case	Girder ID	Material System	10 years			25 years			35 years			50 years		
			Number of Strips	Factored Moment Capacity	β	Number of Strips	Factored Moment Capacity	β	Number of Strips	Factored Moment Capacity	β	Number of Strips	Factored Moment Capacity	β
1	5	SIKA	2	1432	3.96	2	1432	3.96	2	1432	3.96	2	1432	3.96
	20	SIKA	4	3315	3.58	4	3315	3.58	4	3315	3.58	4	3315	3.58
	5	ALL	1	1393	3.66	1	1393	3.66	1	1393	3.66	1	1393	3.66
	20	ALL	4	3333	3.66	4	3333	3.66	4	3333	3.66	4	3333	3.66
2	5	SIKA	1	1381	3.52	1	1381	3.52	1	1380	3.51	2	1428	3.90
	20	SIKA	4	3354	3.75	4	3352	3.75	4	3347	3.73	4	3302	3.60
	5	ALL	2	1483	4.30	2	1491	4.36	2	1491	4.36	2	1421	3.85
	20	ALL	4	3299	3.57	4	3321	3.64	4	3320	3.64	5	3391	3.81
3	5	SIKA	2	1397	3.66	3	1426	3.85	3	1390	3.55	4	1406	3.62
	20	SIKA	6	3311	3.56	7	3320	3.59	8	3444	3.97	8	3194	3.09
	5	ALL	2	1396	3.65	3	1422	3.82	3	1386	3.52	4	1403	3.60
	20	ALL	6	3305	3.54	7	3315	3.58	8	3434	3.93	8	3204	3.18
4	5	SIKA	2	1464	4.15	2	1406	3.68	3	1403	3.62	4	1399	3.55
	20	SIKA	5	3333	3.61	6	3309	3.58	8	3305	3.51	8	3200	3.16
	5	ALL	2	1445	4.00	2	1396	3.60	4	1435	3.96	5	1426	3.81
	20	ALL	6	3354	3.74	8	3330	3.61	8	3251	3.34	8	3160	3.03

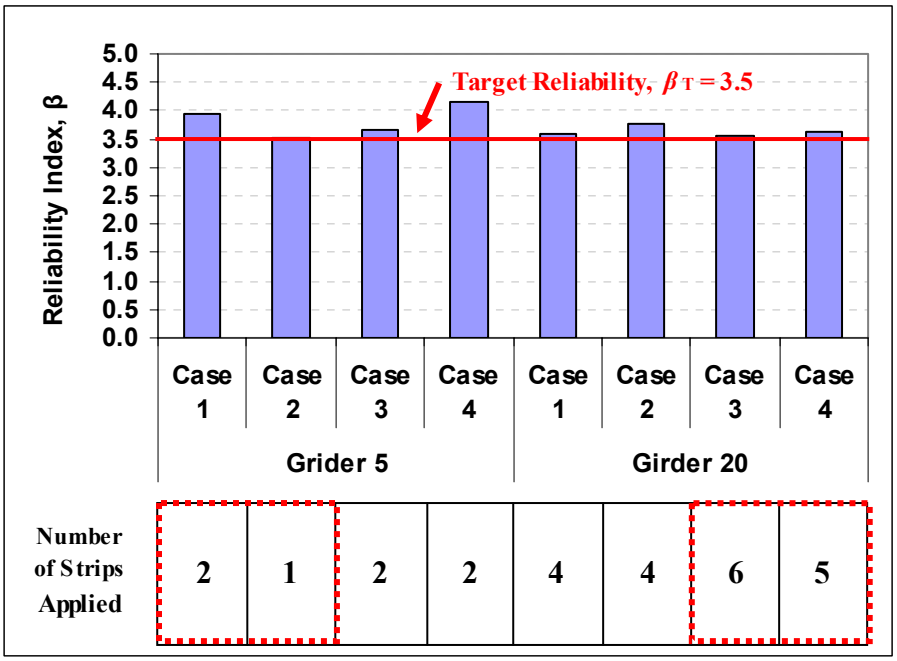

Figure 6-2. Graphical Comparison of β Resulting from Reliability Analysis for SIKA (Assumed Design Life of 10 years)

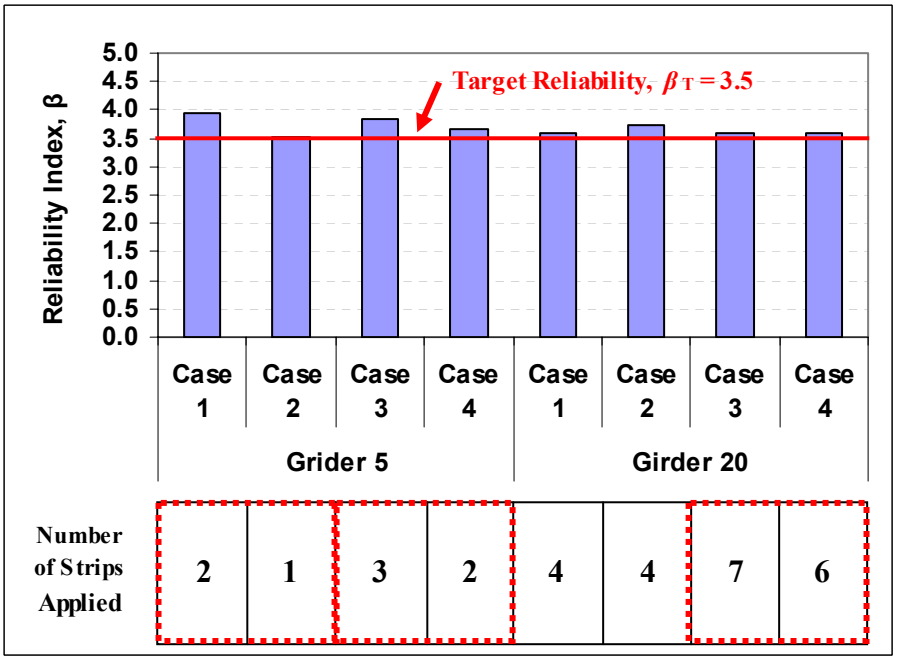

Figure 6-3. Graphical Comparison of β Resulting from Reliability Analysis for SIKA (Assumed Design Life of 25 years)

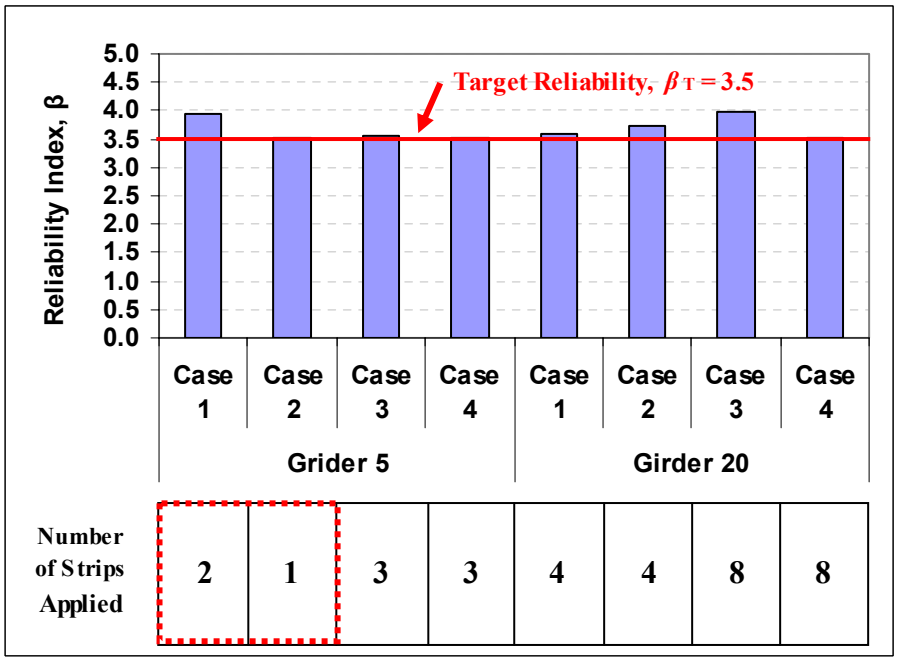

Figure 6-4. Graphical Comparison of β Resulting from Reliability Analysis for SIKA (Assumed Design Life of 35 years)

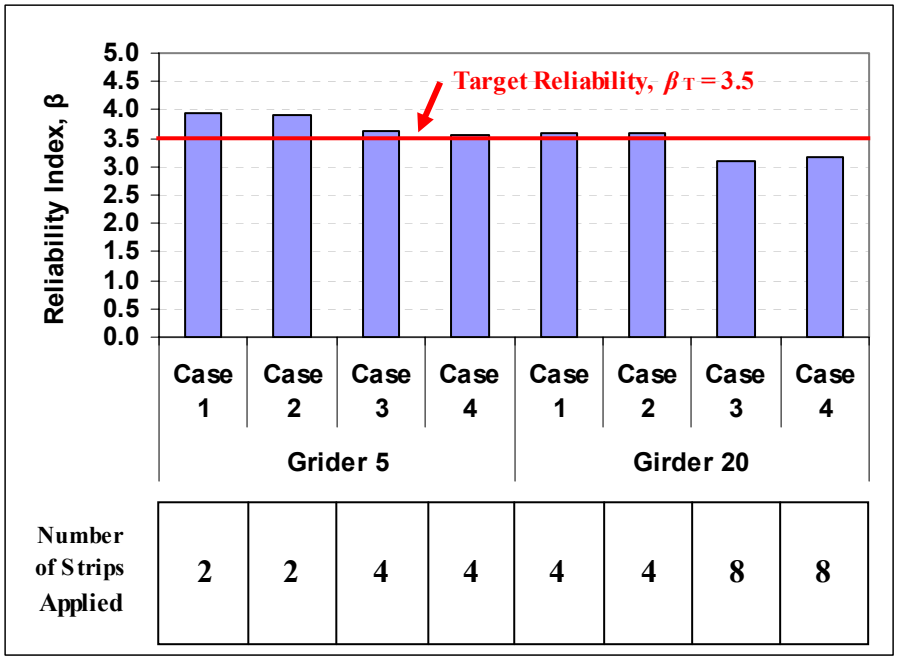

Figure 6-5. Graphical Comparison of β Resulting from Reliability Analysis for SIKA (Assumed Design Life of 50 years)

It is shown in the above figures that the reliability indices of all cases are reasonably consistent with time. For most cases, except for Case 3 and Case 4 of girder 20 for a design life of 50 years as shown in Figure 6-5, the target reliability was met and the resulting reliability indices have a good proximity to the target reliability. This trend serves the purpose of the reliability-based design procedures that a uniform level of reliability among various design cases and conditions can be achieved. While the reliability indices remained fairly constant with time, the general trends of structural and component degradation can be observed from an increase in the required number of FRP strips to meet the target reliability over time. This indicates that more material must be applied to the girders to maintain a reliability index above the target reliability index when time-dependent degradation is included in design. This trend is comparable to the expected theoretical trend that the reliability index would decrease as degradation increases over time if the applied number of FRP strips is fixed constant.

For the purposes of this current investigation, some advantages of using the Weibull design values over the ACI 440 design values are illustrated by comparing the numbers of FRP strips required to meet the target reliability for the same design condition. It should be recalled that cases 1 and 2 represent the same design conditions except that case 1 is based on the ACI 440 design values and case 2 is based on the Weibull design values. The same pattern is true for cases 3 and 4 and details related to the design conditions of each case can be found in Table 6-1. As can be seen from the cases highlighted by red box in Figures 6-2, 6-3, and 6-4, it is observed that the

required number of FRP strips can be reduced by the use of the Weibull design values while maintaining the structural reliability fairly consistent with the target reliability. It should be noted that the occurrence of this advantageous trend decreases significantly from the cases at a period of 25 years to those at 50 years due to the fact that the structural degradation of the example girders becomes dominated by continuous steel degradation which is not addressed through Weibull statistics used in this example. However, this may not be a concern for the purposes of this study since strengthening is not typically designed for 50 years. The aforementioned advantageous trend can be attributed to the fact that the Weibull design values are determined based on a sound approach that considers the stochastic nature of FRP material variability more accurately, as illustrated in Chapter 3, and that accounts for an expected design life and type of exposure to predict FRP degradation, as discussed in Chapter 5. This investigation suggests that overall the use of the Weibull design values provides a more reliable and efficient means to utilize prefabricated FRP strips for use with reliability-based design procedures for rehabilitation of concrete structures.

Chapter 7. Summary and Conclusions

7.1 Summary

This research investigates the experimental and analytical procedures followed to develop a framework for reliability-based design of FRP strengthening for existing concrete structures. The statistical variation in prefabricated FRP composites was characterized for use in reliability analysis based on tensile testing of a number of specimens obtained from sample material systems provided by three suppliers. For the purposes of the current research, the three material systems were grouped as a single class and used as an additional material system throughout this investigation. The combined set of data was treated by the same statistical characterization procedures used for each material system. As a result, although the variation of the combined set of data was greater than that of other single material systems, the level of variation was within an acceptable range for typical FRP materials. However, it is emphasized that the production of more uniform prefabricated FRP materials would be desirable and development of a consistent statistically valid method for testing, statistical analysis, and reporting formats is also needed.

A method for specifying the design value of FRP tensile properties was proposed. This method is based on the use of the FRP characteristic value derived from the two-parameter Weibull distribution, a factor of confidence level to account for statistical uncertainty due to limited data on the basis of which the characteristic value is determined, and the predictive degradation equation with an environmental

modification factor that is specific to the exposure environment and expected service life of the FRP strengthening.

Accelerated degradation experimental techniques have demonstrated the behavior of carbon/epoxy prefabricated FRP strips over time and in typical exposure conditions of FRP strengthening. Predictive analysis based on those techniques illustrates the large deficiency between design guidelines and experimental material degradation behavior. Predictive equations were derived in order to characterize the degradation of material properties more accurately and thus to enable the prediction of the degraded property of interest at any given time in terms of its original manufactured reported value and constants determined through experimental techniques. A direct comparison of the predicted degradation trend of FRP materials and the constant value reduced by an environmental factor recommended in design guidelines was presented. It was apparent that in the case of FRP strips the characteristic design value and environmental factors prescribed by design some guidelines are inaccurate.

Design examples using existing bridge girders were completed using both the ACI 440 (2002) guideline design value and the Weibull design value based on degradation equation predicted properties. These examples were designed according to the procedure prescribed by ACI 440 (2002). Then, a reliability analysis was performed according to the NCHRP Report 368 by Nowak (1999) to validate the results obtained from the ACI 440 procedure and to demonstrate the use of the

proposed Weibull design value. From the results of reliability analysis, it was observed that the required number of FRP strips can be reduced by the use of the FRP design values based on the Weibull distribution and the predictive degradation equations while maintaining the structural reliability fairly consistent with the target reliability. This shows that using the Weibull design value for rehabilitation of concrete girders will make projects more structurally efficient and cost effective. Choosing an expected service life of the rehabilitation and designing with the properties predicted for that time period reduces the amount of material while increasing the effectiveness of the design process. This investigation suggests that overall the use of the Weibull design values provides a more reliable and efficient means to utilize prefabricated FRP strips for use with reliability-based design procedures for rehabilitation of concrete structures.

The ability to determine material properties of FRP prefabricated rehabilitation materials at any time during the intended service life or beyond is the major advantage of the reliability-based approach proposed in this research. Using time-dependent degradation on the steel and FRP materials, the time-dependent degradation equations for material properties presented this research are different than the design guidelines' deterministic factor approach. This provides designers greater flexibility during initial design as well as when evaluating structures over time, since engineers can calculate the actual material properties and determine if the structure needs further rehabilitation or not.

The work developed through this investigation offers a new perspective on the determination of FRP design values than that prescribed by the current guidelines. Currently available design guidelines design with global safety factors by applying these factors over the lifetime of the material regardless of environmental changes or degradation of the material. The philosophy proposed herein provides the opportunity to design with material properties values after degradation so that the values used are accurate over time. Using the degraded value for a predetermined service life of the rehabilitation prevents the use of excessively large environmental or degradation factors which would mandate the use of additional strips due to the reduced design value. Coupling this design approach with continual checks of the status throughout the service life will ensure that the rehabilitation remains effective over time. These checks will also serve as a warning for when further strengthening is necessary to provide the highest standard of public safety.

7.2 Areas for Further Research

In Chapter 3, several different sets of prefabricated FRP composite samples were analyzed to determine appropriate statistical models for composite properties. While the data sets were large compared to sets of five or ten that might commonly be used to assess material properties, they were still quite small from a statistical standpoint. It would be desirable to have many larger data sets, representing even more types of composite materials. This additional data can be used to verify the distributions chosen to model variation in composite properties and identify different

classes of composites that should be modeled in different ways. Also, for the durability test data used for predictive analysis, a minimum number of 5 samples for each time period were adequate according to the ASTM requirement, but more data would be desirable to derive more reliable and accurate predictive degradation equations and thus characterize time-dependent degradation behavior more accurately.

For FRP strengthening with the use of prefabricated FRP strips, it is essential to understand the performance characteristics of adhesives and their interaction with concrete substrate and the FRP strips. Due to the fact that adhesives will be subjected to environmental exposures in service, the long term effects of adhesive degradation on the value of the rehabilitation over time must be studied and a link must be established between the adhesive degradation model and the bond coefficient used in guidelines such as ACI 440 (2002). The degraded value of adhesive should be incorporated into the design procedure in a similar manner as the degraded FRP properties.

When a degradation prediction model based design system is implemented in design as suggested previously, a single, uniform degradation equation for all three material systems considered in this research and other commercially available material systems should be developed for practical purposes. For a single degradation equation to define multiple material systems material manufacturers must adopt a similar set of quality and quality control standards.

There are few existing models for development of environmental factors from experimental data. The extrapolation method used in this research is one of many methods available from experimental data which appears to accurately describe the experimental data for this research. The environmental modification factors developed using this method should be revisited if a more appropriate approach is developed in the future.

References

Abanilla, M. A., Karbhari, V. M., Li, Y. (2006). Interlaminar and intralaminar durability characterization of wet layup carbon/epoxy used in external strengthening, *Composites Part B: Engineering*. vol. 37[7-8], pp 650-661.

Abanilla, M. A., Li, Y., Karbhari, V. M. (2006). Durability characterization of wet layup graphite/epoxy composites used in external strengthening, *Composites Part B: Engineering*. vol. 37[2-3], pp 200-212.

Adams, D.F., Carlsson, L.A., Ripes, R.B. (2003). *Experimental Characterization of Advanced Composite Materials*. CRC Press, New York, NY.

Alqam, M., Bennett, R.M., Zureick, A.H. (2001). Three Parameter vs. Two Parameter Weibull Distribution for FRP Composite Material Properties. *Compos. Struct.*, 58[4], pp 497-503.

American Association of State Highway and Transportation Officials. (2003). *Manual for Condition Evaluation and Load and Resistance Factor Rating (LRFR) of Highway Bridges*; AASHTO: Washington D.C.

American Association of State Highway Transportation Officials. (2004). *AASHTO LRFD Bridge Design Specifications, SI Units*, 3rd edition; AASHTO: Washington D.C.

American Concrete Institute Committee 440 (ACI 440). (2002). *Guide for the Design and Construction of Externally Bonded FRP Systems for Strengthening Concrete Structures.* ACI, Farmington Hills, MI.

American Institute of Steel Construction (AISC LRFD). (2004). *Manual of Steel Construction, Load and Resistance Factor Design*.

ASTM International. E 178-02, Standard Practice for Dealing With Outlying Observations. *Annual Book of ASTM Standards*. 2002

ASTM International. D 2584-02, Standard Test Method for Ignition Loss of Cured Reinforced Resins. *Annual Book of ASTM Standards*. 2002

ASTM International. D 3039/D3039M-05, Standard Test Method for Tensile Properties of Polymer Matrix Composite Materials. *Annual Book of ASTM Standards*. 2005

ASTM International. D 3171-99, Standard Test Method for Constituent Content of Composite Materials. *Annual Book of ASTM Standards*. 2005.

Atadero, R.A. (2006). *Development of Load and Resistance Factor Design for FRP Strengthening of Reinforced Concrete Structures,* Ph.D. Dissertation. Department of Structural Engineering, University of California, San Diego.

Atadero, R., Lee, L., Karbhari, V. M. (2005). Consideration of Material Variability in Reliability Analysis of FRP Strengthened Bridge Decks. *Composite Structures*, vol. 70[4], pp 430-440.

Atadero, R.A, Karbhari, V. M. (2005). Determination of Design Values for FRP Used for Strengthening. *Proceedings of the International SAMPE Technical Conferece,* Long Beach, pp 141-156.

Bain, LJ., Engelhardt, M. (1991). *Statistical Analysis of Reliability and Life-Testing Models, 2nd Edition*. Marcel Dekker, Inc., New York, NY.

Bury, K. (1999). *Statistical Distributions in Engineering*; Cambridge University Press: New York, NY.

Canadian Highway Bridge Design Code (CHBDC). (2006). CAN/CSA-S6-06, Canadian Standards Association (CSA), Ontario,Canada.

Chambers, R.E. (1997). ASCE Design Standard for Pultruded Fiber Reinforced Plastic (FRP) Structures. *Journal of Composites for Construction*, 1, pp 26-38.

Choi, S.K., Grandhi, R.V., Canfield, R.A. (2007). Reliablity-Based Structural Design. Springer, London.

Conte, J.P. (2006). *SE 224: Structural Reliability and Risk Analysis*, Course Reader. Department of Structural Engineering, University of California, San Diego, 2006.

Dai, SH., Wang, MO. (1992). *Reliability Analysis in Engineering Applications*.Van Nostrand Reinhold, New York, NY.

Ellingwood, B. (1994). Probability-Based Codified Design: Past Accomplishments and Future Challenges. *Struct. Safety*, 13[3], pp 159-176.

Ellingwood, B. (2003). Toward Load and Resistance Factor Design for Fiber Reinforced Polymer Composite Structure. J. of *Struct. Engineering*, 129[4], pp 449-458.

Ellingwood, B., Galambos, T.V., MacGregor, J.G. (1982). A Probability–Based Load Criterion for Structural Design. *Civil Engineering*. vol. 51[7], pp 74-76.

Ellingwood, B., MacGregor, J.G., Galambos, T.V., Cornell, C.A. (1982). Probability Based Load Criteria: Load Factors and Load Combinations. *Journal of the Structural Division*., vol. 108[ST5], pp 978-997.

El-Tawil, S., Okeil, A.M. (2002). LRFD Flexural Provisions for Prestressed Concrete Bridge Girders Strengthened with Carbon Fiber-Reinforced Polymer Laminates. *ACI Structural Journal*, vol. 99[2], pp 181-190.

Haldar, A., Mahadevan, S. (2000). *Probability, Reliability, and Statistical Methods in Engineering Design.* Wiley, New York, NY.

Kaw, A.K. (2006). *Mechanics of Composite Materials*. CRC Press, Boca Raton.

King, R.L. (1986). Statistical Methods for Determining Design Allowable Properties for Advanced Composite materials. *Proc., 15th Reinforced Plastics Congress*, British Plastics Federation, pp 79-85.

Lawless, J.F. (1982). *Statistical Models and Methods for Lifetime Data*. Wiley, New York, NY.

Madsen, H.O., Krenk, S., Lind, N.C. (1986). *Methods of Structural Safety.* Prentice Hall, Englewood Cliffs, NJ.

Melchers, R.E. (1999). *Structural Reliability Analysis and Prediction,* 2nd Edition. John Wiley & Sons, New York, NY.

Mirza, S.A., MacGregor, J.G. (1976). *A Statistical Study of Variables Affecting the Strength of Reinforced Normal Weight Concrete Members*, Structural Engineering Report No. 58; Department of Civil Engineering, The University of Alberta: Edmonton, Alberta, Canada.

Murphy, J.F. (1988). *Load and Resistance Factor Design for Engineered Wood Construction – A Pre-Standard Report*. American Society of Civil Engineers, NY.

Nelson, Wayne. (2004). *Accelerated Testing: Statistical Models, Test Plans, and Data Analyses*. John Wiley & Sons Inc.

Nowak, A.S. (1999). *Report 368: Calibration of LRFD Bridge Design Code.* National Academy Press, Washington D.C.

Okeil, A.M., El-Tawil, S., Shabawy, M. (2002). Flexural Reliability of Reinforced Concrete Bridge Girders Strengthened with Carbon Fiber-Reinforced Polymer Laminates. *ASCE Journal of Bridge Engineering*, vol. 7[5], pp 290-299.

Plevris, N., Triantafillou, T.C., Veneziano, D. (1995). Reliability of RC Members Strengthened with CFRP Laminates. *Journal of Structural Engineering*, vol. 121[7], pp 1037-1044.

Rackwitz, R., Fiessler, B. (1978). Structural Reliability under Combined Random Load Sequences. *Computers & Structures,* vol. 9[5], pp 489-494.

Sutherland, L.S., and Soares, C.D. (1997). Review of probabilistic models of the strength of composite materials. *Reliability Eng. and System Safety*, 56, pp183-196.

The Concrete Society: Technical Report 55 (TR 55). (2004). *Design Guidance for Strengthening Concrete Structure using Fibre Composite Materials,* 2nd Edition. The Concrete Society, Berkshire, UK.

Täljsten, B. (2002). FRP Strengthening of Existing Concrete Structures, Design Guidelines. Luleå University Printing Office, Luleå, Sweden.

The Composite Materials Handbook (HDBK-MIL17). (2002). Guidance for Characterization of Structural Materials, Vol. 2. Materials Science Corporation in Cooperation with ASTM, Lancaster, PA.

Wang, Y., Yam, R.C.M., Zuo, M.J. (2004). A Multi-Criterion Evaluation Approach to Selection of the Best Statistical Distribution. *Computers and Industrial Engineering*, vol. 47[2-3], pp 165-180.

Wilcox, P. (2008). *Reliability Based Assessment of FRP Rehabilitation of Reinforced Concrete Girders*, M.S. Thesis. Department of Structural Engineering, University of California, San Diego.

Yang, Q., Karbhari, V.M. (2008). *Durability Database for FRP Materials for Strengthening*. Report to the California Department of Transportation.

Zureick, A., Bennett, R.M., Ellingwood, B.R. (2006). Statistical Characterization of Fiber-Reinforced Polymer Composite Material Properties for Structural Design. *ASCE Journal of Structural Engineering*, vol. 132[8], pp 1320-1327.

Appendix A. MATLAB Programs Developed for this Research

The MATLAB programs written to carry out the analyses conducted in this research are provided below. Example code for a single material type and analysis case is given in Section A.1. Modifications to the code were made when necessary for the remaining analysis cases and material systems. The program describes the process for EXCEL girder analysis as shown in Appendix B, using random variables where applicable to create the necessary distributions of load and resistance such that the reliability index could be calculated for each girder. The processes used to determine the reliability index, β, are shown in Section A.2. Section A.3 shows the subroutine used in each analysis to tabulate the reliability index, β.

A.1. Example MATLAB Code for Girder Analysis

The code shown below was developed to evaluate the ACI 440 [2002] design procedure and incorporates the variability in the materials used in the girder rehabilitation. The program calls a procedure to calculate the reliability index, which can be seen in Section A.2.

```
%Monte Carlo Simulations to get design parameters,
%mean and standard deviation of FRP materials.
warning off MATLAB:divideByZero
clear all
close all
clc
format short g;

%%%%%%%%%%%%%%%%%%%%%%%%%%%%%%%%%%
%%%SIKA CASE 1.   MEAN - 3SD  %%%
%%%CE = 0.85  NCHRP 368 Beta  %%%
%%%Initial Steel Loss 10%     %%%
%%%%%%%%%%%%%%%%%%%%%%%%%%%%%%%%%%

file = 'F_SIKA_CASE1_G5.txt';
fid = fopen(file,'wt');

s1 = sprintf('Girder 5, SIKA Case 1 Results. (Time Dependent) \n\n');
fprintf(fid,s1);

%Maximum number of plys to attempt
%b_w = 304.8mm for girder 5
%b_w = 406.8mm for girder 20
max_plys = 6   %Girder 5
%max_plys = 8   %Girder 20
start_plys = [1];

case_var = 1;   %1 = %degradation, 2 = degradation time
if case_var == 1
    deg_values = [0.1];
    time_values = [0];
end
if case_var == 2
    deg_values = [0];
    time_values = [50];
end
```

```
plystart_count=0;
for init_deg = deg_values
    for time = time_values
        plystart_count = plystart_count+1;
        plys=start_plys(plystart_count);
while 1==1
    %number of sets of 100,000 iterations.
num_sets=30;
for set=1:1:num_sets;
num_runs(set)=100000;
display(['    ' ])
display(['Current Number of Iterations ' num2str(num_runs(set))])
%number of simulations to fit Mn_strengthened to a distribution
num_fits=1;
begin=cputime;

ar=clock;
br=mod(ar(1,6),1);
rand('state',br);
%%%%%%%%%%%%%%%%%%%%%%%%%%%%%%%%%%%%%%%%%%%%%%%%%%%%%%%%%%%%%%%%%%%%%%%%%%%%
%Big Loop to determine Which Distribution Mn_Strengthened best fits.
for bigloop=1:num_fits
%%%%%%%%%%%%%%%%%%%%%%%%%%%%%%%%%%%%%%%%%%%%%%%%%%%%%%%%%%%%%%%%%%%%%%%%%%%%
%%%%%%%%%%%%%%%%%%%%%%%%%%%%%%%%%%%%%%%%%%%%%%%%%%%%%%%%%%%%%%%%%%%%%%%%%%%%
%GIRDER 5 LOADS
%1355.82 is conversion factor from kip-ft to N-m.
%other numbers are bias factor and COV.

%GIRDER 5 DISTRIBUTION FACTOR, FRom Becki's Research, See AASHTO for
explaination.
DF=0.638296;

clear M_DL
%Dead Load

M_DL(:,1)=normrnd(228500,228500*0.10,num_runs(set),1);
%N-m DL_COV=0.10;  %Coefficient of Variation for Dead Load,
from %NCHRP 368.

clear M_W
%Wearing Moment
M_W(:,1)=normrnd(54000,54000*0.25,num_runs(set),1);
%N-m COV=0.25;  %Coefficient of Variation for wearing, from NCHRP 368.

clear M_LL_PLUS_IMPACT
%Live Load Plus Impact, the static portion only from qconcrete
program, >From Becki's Research.
%1.325 is Bias Factor, from NCHRP 368.

M_LL_PLUS_IMPACT(:,1)=normrnd(930100,930100*0.18,num_runs(set),1)*1.1
*DF; %N-m

LLPI_COV=0.18; %Coefficient of Variation for LL+Impact, from NCHRP
368.
```

```
M_S=M_DL+M_W+DF*M_LL_PLUS_IMPACT; %Service Load.
M_LL=1.15*M_DL+1.5*M_W+1.35*M_LL_PLUS_IMPACT; %LRFR LOAD FACTORS.

disp('Done with Loads');

%%%%%%%%%%%%%%%%%%%%%%%%%%%%%%%%%%%%%%%%%%%%%%%%%%%%%%%%%%%%%%%%%%%%%%%
%GIRDER 5 GEOMETRY AND FRP CONFIGURATION
%Design FRP Values, Step 1 of Excel Sheets.
%Calculated above using random numbers from appropriate

%%%%%%%%%%%%%%%%%%%%%%%%%%%%%%%%%%%%%%%%%%%%%%%%%%%%%%%%%%%%%%%%%%%%%%%
%ACI 440 APPROACH

%ACI 440 ENVIRONMENTAL FACTOR
CE=0.85;  %ACI 440 Environmental Factor.

%SIKA FRP Pultruded Strip Mechanical Properties
%FRP STRENGTH (NORMAL)
%mean = 2504.59 MPa,  std. dev = 82.85 MPa
%FRP MODULUS (NORMAL)
%mean = 138090 MPa  Std. Dev = 5220 MPa

frp_strength=CE*(2504.59-3*82.85);

frp_strength=normrnd(frp_strength_des,82.85,num_runs(set),1)*CE;
Ef=normrnd(138090,5220,num_runs(set),1);
%Ef=138090;
frp_strain=frp_strength./Ef;
%%%%%%%%%%%%%%%%%%%%%%%%%%%%%%%%%%%%%%%%%%%%%%%%%%%%%%%%%%%%%%%%%%%%%%%

%%%%%%%%%%%%%%%%%%%%%%%%%%%%%%%%%%%%%%%%%%%%%%%%%%%%%%%%%%%%%%%%%%%%%%%
%WEIBULL APPROACH (PROPOSED METHOD OF THE CURRENT RESEARCH
%
frp_strength=wblrnd(1507.45,36.27,num_runs(set),1);
%
Ef=wblrnd(125460,31.76,num_runs(set),1);
%
frp_strain=wblrnd(0.0099,22.55,num_runs(set),1);
%%%%%%%%%%%%%%%%%%%%%%%%%%%%%%%%%%%%%%%%%%%%%%%%%%%%%%%%%%%%%%%%%%%%%%%

%FRP GEOMETRICAL PROPERTIES
%SCCI FRP Strip Thickness (LOGNORMAL)
frp_thick=lognrnd(0.235703447341952,0.008216847887475,num_runs(set),1
);
%mean = 1.2654", std dev = 0.0104" (x 25.4 mm/in.)
%from SCCI Ambient Tensile Entire Coupon Population.

%FRP Width (Assumed Constant and Exact)
frp_width=50.8*plys;

%Area of SCCI FRP Pultruded Strip
Af=frp_width*frp_thick;
```

```
disp('Done with Geometry');
%%%%%%%%%%%%%%%%%%%%%%%%%%%%%%%%%%%%%%%%%%%%%%%%%%%%%%%%%%%%%%%%%%%%%%%%%%%%
%%%%%%%%%%%%%%%%%%%%%%%%%%%%%%%%%%%%%%%%%%%%%%%%%%%%%%%%%%%%%%%%%%%%%%%%%%%%
%GIRDER 20 GEOMETRICAL & MECHANICAL PROPERTIES
%all dimensions in mm, unless noted.
bw=406.4;
bf=normrnd(2425.7+(1/32*25.4),(15/32*25.4),num_runs(set),1);
h=normrnd(1524-(1/8*25.4),(1/4*25.4),num_runs(set),1);
derror=normrnd((h-1370.34422-
(3/16*25.4)),(1/2*25.4),num_runs(set),1);
d=h-derror; %1370.34422;
slab_depth=normrnd(168.275+(1/32*25.4),(15/32*25.4),num_runs(set),1);
cover=normrnd((50.8+(1/16*25.4)),(5/16*25.4),num_runs(set),1); %mm,
=2 in.

%REBAR INFO
%Grade 40 Steel Degradation depends on water-cementitious material
ratio.
bar_num=9;  %number of bars in girder
%%init_deg=0; %initial reduction in bar diameter
%Time Degradation of Steel
%%time=0;     %time of steel corrosion
wc=normrnd(.45,0.0225,num_runs(set),1); %for corrosion model, water
content of concrete.
init_bar_diam=35.8*(1-init_deg); %mm, initial bar diameter
init_bar_area=(init_bar_diam^2)/4*pi;
bar_area=normrnd(0.988*init_bar_area,.024*.988*init_bar_area,num_runs
(set),1); %Variation in Bar Size, %from Mirza &MacGregor, 1976
in_limits=0.94*init_bar_area<bar_area<1.06*init_bar_area;
out_limits=0.94*init_bar_area>bar_area | bar_area>1.06*init_bar_area;
while min(in_limits==0)

bar_area_out_limit=normrnd(0.988*init_bar_area,.024*.988*init_bar_are
a,num_runs(set),1).*out_limits;
    bar_area_in_limit=bar_area.*in_limits;
    bar_area=bar_area_in_limit+bar_area_out_limit;
end
bar_diam=sqrt(4*bar_area./pi);
temp_calc=(1-wc);
icorr=(37.8*temp_calc.^-1.64)./cover;
Pav=0.0116*icorr;
new_bar_diam=bar_diam-2*Pav*time; %mm, number 11 bars.
temp_calc=new_bar_diam./2;
bar_area=temp_calc.^2*pi;
As=bar_area*bar_num; %sq. mm. @ time of corrosion.
%%%%%%%%%%%%%%%%%%%%%%%%%%%%%%%%%%%%%%%%%%%%%%%%%%%%%%%%%%%%%%%%%%%%%%%%%%%%
%%%%%%%%%%%%%%%%%%%%%%%%%%%%%%%%%%%%%%%%%%%%
%Grade 40 Yield Strength and Modulus
%Yield Strength Varies via Beta Distribution, According to Mirza and
%MacGregor, 1976.
steel_strength=betarnd(3.2105,4.8157,num_runs(set),1);
fy=(468.843495936-248.211262554)*steel_strength+248.211262554;
Es=normrnd(29200*6.894757293,29200*6.894757293*0.024,num_runs(set),1)
;  %for Modulus of Steel, Mirza and %MacGregor (1979)
clear Pav icorr temp_calc bar_diam bar_area bar_num
```

```
disp('Done with Steel Degradation');
%%%%%%%%%%%%%%%%%%%%%%%%%%%%%%%%%%%%%%%%%%%%%%%%%%%%%%%%%%%%%%%%%%%%%%%%%%%%
%CONCRETE INFO
%Concrete variation from M&M 1976.
fcpsi=normrnd(3293.75,494.0625,num_runs(set),1);
fc=fcpsi./1000*6.894757293; %22.407961203; %MPa, 3.25ksi
Ecpsi=60400*sqrt(fcpsi);
Ec=Ecpsi./1000*6.894757293;
disp('Finished With Initial Parameter and Strength Calculations');
%%%%%%%%%%%%%%%%%%%%%%%%%%%%%%%%%%%%%%%%%%%%%%%%%%%%%%%%%%%%%%%%%%%%%%%%%%%%
%%%%%%%%%%%%%%%%%%%%%%%%%%%%%%%%%%%%%%%%%%%%%%%%%%%%%%%%%%%%%%%%%%%%%%%%%%%%
%Girder Geometry, FRP Geometry and Strength, Girder Reinforcement.
%[frp_strength,Ef,frp_strain,frp_width,frp_thick,bw,bf,h,d,slab_depth
,As,Es,fy,fc,Ec,Af]=GIRDER_20(num_runs);
%%%%%%%%%%%%%%%%%%%%%%%%%%%%%%%%%%%%%%%%%%%%%%%%%%%%%%%%%%%%%%%%%%%%%%%%%%%%
%Programming the ACI 440 Method.
%
%transformed section ratio
n=Es./Ec;
%compression block depth, a:
a=As.*fy./(0.85*fc.*bf);
%steel and fiber ratios
rho_s=As./((slab_depth.*bf)+((d-slab_depth)*bw));
rho_f=Af./((slab_depth.*bf)+((d-slab_depth)*bw));

%Multiplier for simplified code: n*As.
n_As=n.*As;
%  All cases T beams analyzed as rectangular sections.  Neutral Axis:
% NA=(-n_As+sqrt(n_As.^2+2*bf.*n_As.*d))./bf;

%Compressive Stress Block, Beta_1 Factor B1
if 1.09-0.008*fc<0.65
    B1=0.65;
elseif 1.09-0.008*fc>0.85
    B1=0.85;
else
    B1=1.09-0.008*fc;
end
%
%Calculation of Existing Strain at Soffit, Step 3 of Excel Sheets.
%LOOP TO DETERMINE IF RECTANGULAR OR T-BEAM.
waiting=waitbar(0,['Calculating Neutral Axis ' num2str(num_runs(set))
' times.']);
for i=1:num_runs(set)
    waitbar(i/num_runs(set));
    if a(i)<slab_depth(i)     %Calculation as Rectangular Beam.
            NA(i)=(-
n(i)*As(i)+sqrt(n(i)^2*As(i)^2+2*bf(i)*n(i)*As(i)*d(i)))/bf(i);
            kd(i,1)=NA(i);
            Icr(i,1)=bf(i)*NA(i)^3/3+n(i)*As(i)*(d(i)-NA(i))^2;
        else                  %Calculation as T-Beam.
            NA(i)=(-(bf(i)*slab_depth(i)-
bw*slab_depth(i)+n(i)*As(i))+sqrt((bf(i)*slab_depth(i)-
bw*slab_depth(i)+n(i)*As(i))^2-4*(bw/2)*((bw*slab_depth(i)^2)/2-
(bf(i)*slab_depth(i)^2)/2-n(i)*As(i)*d(i))))/bw;
```

```
            kd(i,1)=NA(i);

Icr(i,1)=((bf(i)*slab_depth(i)^3)/12+bf(i)*slab_depth(i)*(kd(i)-
slab_depth(i)/2)^2)+(bw*((kd(i)-
slab_depth(i))^3)/3)+n(i)*As(i)*(d(i)-kd(i))^2;
    end
end
close(waiting)
clear i
%
%
waiting=waitbar(0,['Calculating Mn ' num2str(num_runs(set)) '
times.']);
%LOOP FOR ACI NEUTRAL AXIS' AND OTHER PARAMETERS.
for i=1:num_runs(set)
    waitbar(i/num_runs(set));
    initial_soffit_strain_bi=zeros(num_runs(set),1);
    %Determining The Bond-Dependent Coefficient, Km
    if Ef(i,1)*frp_thick(i,1)<=180000
        K=1/(60*frp_strain(i))*(1-((Ef(i,1)*frp_thick(i,1))/360000));
        if K<=0.9
            Km(i,1)=K;
        else
            Km(i,1)=0.9;
        end
    else
        K=1/(60*frp_strain(i))*(90000/(Ef(i,1)*frp_thick(i,1)));
        if K<=0.9
            Km(i,1)=K;
        else
            Km(i,1)=0.9;
        end
    end
    %%%%%%%%%%%%%%%%%%%%%%%%%%%%%%%%%%%%%%%%%%%%%%%%%%%%%%%%%%%%%%%%%
%%%%%%%%%%%%%%%%%%%%%%%%%%%%%%%%%%%%%%%%%%%%%%%%%%%%%%%%%%%%%%%%%%%%%
%%%%    % AXIS C PROGRAM
    %Initial Estimate of Neutral Axis c;
    w=0.2;
    c(i,1)=w*d(i,1);
    c_new(i,1)=0;

    %Loop until convergence of c.
    while c(i,1)~=c_new(i,1)
        %Determination of Effective FRP Strian
        frp_strain_eff_1(i,1)=((h(i,1)-c(i,1))/c(i,1)).*0.003-
initial_soffit_strain_bi(i,1);

        %Determination of governing FRP Effective Strain
        if frp_strain_eff_1<=(Km(i,1)*frp_strain(i,1))
            frp_strain_eff(i,1)=frp_strain_eff_1(i,1);
        else
            frp_strain_eff(i,1)=Km(i,1)*frp_strain(i,1);
        end

        %Determination of Existing Strain in Reinforcing Steel.
```

```
steel_strain_s(i,1)=(frp_strain_eff(i,1)+initial_soffit_strain_bi(i,1
))*((d(i,1)-c(i,1))./(h(i,1)-c(i,1)));

        %Determination of Stress Level in FRP and Steel
        %Stress in Steel
        if (Es(i,1)*steel_strain_s(i,1)) <= fy(i,1)
            stress_steel(i,1)=Es(i,1)*steel_strain_s(i,1);
        else
            stress_steel(i,1)= fy(i,1);
        end

        %Stress in FRP
        stress_FRP(i,1)=Ef(i,1)*frp_strain_eff(i,1);

        %Calculate Internal Force Resultants and Check Equilibrium on
C.

c_new(i,1)=((As(i,1)*stress_steel(i,1))+(Af(i,1)*stress_FRP(i,1)))/(0
.85*fc(i,1)*B1(i,1)*bf(i,1));

        if ((c_new(i,1)-c(i,1))/c_new(i,1)) < 0.01
            c(i,1)=c_new(i,1);
        elseif c_new(i,1)~=c(i,1)
            w=c_new(i,1)/d;
            c(i,1)=w*d;
        end
    end % END AXIS C PROGRAM
end  %END OF ACI 440 ROUTINE
close(waiting)
%%%%%%%%%%%%%%%%%%%%%%%%%%%%%%%%%%%%%%%%%%%%%%%%%%%%%%%%%%%%%%%%%%%%%%
%%%%%%%%%%%%%%%%%%%%%%%%%%%%%%%%%%%%%%%%%%%%%%%%%%%%%%%%%%%%%%%%%%%%%%
format short g;

%determining the design flexural strength of the section.

% Mn_strengthened=(1.0*((As.*stress_steel(i,1).*(d-
B1.*c./2))+1.0*((Af.*stress_FRP(i,1)).*(h-B1.*c./2))))/1000;
Mn_strengthened=(0.9*(((As.*stress_steel(i,1)).*(d-
B1.*c./2))+0.85*((Af.*stress_FRP(i,1)).*(h-B1.*c./2))))/1000;

%%%%%%%%%%%%%%%%%%%%%%%%%%%%%%%%%%%%%%%%%%%%%%%%%%%%%%%%%%%%%%%%%%%%%%
%Calculation of Probability of Failure, Using Strict Monte Carlo
Simulation
%%%%%%%%%%%%%%%%%%%%%%%%%%%%%%%%%%%%%%%%%%%%%%%%%%%%%%%%%%%%%%%%%%%%%%
fail(set)=sum(M_LL>Mn_strengthened);

%   Determine Probability of Failure From MCS
pf(set)=fail(set)/num_runs(set);
%   Determine Reliability Beta Factor From MCS
Beta_MCS(set)=-norminv(pf(set));
%   Determine covariance of probability of failure
cov(set)=sqrt((1-pf(set))/(num_runs(set)*pf(set)));
%   Determine standard deviation of probability of failure
```

```
std(set)=cov(set)*pf(set);
%   Determine probability of failure plus 1 standard deviation
pf_plus_1(set)=pf(set)+std(set);
%   Determine probability of failure minus 1 standard deviation
pf_minus_1(set)=pf(set)-std(set);

mean_R(set,1)=mean(Mn_strengthened);
%%%%%%%%%%%%%%%%%%%%%%%%%%%%%%%%%%%%%%%%%%%%%%%%%%%%%%%%%%%%%%%%%%%%%%%%%%%%
%END OF STRICT MCS.
%%%%%%%%%%%%%%%%%%%%%%%%%%%%%%%%%%%%%%%%%%%%%%%%%%%%%%%%%%%%%%%%%%%%%%%%%%%%
%   %Fitting Mn_strengthened Data to a Distribution each iteration
to %   %average and see which distribution is best.
%       if bigloop==1
%             [mout,W,DIST_SCORES_lower_is_better] =
fitdist(num_runs(set),Mn_strengthened,bigloop);
%       else
%             [mout,W,DIST_SCORES_lower_is_better] =
fitdist2(num_runs(set),Mn_strengthened,bigloop,DIST_SCORES_lower_is_b
etter);
%       end
%END OF DISTRIBUTION FITTING ROUTINE
%%%%%%%%%%%%%%%%%%%%%%%%%%%%%%%%%%%%%%%%%%%%%%%%%%%%%%%%%%%%%%%%%%%%%%%%%%%%
%%%%%%%%%%%%%%%%%%%%%%%%%%%%%%%%%%%%%%%%%%%%%%%%%%%%%%%%%%%%%%%%%%%%%%%%%%%%
%   %Calculation of Reliability Factor Beta via FORM
%   R_parameter_GAM = gamfit(Mn_strengthened);
%   [Rm,Rv] = gamstat(R_parameter(1,1),R_parameter(1,2));
%   [Rm,Rsd,Rm_ci,Rsd_ci] = normfit(Mn_strengthened);
%   [Rm2,Rv] = normstat(Rm,Rsd);
R_parameter_LN = lognfit(Mn_strengthened);
[Rm,Rv] = lognstat(R_parameter_LN(1,1),R_parameter_LN(1,2));
    LN_mean_R(set,1)=Rm;
    LN_sd_R(set,1)=sqrt(Rv);
%      R_parameter_GAM = gamfit(Mn_strengthened);
%     [Rmg,Rvg] = gamstat(R_parameter_G(1,1),R_parameter_G(1,2));
%
    [Sm,Ssd,Sm_ci,Ssd_ci] = normfit(M_LL);
    [Sm2,Sv] = normstat(Sm,Ssd);

% Sm=M_LL;
% Sv=SD_LOAD^2;
%
[Beta_NCHRP] = reliability_NCHRP(Rm,Rv,Sm,Sv);
%     [BETA_form] = reliability2_LN(R_parameter_LN,Rm,Rv,Sm,Sv);
%     [BETA_form_gamma] =
reliability2_Gamma(R_parameter_G,Rmg,Rvg,Sm,Sv);
%     [BETA_form,alpha_form] = reliability3(Rm,Rv,Sm,Sv);
%     [r2] = dist_comparison(Rm,Rv,Sm,Sv,R_parameter);
%     [r2] = dist_plotting_LN(Rm,Rv,Sm,Sv,R_parameter_LN);

format short g;
display(['Mean of Resistance is: ' num2str(Rm)])
display(['SD of Resistance is: ' num2str(sqrt(Rv))])
display(['Pf is: ' num2str(pf(set))])
display(['SD of Pf is: ' num2str(std(set))])
display(['Beta_MCS is: ' num2str(Beta_MCS(set))])
```

```
display(['Number of Iterations: ' num2str(num_runs(set))])

Total_Time=cputime-begin  %Total time taken to run set of iterations.
end  %END OF BIGLOOP FOR FITTING DISTRIBUTIONS.
set
end  %END OF NUMBER OF SETS OF RUNS.
display('Mean of Resistances per Set:')
mean_R;

%average of averages;
mean_10_sets=mean(LN_mean_R);
Rm2=mean_10_sets;
sd_10_sets=mean(LN_sd_R);
Rv2=sd_10_sets^2;
display(['    ' ])
display(['    ' ])
display(['    ' ])
[Beta_NCHRP_total] = reliability_NCHRP_total(Rm2,Rv2,Sm,Sv);

%Print results of results file.
s = sprintf('Initial Degradation: %f\tTime: %f\nTotal Mean: %f\tTotal
SD: %f\nPlys
= %f\tBeta: %f\n\n',init_deg,time,Rm2,sd_10_sets,plys,Beta_NCHRP_tota
l(end));
fprintf(fid,s);

if Beta_NCHRP_total(end) >= 3.5
    break
else
    plys=plys+1;
    if plys > max_plys
        fprintf(fid,'TOO MANY PLYS WIDE\n\n');
        break
    end
end
end
warning on MATLAB:divideByZero
    end
end
fclose(fid);
```

A.2. Example MATLAB Code for the Calculation of the Reliability Index β for an Example Case

The program shown below was developed to determine the reliability index for each girder, material system, and example case. A reliability index is determined for each iteration of the analysis, totaling 3 million indices, by the code shown in Section A.3. The combined results of the 3 million runs are used by this script to determine the reliability index reported for each case.

```
function [Beta_NCHRP_total] = reliability_NCHRP_total(Rm2,Rv2,Sm,Sv)

%Procedure to Calculate Reliability (Beta) According to NCHRP Report
368.

%Uses Resistances as found in the MCS of ACI 440 Coded Previously and
%Linked to this code via function call.

%Uses Loads as outlined in NCHRP Report 368 with bias factors
as %applicable in the specific cases of the girders used in
this %research.  Uses Loads as described in as built drawings of
the %bridges from which the girders were taken.

%%%%%%%%%%%%%%%%%%%%%%%%%%%%%%%%%%%%%%%%%%%%%%%%%%%%%%%%%%%%%%%%%%%%%%%%%%%%
%Mean Resistance
meanR = Rm2;

%Standard Deviation of Resistance
sdR = sqrt(Rv2);

%Coefficient of Variation of Resistance, V = sd/mean.
covR = sdR / meanR;

%Mean of Load
meanL = Sm;

%Standard Deviation of Load
sdL = sqrt(Sv);

%Coefficient of Variation of Load, V = sd/mean.
covL= sdL/ meanL;
```

```
%initially k=2, assumption
k = 2;

%Initial Calculation of Design Point, R*.
R_star(1) = meanR * (1 - k * sdR);

%Initialize a recording mechanism for vectorization of results.
ri=1;

%Set Error Flag = 1 and loop until its value changes.
Flag = 1;

%Loop until design point R_star is found for approximating
Normal %Distribution using while loop.  Loop until flag is not equal
1.  %Flag value determined by error between new and old R_star values
of
%each iteration.
while Flag == 1

    %Determine distribution parameter alpha (a) for calculation of
CDF & PDF
    a(ri) = (real((log(R_star(ri)) - log(meanR)) / covR));

%Determine values of lognormal distribution of Resistance
using %initial R*
    FRRstar(ri) = normcdf(a(ri));
    fRRstar(ri) = normpdf(a(ri)) / (covR * R_star(ri));

    %Calculate the MEAN and SD of the approximating normal
    %distribution of R, at R*, using EQN D-8 and D-9 of NCHRP Report
    %368.
    % sigmaR = normpdf(norminv(normcdf(a(i)))) / (normpdf(a(i)) /
(sdR*R_star(i)));
    sigmaR(ri) = covR * R_star(ri);
    % muR = R_star(i) - simgaR * norminv(normcdf(a(i)));
    muR(ri) = R_star(ri) - a(ri) * sigmaR(ri);

    %Calculate Reliability Index, Beta, using EQN D-14
    Beta_NCHRP_total(ri) = (R_star(ri)-a(ri)*covR*R_star(ri)-
meanL)/((covR*R_star(ri))^2 + sdL^2)^(1/2);

    %Calculate New Design Point
    R_star(ri+1) = muR(ri) - Beta_NCHRP_total(ri) *
(covR*R_star(ri))^2 / ((covR*R_star(ri))^2 + sdL^2)^(1/2);

    %Calculate Difference between Design Points R_star(i) and
R_star(i+1) after first iteration.
    if ri >= 2
        diff=abs((R_star(ri)-R_star(ri-1))^2);
        if diff < 1e-10
            %Change Flag to end loop if error is within tolerance.
            Flag = 2;
```

```
        end
    end

    %Next Index Number
    ri = ri+1;

end  %end while loop.

display(['Beta_NCHRP is: ' num2str(Beta_NCHRP_total(end))]);
```

A.3. Example MATLAB Code for the Calculation of the Reliability Index β per Iteration of a Case

The code presented here is used during each of the 3 million iterations of the analysis of each example case for each material system. β is calculated using the Rackwitz and Fiessler (1978) and then passed back to the analysis program shown in Section A.2.

```
function [Beta_NCHRP] = reliability_NCHRP(Rm,Rv,Sm,Sv)

%Procedure to Calculate Reliability (Beta) According to NCHRP Report
368.

%Uses Resistances as found in the MCS of ACI 440 Coded Previously and
%Linked to this code via function call.

%Uses Loads as outlined in NCHRP Report 368 with bias factors
as %applicable in the specific cases of the girders used in
this %research.  Uses Loads as described in as built drawings of
the %bridges from which the girders were taken.

%%%%%%%%%%%%%%%%%%%%%%%%%%%%%%%%%%%%%%%%%%%%%%%%%%%%%%%%%%%%%%%%%%%%%%%%%%%%%%%%
%Mean Resistance
meanR = Rm;

%Standard Deviation of Resistance
sdR = sqrt(Rv);

%Coefficient of Variation of Resistance, V = sd/mean.
covR = sdR / meanR;

%Mean of Load
meanL = Sm;

%Standard Deviation of Load
sdL = sqrt(Sv);

%Coefficient of Variation of Load, V = sd/mean.
covL= sdL/ meanL;


%initially k=2, assumption
```

```
k = 2;

%Initial Calculation of Design Point, R*.
R_star(1) = meanR * (1 - k * sdR);

%Initialize a recording mechanism for vectorization of results.
ri=1;

%Set Error Flag = 1 and loop until its value changes.
Flag = 1;

%Loop until design point R_star is found for approximating
Normal %Distribution using while loop.  Loop until flag is not equal
1.  %Flag value determined by error between new and old R_star values
of %each iteration.
while Flag == 1

%Determine distribution parameter alpha (a) for calculation of CDF
& %PDF
    a(ri) = (real((log(R_star(ri)) - log(meanR)) / covR));

%Determine values of lognormal distribution of Resistance using
initial R*
    FRRstar(ri) = normcdf(a(ri));
    fRRstar(ri) = normpdf(a(ri)) / (covR * R_star(ri));

%Calculate the MEAN and SD of the approximating normal distribution
of R, at R*, using EQN D-8 and
    %D-9 of NCHRP Report 368.
    % sigmaR = normpdf(norminv(normcdf(a(i)))) / (normpdf(a(i)) /
(sdR*R_star(i)));
    sigmaR(ri) = covR * R_star(ri);
    % muR = R_star(i) - simgaR * norminv(normcdf(a(i)));
    muR(ri) = R_star(ri) - a(ri) * sigmaR(ri);

    %Calculate Reliability Index, Beta, using EQN D-14
    Beta_NCHRP(ri) = (R_star(ri)-a(ri)*covR*R_star(ri)-
meanL)/((covR*R_star(ri))^2 + sdL^2)^(1/2);

    %Calculate New Design Point
    R_star(ri+1) = muR(ri) - Beta_NCHRP(ri) * (covR*R_star(ri))^2 /
((covR*R_star(ri))^2 + sdL^2)^(1/2);

    %Calculate Difference between Design Points R_star(i) and
R_star(i+1) after first iteration.
    if ri >= 2
        diff=abs((R_star(ri)-R_star(ri-1))^2);
        if diff < 1e-10
            %Change Flag to end loop if error is within tolerance.
            Flag = 2;
        end
    end
```

```
    %Next Index Number
    ri = ri+1;

end  %end while loop.

display(['Beta_NCHRP is: ' num2str(Beta_NCHRP(end))]);
```

A.4. Script for Statistical Distribution Fitting

The code shown here was developed to carry out the multi criterion approach to statistical distribution fitting outlined in Section 3.2.2.3. Tensile testing data from the current research were used as inputs to the routine to determine the distributions of FRP strength, modulus, and thickness. The procedure adapted from Wang et al (2005) is the basis for this code.

```
%Program to check fit of empirical or calculated data
to %distributions following Wang et al, 2004.
%
function [mout,W,DIST_SCORES_lower_is_better] =
fitdist2(num_runs,Mn_strengthened,bigloop,DIST_SCORES_lower_is_better
)
%
close all
%
%Data to Which a Distribution Must Be Fit:
  M=Mn_strengthened;  %Data Source from Monte Carlo Simulation Prog.
   %If running for data not obtained via matlab and passed in,insert
   %a vector of the data such that M = [ ... ];
%   stddev=std(M);
%   skew=skewness(M);
%   kurt=kurtosis(M);
%   Beta1Hat=skew^2/stddev^6;
%   Beta2Hat=kurt/stddev^4;
%Criteria number 4, Distance of skewness and kurtosis to
appropriate %distribution skewness and kurtosis omitted due to
unknown Weibull %benchmark value, see Wang et al, 2004.
%
%Criteria 5, expert opinion omitted as no such expert opinion in
any %quantity is available in this case.
%
%Sort the Observed Data, Smallest to Largest for CDF Plotting Later.
    M_NUMS=sort(M);
%
%DETERMINE HYPOTHESES DISTRIBUTION PARAMETERS
    %DETERMINE NORMAL DISTRIBUTION PARAMETERS
        %Get Parameters of Data for Normal Distribution
        [muNormhat,sigmaNormhat,muci,sigmaci] = normfit(M);
    %DETERMINE WEIBULL DISTRIBUTION PARAMETERS
        %Get Parameters of Data for Normal Distribution
        [weibphat,weibci] = wblfit(M);
    %DETERMING LOGNORMAL DISTRIBUTION PARAMETERS
        [LNhat,LNci] = lognfit(M);
```

```
        muLNhat=LNhat(1,1);
        sigmaLNhat=LNhat(1,2);
        %From Bury, 1999, Lognormal may be taken as the same as
Normal.
    %DETERMINGE GAMMA DISTRIBUTION PARAMETERS
        [GammaHat,gammaci] = gamfit(M);
%
%CRITERIA 1: KOLMOGOROV-SMIRNOV GOODNESS OF FIT HYPOTHESIS
TEST %RESULTS
            %Test for Normal Distribution CDF
            [hn,pn,kn,cn] = kstest(M, [M
normcdf(M,muNormhat,sigmaNormhat)]);
%
            %Test for Weibull Distribution CDF
            [hw,pw,kw,cw] = kstest(M, [M
weibcdf(M,weibphat(1,1),weibphat(1,2))]);
%
            %Test for Lognormal Distribution CDF
            [hl,pl,kl,cl] = kstest(M, [M
logncdf(M,muLNhat,sigmaLNhat)]);
%
            %Test for Gamma Distribution CDF
            [hg,pg,kg,cg] = kstest(M, [M
gamcdf(M,GammaHat(1,1),GammaHat(1,2))]);
%
%CRITERIA 2: AVERAGE ERROR IN HYPOTHESIS CDF TO EMPIRICAL CDF
    %EMPIRICAL CDF INFORMATION
        figure
        %EXPERIMENTAL DATA CDF
            [F,L] = ecdf(M);
            [H,STATS]=cdfplot(M);
                title('CDF Comparison of Hypothesis Distributions to
Observed Data');

legend('Empirical','Normal','Weibull','Lognormal','Gamma',2);
            hold on
%
    %NORMAL DISTRIBUTION CDF
        NORM_CDF=sort(normcdf(M,muNormhat,sigmaNormhat));
        plot(M_NUMS,NORM_CDF,'r--');
%
        %Average deviation in CDF Test
            delFn=0;
            for i=1:num_runs
                delFn=delFn+abs(NORM_CDF(i)-F(i));
            end
            delFn=1/num_runs*delFn;
%
    %WEIBULL DISTRIBUTION CDF
        WEIB_CDF=sort(weibcdf(M,weibphat(1,1),weibphat(1,2)));
        plot(M_NUMS,WEIB_CDF,'g:');
%
        %Average deviation in CDF Test
            delFw=0;
            for i=1:num_runs
```

```
                delFw=delFw+abs(WEIB_CDF(i)-F(i));
            end
            delFw=1/num_runs*delFw;
%
    %LOGNORMAL DISTRIBUTION CDF
        LOGN_CDF=sort(logncdf(M,muLNhat,sigmaLNhat));
        plot(M_NUMS,LOGN_CDF,'c-.');
%         legend('Empirical','Normal','Weibull','Lognormal',2);
%
        %Average deviation in CDF Test
            delFl=0;
            for i=1:num_runs
                delFl=delFl+abs(LOGN_CDF(i)-F(i));
            end
            delFl=1/num_runs*delFl;
%
%   %GAMMA DISTRIBUTION CDF
        GAMMA_CDF=sort(gamcdf(M,GammaHat(1,1),GammaHat(1,2)));
          plot(M_NUMS,GAMMA_CDF,'m-.');
        legend('Empirical','Normal','Weibull','Lognormal','Gamma',2);
    hold off
%
        %Average deviation in CDF Test
            delFg=0;
            for i=1:num_runs
                delFg=delFg+abs(GAMMA_CDF(i)-F(i));
            end
            delFg=1/num_runs*delFg;
%
%CRITERIA 3: AVERAGE ERROR IN HYPOTHESIS PDF TO EMPIRICAL PDF
    %HISTOGRAM (PDF) OF EXPERIMENTAL DATA
        num_bins=30;
        [n,mout]=hist(M,num_bins);
        bar(mout,n)
        %Set Color of Histogram Output
            h = findobj(gca,'Type','patch');
            set(h,'FaceColor','r','EdgeColor','w')
            xlabel('Value of Observed Data')
            ylabel('Number of Occurances')
            title('Histogram of Observed Data')
       figure
%
    %EXPERIMENTAL DATA PDF
        f = ksdensity(M,mout,'kernel','triangle');
        plot(mout,f,'b')
            xlabel('x')
            ylabel('f(x)')
            title('PDF Comparison of Hypothisis Distributions to
Observed Data')
        hold on
%
    %NORMAL DISTRIBUTION PDF
        NORM_PDF = normpdf(mout,muNormhat,sigmaNormhat);
        plot(mout,NORM_PDF,'r--')
%
```

```
        %Average Deviation of Normal PDF from Empirical PDF
            delfn=0;
            for i=1:num_bins
                delfn=delfn+abs(NORM_PDF(i)-f(i));
            end
            delfn=1/num_bins*delfn;
%
    %WEIBULL DISTRIBUTION PDF
        WEIB_PDF = weibpdf(mout,weibphat(1,1),weibphat(1,2));
        plot(mout,WEIB_PDF,'g:')
%
        %Average Deviation of Weibull PDF from Empirical PDF
            delfw=0;
            for i=1:num_bins
                delfw=delfw+abs(WEIB_PDF(i)-f(i));
            end
            delfw=1/num_bins*delfw;
%
    %LOGNORMAL DISTRIBUTION PDF
        LOGN_PDF = lognpdf(mout,muLNhat,sigmaLNhat);
        plot(mout,LOGN_PDF,'c-.')
        legend('Empirical','Normal','Weibull','Lognormal',2);
%
        %Average Deviation of Normal PDF from Empirical PDF
            delfl=0;
            for i=1:num_bins
                delfl=delfl+abs(LOGN_PDF(i)-f(i));
            end
            delfl=1/num_bins*delfl;
%
%     %GAMMA DISTRIBUTION PDF
        GAMMA_PDF = gampdf(mout,GammaHat(1,1),GammaHat(1,2));
        plot(mout,GAMMA_PDF,'m-.')

legend('Empirical','Normal','Weibull','Lognormal','Gamma',2);
        hold off
%
        %Average Deviation of Normal PDF from Empirical PDF
            delfg=0;
            for i=1:num_bins
                delfg=delfg+abs(GAMMA_PDF(i)-f(i));
            end
            delfg=1/num_bins*delfg;
%
%DETERMINATION OF RANKING OF FIT OF THE HYPOTHESIS DISTRIBUTIONS
    %CREATE PERFORMANCE MATRIX R, per Wang et al, 2004.
        R=[ kn,    kw,    kl,    kg;    ...
           delFn, delFw, delFl, delFg;  ...
           delfn, delfw, delfl, delfg   ];

   %CREATE WEIGHTING VECTOR W
%     W=[0.18, 0.28, 0.28];
%         Weighting vector taken from Wang et al, 2004, as this data
is all that it available to date
%         for ranking weights.
```

```
  W=[1, 1, 1];
%         Unity Weighting vector used as no expert advice
is %available to determine the appropriate importance of the fit
tests %conducted.

    %CALCULATE WEIGHTED AVERAGE PERFORMANCES OF DISTRIBUTIONS
    DIST_SCORES_lower_is_better(bigloop,:)=W*R;
%     In this method, the larger the result of each test, the
worse %fit, therefore the smallest value in the B matrix correlates
to the %best fitting distribution.
```

Appendix B. Example of Sectional Analysis of Girders

This appendix contains examples of the calculations used throughout this work. Sectional analysis calculations are presented followed by examples of the code written for analysis programs created for this research. Girder analyses were performed as described in Section 6.5, first using Microsoft Excel to determine analytically the moment capacity of each girder in each case. The process used is shown below for girder 5 using material system SIKA+SCCI+FYFE in example case one (the ACI 440 design value, C_E = 0.85, 20% Steel Initial Loss). Changes were made where necessary to adapt the analysis process for the other material systems and analysis cases.

Design Example "Sectional Analysis"

Girder #	**5**	5 or 20
Material	**ALL**	
Design Case	**1**	

FRP Degradation	**Continuous**	
Initial steel loss	**10%**	
Continuous steel loss	**2**	1(Yes) or 2 (No)
Design Life	**50**	years

Girder Properties

	Girder 5	Girder 20	
b_w=	304.8	406.4	mm
b_f=	2235.2	2425.7	mm
h=	1066.8	1524.0	mm
d=	922.1	1370.3	mm
w/c ratio=	0.45	0.45	mm
Cover=	50.80	50.80	mm
Rebar #=	6	9	
Rebar dia=	36	36	mm
slab depth, ts=	177.8	168.3	mm

Experimental FRP Properties

		Mean	STD	
SIKA	Strength=	2504.59	82.85	Mpa
	Modulus=	138090	5220	MPa
	Strain=	0.0158	0.00084	mm/mm
SIKA+SCCI+FYFE	Strength=	2497.64	223.95	Mpa
	Modulus=	127230	12850	MPa
	Strain=	0.01972	0.00154	mm/mm

StripThickness, tf=	1.31	mm/strip
Strip Width, wf=	50.8	mm/strip

Design Moment Demand

	Girder 5	Girder 20	
M_DL=	282.5	599.3	kN-m
M_S=	876.7	2070.5	kN-m
LRFR Factored=	1168.1	2754.5	kN-m

C_E= 0.85

		ACI 440 (μ-3σ)	WEIBULL	
SIKA	Strength, f_{fu}=	1917.634	1465.21	Mpa
	Modulus, E_f=	138090	121450	MPa
	Strain, ε_{fu}=	0.0133	0.0095	mm/mm
SIKA+SCCI+FYFE	Strength, f_{fu}=	1551.9215	1492.6	Mpa
	Modulus, E_f=	127230	106540	MPa
	Strain, ε_{fu}=	0.0128	0.0123	mm/mm

1. Girder Properties

b_w=	304.8	mm
b_f=	2235.2	mm
h=	1066.8	mm
d=	922.1	mm
w/c ratio=	0.45	mm
Cover=	50.80	mm
Rebar #=	6	
Rebar dia=	36	mm
slab depth, ts=	177.8	mm
A`s=	5496.53	mm^2

Steel & Concrete Properties

Rebar diameter=	36	mm
Rebar #=	6	
Initial A_s=	6107.26	mm^2
f_y=	275.8	MPa
E_s=	200000	MPa
f'_c=	22.41	MPa
E_c=	22,700	MPa
n=	8.81	=Es/Ec

Initial steel loss alone

Initial steel loss %=	10%	
Loss As=	610.73	mm^2
Final As=	5496.53	mm^2

Plus Continuous steel loss with time

icorr=	1.99	
Pav=	0.023057	
Do=	36	mm
Design life=	50	years
Dloss=	33.69	mm
Loss As=	757.26	mm^2
Total Final As=	4739.27	mm^2

2. FRP Design Values

Strength, f_{fu}=	1551.9215	Mpa
Modulus, E_f=	127230	MPa
Strain, ε_{fu}=	0.0128	mm/mm

3. Choose a trial quantity of FRP by specifying the number of strips

N= 1 <= # of Strips directly applied to the concrete girder

n= 1 <=# of plies applied on top of each other (Assumed as 1.0 for the current research: See P.126 in Wilcox (2008))

wf_total= 50.8 mm **WIDE OK** <=checking the width limitation

bw= 304.8 mm

4. Determine the analytical girder section

a= 30.27 mm

ts= 177.8 mm

=> Rectangular section

5. Determine the reinforcement ratio of steel and FRP

At= 624295.5 mm^2

Af= 66.55 mm^2

ρ_s= 0.008804

ρ_f= 0.000107

6. Determine the existing strain at the bottom soffit of the girder

$$\varepsilon_{bi} = \frac{M_{DL}(h-kd)}{I_{cr}E_c}$$

k= 0.325112376

Icr= 21494438074 mm^4

DL= 282500 N-m

<= n represents the transformed ratio (Es/Ec)

ε_bi= 0.000444 mm/mm

7. Determine the bond coefficient

$$\kappa_m = \begin{cases} \dfrac{1}{60\varepsilon_{fu}}\left(1-\dfrac{nE_f t_f}{360{,}000}\right) \le 0.90, & for \quad nE_f t_f \le 180{,}000 \\ \dfrac{1}{60\varepsilon_{fu}}\left(\dfrac{90{,}000}{nE_f t_f}\right) \le 0.90, & for \quad nE_f t_f > 180{,}000 \end{cases}$$

**n represents the number of strips used.

nE_ft_f = 166671.3 N/mm

κ_m = 0.701

8. Estimate a trial value for the neutral axis depth

c0= 44 mm <= Typically, c=0.2d

9. Determine the effective strain in the FRP

$$\varepsilon_{fe} = \varepsilon_{cu}\left(\frac{h-c}{c}\right) - \varepsilon_{bi} < \kappa_m \varepsilon_{fu}$$

ε_cu= 0.003 mm/mm

$\kappa_m\varepsilon_{fu}$= 0.00895 mm/mm

ε_fe= 0.00895 mm/mm

10. Determine the strain in the reinforcing steel

$$\varepsilon_s = \left(\varepsilon_{fe} + \varepsilon_{bi}\right)\left(\frac{d-c}{h-c}\right)$$

ε_s = 0.008066 mm/mm

11. Determine the stresses in the steel and FRP

$$f_s = E_s\varepsilon_s \le f_y$$ fs= 275.79 MPa

$$f_{fe} = E_f\varepsilon_{fe}$$ f_fe= 1138.76 MPa

12. Estimate the Whitney compressive stress block constant

$$\beta_1 = \begin{cases} 0.65 & \text{if} \quad \left(1.09 - 0.008 f_c'\right) < 0.65 \\ 0.85 & \text{if} \quad \left(1.09 - 0.008 f_c'\right) > 0.85 \\ 1.09 - 0.008 f_c' \left[N/mm^2\right] & \text{if} \quad \text{otherwise} \end{cases}$$

1.09-0.008*f'c= 0.911 β1= 0.85

13. Use equilibrium to caluculate a new estimate of the neutral axis depth

$$c = \frac{A_s^* f_s + A_f f_{fe}}{\gamma f_c' \beta_1 b}$$

γ= 0.85

c= 43.98 mm

c_o= 44 mm <= Assumed c

% difference= 0 %

14. Iterate to find the final satisfying neutral axis

Iteration	c_o	New c	% difference	Check
1st	44	43.98	0.0	OK
2nd			#DIV/0!	#DIV/0!
3rd			#DIV/0!	#DIV/0!
4th			#DIV/0!	#DIV/0!
5th			#DIV/0!	#DIV/0!

Selected c= 44 mm

15. Determine the factored moment capacity of the section

$$\phi M_n = \phi\left[A_s f_s\left(d - \frac{\beta_1 c}{2}\right) + \psi A_f f_{fe}\left(h - \frac{\beta_1 c}{2}\right)\right]$$

ψ = 0.85
Φ = 0.9

ΦM_n = 1293335333 N-mm
1293335.3 N-m

ΦM_n =	1293.34	kN-m
Moment Demar	1168.10	kN-m

=> OK

Iteration	N	c [mm]	ΦM_n	Moment Demand	Check
1st	1	44	1293.34	1168.10	OK
2nd				1168.10	ITERATE
3rd				1168.10	ITERATE
4th				1168.10	ITERATE
5th				1168.10	ITERATE

Final ΦM_n =	1293.34	kN-m

16. Check the service stress in the steel reinforcement

$$f_{s,s} = \frac{\left[M_s + \varepsilon_{bi} A_f E_f \left(h - \frac{kd}{3}\right)\right](d - kd) E_s}{A_s E_s \left(d - \frac{kd}{3}\right)(d - kd) + A_f E_f \left(h - \frac{kd}{3}\right)(h - kd)} \le 0.80 f_y$$

$$f_{f,s} = f_{s,s}\left(\frac{E_f}{E_s}\right)\left(\frac{h - kd}{d - kd}\right) - \varepsilon_{bi} E_f \le 0.55 f_{fu}$$

M_S= 876741003.0 N-mm

f_ss=	192.65	Mpa	0.90fy=	248.21	Mpa	**OK**
f_fs=	94.54	Mpa	0.55f_fu=	853.56	Mpa	**OK**

17. Final Design and Summary

=> DESIGN SATISFIED

=> Apply 1 50.8mm wide layers of prefabricated FRP strips to the girder

ε_fe=	0.00895	mm/mm
c=	44	mm
ε_s =	0.008066	mm/mm
fs=	275.79	Mpa
f_fe=	1138.76	MPa
β1=	0.85	
Final ΦM_n =	1293.34	kN-m

Appendix C. Table of U_γ for Confidence Levels

The method presented by Bain (1991) determines the confidence level for the p-percentile value of the Weibull distribution, as shown in Eq. 4-10 from Section 4.2.3, that only depends on the desired probability percentile, p, the confidence level desired, γ, and the sample size. The parameter U_γ is tabulated as a function of sample size and confidence level and can be taken from Table 4A of Bain (1991) which is reproduced herein.

n	γ								
	0.02	0.05	0.1	0.25	0.5	0.75	0.9	0.95	0.98
5	-3.647	-2.788	-1.986	-0.993	-0.125	0.780	1.726	2.475	3.537
6	-3.419	-2.467	-1.813	-0.943	-0.110	0.740	1.631	2.300	3.162
7	-3.164	-2.312	-1.725	-0.910	-0.101	0.720	1.582	2.193	2.963
8	-2.987	-2.217	-1.672	-0.885	-0.091	0.710	1.547	2.124	2.837
9	-2.862	-2.151	-1.632	-0.867	-0.087	0.705	1.521	2.073	2.751
10	-2.770	-2.103	-1.603	-0.851	-0.082	0.702	1.502	2.037	2.691
11	-2.696	-2.063	-1.582	-0.839	-0.076	0.700	1.486	2.007	2.643
12	-2.640	-2.033	-1.562	-0.828	-0.073	0.700	1.472	1.981	2.605
13	-2.592	-2.008	-1.547	-0.822	-0.069	0.699	1.464	1.961	2.574
14	-2.556	-1.991	-1.534	-0.812	-0.067	0.700	1.456	1.946	2.548
15	-2.521	-1.971	-1.522	-0.806	-0.062	0.697	1.448	1.933	2.529
16	-2.496	-1.956	-1.516	-0.800	-0.060	0.700	1.440	1.920	2.508
18	-2.452	-1.930	-1.498	-0.793	-0.055	0.700	1.434	1.896	2.478
20	-2.415	-1.914	-1.485	-0.783	-0.054	0.702	1.422	1.883	2.455
22	-2.387	-1.895	-1.473	-0.779	-0.052	0.704	1.417	1.867	2.434
24	-2.366	-1.881	-1.465	-0.774	-0.044	0.705	1.411	1.857	2.420
28	-2.334	-1.863	-1.450	-0.762	-0.042	0.709	1.402	1.836	2.397
32	-2.308	-1.844	-1.437	-0.758	-0.034	0.707	1.397	1.827	2.376
36	-2.292	-1.830	-1.428	-0.750	-0.030	0.708	1.392	1.812	2.358
40	-2.277	-1.821	-1.417	-0.746	-0.025	0.715	1.391	1.802	2.346
45	-2.261	-1.808	-1.412	-0.741	-0.023	0.714	1.385	1.794	2.334
50	-2.249	-1.796	-1.400	-0.735	-0.021	0.714	1.379	1.789	2.319
55	-2.240	-1.791	-1.394	-0.734	-0.015	0.716	1.376	1.784	2.314
60	-2.239	-1.782	-1.387	-0.728	-0.015	0.713	1.371	1.774	2.301
70	-2.226	-1.765	-1.380	-0.720	-0.008	0.711	1.372	1.765	2.292
80	-2.218	-1.762	-1.368	-0.716	0.000	0.689	1.324	1.699	2.200
100	-2.21	-1.74	-1.36	-0.71	0.00	0.71	1.36	1.75	2.26
120	-2.21	-1.73	-1.35	-0.70	0.01	0.70	1.35	1.74	2.25
∞	-2.16	-1.73	-1.35	-0.71	0.00	0.71	1.35	1.73	2.16